The Thesis Committee for Victoria Elizabeth McCammon
Certifies that this is the approved version of the following thesis:

IN-PLANE SHEAR STRENGTH AND STIFFNESS OF PRECAST CONCRETE PANELS

APPROVED BY
SUPERVISING COMMITTEE:

Supervisor:

Todd A. Helwig

Patricia Clayton

IN-PLANE SHEAR STRENGTH AND STIFFNESS OF PRECAST CONCRETE PANELS

by

Victoria Elizabeth McCammon, B.S.C.E.

Thesis

Presented to the Faculty of the Graduate School of

The University of Texas at Austin

in Partial Fulfillment

of the Requirements

for the Degree of

Master of Science in Engineering

The University of Texas at Austin

December 2015

Dedication

To my family, for putting up with me, and to my friends, for dogging me when I needed it.

Acknowledgements

This research was conducted at the Phil M. Ferguson Structural Engineering Laboratory at the Pickle Research Campus of the University of Texas at Austin. Funding for this research was provided by the Texas Department of Transportation.

The author wishes to express her appreciation for the faculty, staff, and other students at Ferguson lab. In particular the help of the other students on this project, Colter Roskos and Paul Biju-Duval, was greatly appreciated. Without their help, knowledge, creativity, and hard work this project would not have been possible.

Abstract

IN-PLANE SHEAR STRENGTH AND STIFFNESS OF PRECAST CONCRETE PANELS

Victoria Elizabeth McCammon, M.S.E.

The University of Texas at Austin, 2015

Supervisor: Todd A. Helwig

Pre-Cast-Panels (PCP) have been used for decades as stay-in-place forms to support the wet concrete during the placement of bridge decks and as part of the composite slab for typical straight bridges. The typical connection detail in Texas is to set the panel on a foam bedding strip, leaving a ledge for the slab concrete to flow under; this ledge provides the long-term support for the panel. The PCP is not structurally connected to the bridge until the slab has set up; it provides no in-plane shear resistance under construction loads, when the superstructure is the most vulnerable to lateral forces. If the PCP is connected to the girders during deck casting they can provide bracing to the top flanges of the beams and forces in the traditional lateral resisting system can be reduced, potentially leading a reduction in the number of cross-frames and top lateral truss member sizes.

The objective of this research is to measure the in-plane shear strength and stiffness of PCP attached to girder systems using different connections and to

determine the stability of the traditional connection method with respect to in-plane shear movement. The research included testing conventionally reinforced full scale PCP in a shear frame. The typical Texas detail was tested at three different bedding strip heights. Variations of two additional connection methods were tested to determine their behavior.

Bolting the PCP to the shear studs provides only a small in-plane shear stiffness and strength. Welding the PCP to a steel shape that is welded to the top flange of the beam provides a much stronger and stiffer connection.

Table of Contents

List of Tables

List of Figures

CHAPTER 1

Introduction

1.1 PROBLEM DESCRIPTION

Precast concrete panels (PCPs) have been successfully used on straight bridges since the late 1950's. The panels enhance the construction efficiency since they provide an immediate work surface for construction materials, equipment, and personnel. However, their use on curved girders has been disallowed due to a lack of testing in this configuration. Because there is no positive connection between the girders and panels, there are concerns with the use of PCPs on horizontally curved bridges since the girders experience significant lateral and torsional deformations. The use of conventional forming or permanent metal deck forms (PMDF) is typically used to form the slab on curved girder bridges.

Curved bridge superstructures are predominantly constructed of steel or concrete beams with a composite slab. Bridges with large radii of curvatures or short spans can be constructed with straight beams that chord the curves. The use of chorded beams is limited by the strength of the slab overhang as it gets larger near mid-span. These bridges typically have low levels of torsion and are often designed as straight bridges.

Bridges with smaller radii of curvature and longer spans use curved beams. Bridges of this type are often found in highway interchanges; the space limitations of available right-of-way results in a smaller radius of curvature and the geometric constraints of the lower roadways often result in longer spans. These bridges have a higher torsional load that can result in complex beam to slab behavior. PCP composite

decks have not been tested for this complex beam to slab interaction, which is one of the reasons the precast panels are not allowed on curved bridges.

While most bridge systems may utilize some form of bracing, curved girder systems generally require more substantial bracing systems compared to straight girders. The most common bracing that is used for steel I-girder are cross-frames. Steel tub girders utilize a wider array of bracing, including a top lateral truss and interior K-frames, and often also have exterior cross-frames between the tubs. For concrete U-Beams the lateral bracing system can include a cast-in-place lid slab to close the open cross-section of the beams. Current details for PCPs do not include a positive connection to the girders, and as a result there is no significant lateral force transfer between the panels and the girders prior to the slab curing. The results outlined in this thesis are part of a study on the behavior of PCPs in horizontally curved bridge applications. The goals of the study include determining if PCPs can be used in curved bridge applications using existing panel support details as well as developing connection details so the panels can provide some lateral bracing to the girders.

1.2 OBJECTIVE OF STUDY

An investigation of the ability for using PCPs on curved bridges is currently being conducted at the University of Texas at Austin with the sponsorship of the Texas Department of Transportation (TxDOT). This project includes both computational studies as well as full-scale experiments. The experimental work provides valuable data for validating the finite element model so that parametric studies can be conducted to develop a comprehensive understanding of the behavior of the panels.

The full-scale testing has been divided into a series of studies, including tests on the individual panels as well as tests on girder systems with the PCPs utilized for bracing.

The initial focus of the testing has targeted the behavior of the individual panels and has included in-plane shear tests of full-scale PCPs attached to the top flange of a girder. Different attachment methods have been investigated. Although the focus of the study is on the behavior of commercially fabricated prestressed PCPs, for efficiency the initial testing program has utilized reinforced concrete panels that were fabricated at Ferguson Structural Engineering Laboratory at the University of Texas. The first series of tests have been conducted to develop suitable connection details. The focus of this thesis is these initial in-plane shear tests of the conventionally reinforced PCPs. Based upon these initial series of tests, the research team is working with commercial precast plants to test the connection details on prestressed PCPs.

In addition to the in-plane shear tests, experiments will also be carried out on girder systems with PCPs for bracing. While the focus of the study is on curved girder systems, the test program will utilize straight girders with eccentric loads to simulate the torsion caused by the horizontally curved geometry. The test setup for the girder experiments has been designed and is currently being fabricated.

1.3 DESCRIPTION OF CURRENT CURVED BRIDGES

Most curved beam bridges make use of steel I-girders or steel tub-girders such as those shown in Figure 1.1 and Figure 1.2. Although most horizontally curved bridges make use of steel girders, some applications of prestressed, post-tensioned, spliced, concrete U-Beams have been utilized in Colorado. Bridges in Texas have been designed using this beam as an alternative, but the contractors have not chosen to construct them. However, it is likely that such a bridge will be constructed in the future, and the state of Texas is interested in the use of PCPs as the forming system in such an application. Therefore, this bridge type is included in the scope of the current research study.

Figure 1.1: *Curved Steel I-Girder Bridge with PMDF*

Figure 1.2: *Curved Steel Tub-Girder Bridge with PMDF*

The composite slabs on the curved beam bridges have historically been constructed using permanent metal deck forms (PMDF). Conventional wood forming can also be used to form the slab; however this formwork is temporary and must be removed. The Concrete U-Beam bridges in Colorado have utilized PCPs both as lid slabs to close the section and between the beams in the cross section. These PCPs are not considered structural members in the design of these bridges, but were used as stay-in-place formwork only. Figure 1.3 shows a bridge with chorded U-beams. Curved, post-tensioned U-Beams are comparatively deeper and wider than their prestressed straight counterpart with thicker webs and substantial end blocks to accommodate the post-tensioning ducts.

Figure 1.3: *Chorded Concrete U-Beam Bridge with PCP*

1.4 SCOPE

As noted earlier, this thesis presents results on a research study focused on the use of precast concrete panels (PCPs) in curved girder applications. This thesis focuses on the initial testing phase, consisting of experiments to measure the in-plane shear stiffness and strength of the panels. This thesis has been divided into 6 chapters. Following this introductory chapter, Chapter 2 provides an overview of background information related to horizontally curved girders and PCPs. Chapter 3 describes the test setup that was designed and fabricated to measure the shear properties of the PCPs. Results from the first stage of testing are presented in Chapter 4, followed by a comparison and discussion of the results in Chapter 5. A summary of the work presented in this thesis is provided in Chapter 6 as well as an overview of future work.

CHAPTER 2

Background

2.1 PRECAST CONCRETE PANELS

Precast concrete panels (PCP) are prefabricated panels of concrete that span between the top flanges of girders. Historically, both full depth and partial depth panels have been used. The thickness of full depth PCPs is the depth of the slab; closure joints are poured between the panels to make them composite. The top of the full depth PCP is the riding surface of the bridge deck. As implied by the name, the partial depth PCPs are thinner than the final thickness of the slab and a cast-in-place (C-I-P) topping concrete is placed over a layer of PCPs and poured between the panel ends over the girders to make the PCPs composite with the girders and the C-I-P topping. The partial depth PCPs serve two purposes; they provide stay-in-place formwork for the C-I-P topping concrete and they provide the bottom layer of reinforcing in the final composite slab. The reinforcement in the PCPs may be mild steel or prestressed steel. The topping concrete is thick enough to provide adequate cover to the slab's top layer of reinforcing. Although full depth PCPs have been successfully used in the past, the focus of the research outlined in this thesis is on partial depth PCPs, which will be the focus of the remainder of this chapter.

Different connections have been proposed since PCPs were first used in bridges. The first use of PCPs included support details in which the panels were supported on fiberboard. The current state of practice on Texas bridges is to set the panels on a strip of polystyrene, called the bedding strip, leaving a ledge for the slab concrete to flow under; this ledge provides the long-term support for the panel. The bedding strip is only a

temporary support of the PCP until the topping concrete sets up. When the topping concrete is cast on the deck, it fills in the space between the PCPs over the beam top flanges and it flows under the overhang of the PCP. This line of concrete under the panel then becomes the long term support of the panel.

2.2 LITERATURE REVIEW

A search of the literature yielded no previous studies or applications on the use of PCPs on curved bridges. There is literature on the use of PCPs on straight bridges and the use of precast panel for shear walls.

2.2.1 Historical Use of and Research on PCPs

The first documented use of PCPs on bridges was on the North Illinois Tollway in 1957. A trial bridge, the Beverly Road Bridge, was constructed to try out new construction methods proposed for the Illinois Tollway project including the use of PCPs called "concrete planks" (Bender, 1957). The PCPs were determined to act compositely with both the bridge girders and the C-I-P topping after a suite of tests on both the test bridge and laboratory specimens (Janney & Eney, 1957). The test bridge was subjected to static loads during different construction stages and dynamic loads after the bridge was finished. The laboratory specimens, tested at Lehigh University, were sections of deck comprised of a PCP with a C-I-P topping. The laboratory specimens were subjected to static and dynamic loading then loaded to failure; there was no evidence of delamination between the PCPs and the C-I-P topping (Janney & Eney, 1957). After the construction of the Beverly test bridge, nine bridges on the Illinois Tollway were constructed using PCPs. The PCPs used on the Illinois Tollway were 2 ½ inches thick and laid in a thin mortar bed on the beams. A 5-inch thick topping slab was cast on top of the PCPs (Bender, 1957). Figure 2.1 shows a cut-away drawing of the Beverly Road Bridge.

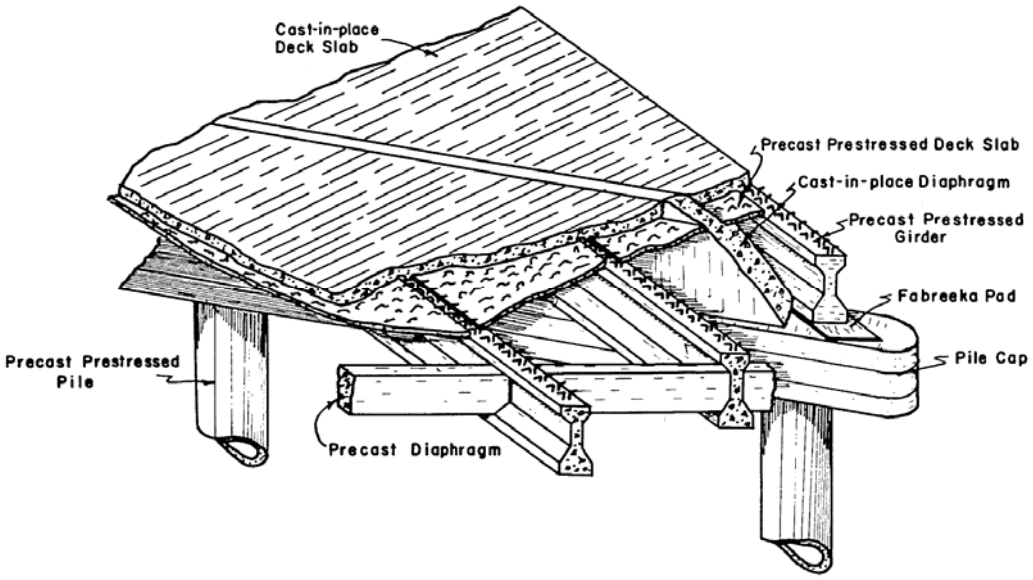

Figure 2.1: *Cutaway of Beverly Road Test Bridge (Janney & Eney, 1957)*

The State of Texas built three bridges with PCPs that were open to traffic in 1963. The Texas Highway Department field tested two of these bridges several months after they were in service (Texas Highway Department, undated) and researchers from Texas A&M University field tested on one of these bridges seven years later (Jones & Furr, Res Rept. No.145-1, 1970). The researchers from Texas A&M University also surveyed all three bridges for cracks. Both the Texas Highway Department and the researchers from Texas A&M University concluded that the PCPs adequately distributed the load to the adjacent beams and that the panels were therefore acting compositely with the C-I-P slab. The cracking that was present was in the topping slab above the transverse butt joints between adjacent PCPs. These cracks did not extend more than halfway into the topping slab and were thus not indicative of non-composite behavior (Jones & Furr, Res Rept. No. 145-1, 1970). These early PCPs were 3-inches thick and set on a ¼-inch thick fiberboard. The PCPs were topped with a 3-inch thick cast-in-place topping slab.

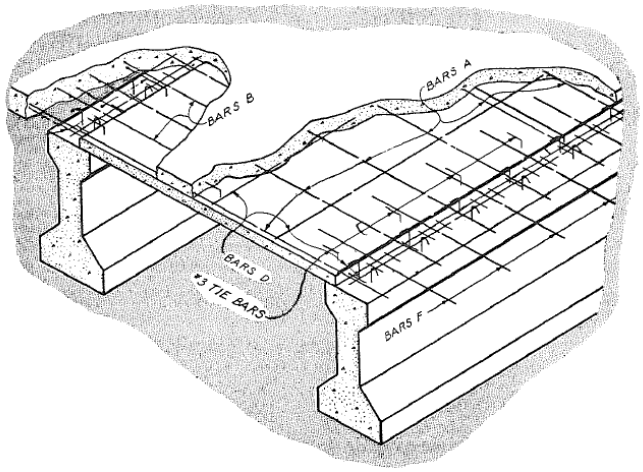

Figure 2.2: *Cutaway of First Texas Bridges with PCP (Texas Highway Department, undated)*

Further testing on small laboratory specimens demonstrated that the panel stiffness was not significantly affected by cyclic loading (Jones & Furr, Res Rept. No. 145-2, 1970). Adding interface reinforcement between the PCPs and the C-I-P topping did not improve the service performance of the system (Buth, Furr, & Jones, 1972) but mildly improved the deflections after millions of cycles of loading at twice the design load (Furr & Ingram, 1972).

Full-scale testing of laboratory-built bridge spans resulted in determining the failure mode of the composite PCP and C-I-P slab was punching shear and the PCP to C-I-P slab interface did not show any distress under the cyclic loading (Buth, Furr, & Jones, 1972). Adding dowels across the butt joints between the panels did not improve the live load transfer between adjacent PCPs (Buth, Furr, & Jones, 1972). Cracks in the C-I-P topping at these butt joints did not affect the performance and were likely caused by thermal shrinkage (Buth, Furr, & Jones, 1972). Removing the pre-stressing strand extension beyond the end of the panel into the gap between the panels above the girders

does not negatively affect the local or global behavior of the composite PCP and C-I-P deck (Bieschke & Klingner, 1982).

Decks built with PCPs were found to be stiffer, stronger, and more crack resistant than fully C-I-P decks (Tsui, Burns, & Klingner, 1986). Both the fully C-I-P decks and the composite PCP and C-I-P decks failed in punching shear, with capacities higher than those predicted using the existing ACI and AASHTO provisions (Tsui, Burns, & Klingner, 1986). The out-of-plane loading causes in-plane membrane forces, or "arching action," due to the restraint provided by the girders; these forces have a negligible effect on the response of the panels prior to cracking but substantially improved the flexural capacity of the slab after the slab had cracked (Fang, Worley, Burns, & Klingner, 1990).

More recent research has focused on quantifying the capacity of a slab constructed with PCPs and a C-I-P topping. Mander et al (2011) from Texas A&M University were able to predict the failure load of test specimens subjected to a tandem load by adding the contributions of the punching shear capacity of the cast-in-place topping and the flexural capacity of the PCP. Kwon (2012) calculated the capacity of the slab taking advantage of the membrane forces which cause arching action and found the reinforcing in the PCP/CIP slab to be conservative; the reinforcement in the C-I-P topping could be reduced.

2.2.2 In-Plane Shear Behavior of Concrete

The in-plane behavior of PCPs has not been the subject of past research because they are predominantly loaded out-of-plane. Literature on the in-plane shear behavior of reinforced concrete shear walls can lend insight to the in-plane behavior of PCPs even though the dimensions and thicknesses differ from the typical PCP.

The Modified Compression Field Theory (MCFT) was developed to predict the shear behavior of reinforced concrete panels subject to combined in-plane shear stress and biaxial normal stresses (Vecchio, 1981). The MCFT assumes the stress and strain fields for the concrete are coincident, the average strain in the panel is equal to the average strain in the reinforcement and the concrete, and the average stress in the panel is the average stress in the reinforcement plus the average stress in the concrete. The model for the reinforcing behavior is elastic-perfectly plastic, with the maximum stress equal to the yield strength. The concrete model includes compression softening and tension stiffening of cracked concrete. The MCFT is only appropriate to use on members with sufficient reinforcing for crack control; it does not adequately model the behavior for members with a shear response governed by a single dominant crack.

The Disturbed Stress Field Model (DSFM) modifies the original MCFT to increase the accuracy of the model where the MCFT was known to be lacking (Vecchio F. J., 2000; Vecchio F. J., 2001) . The DSFM assumes the stress and strain fields for the concrete are not coincident. The DSFM considers the local conditions at crack; shear crack slip is checked. The DSFM uses a modified compression softening model that more closely matched observed behavior.

The Continuum Strong Discontinuity Approach (CSDA) was developed to predict the post-cracking behavior of reinforced concrete (Oliver et al, 2008). The CSDA uses mixture theory to create a continuum composite model that is used in a finite element approach. The composite element is composed of a matrix representing the concrete and two orthogonal fibers representing the reinforcement. This composite model accounts for the failure of the concrete, the failure of the rebar, the effects of rebar bond and slip, and dowel action of the rebar. By incorporating all of these behaviors in the composite model instead of modeling these effects directly, the finite element analysis is simplified.

Gérin and Adebar presented a "simple rational model" for reinforced concrete that can be used to predict the force-deformation response of a shear wall that is cyclically loaded (Gérin & Adebar, 2009). This model treats the strain in the cracks separately from the concrete between the cracks which allows the orientation of the principal strain and the principal stresses to be in different directions. It allows average tensile strains at the same time there are compressive concrete stresses, this allows the model to capture the effects of load reversal.

2.3 CURRENT PRACTICE

On most straight beam bridges the contractor has the option of using PCPs, PMDFs, or conventional plywood forming to construct the slab. PCPs are prohibited in cases where the top flange is too narrow, where a traffic rail is founded in the bay, where the bay is adjacent to a phased construction joint, and on curved bridges. When the top flange is too narrow, as in the case of some rolled steel I-beams, there is not enough room to attach shear studs between the edges of the panels. A traffic rail typically requires anchor bars that lap with the bottom slab reinforcement; in this case the bay needs to have bottom reinforcement and therefore PCPs are not allowed. The prohibition of PCPs on curved bridges is due to concerns about the girder deformations from torsional loads and the absence of a positive connection between the panel and the girders. Because of the absence of past studies demonstrating suitable behavior of the panels in curved girder applications, the PCPs are disallowed in these applications. In curved bridge applications there is the potential for complex interaction of the slab and girders as the girders are subjected to a significant amount of torsion as well as additional shear and moment. The slab acts as a diaphragm that distributes the vertical displacement across the cross section and limits the torsional movement of the top flange of the beam.

2.3.1 PCP Details

The PCPs used in TxDOT bridges are reinforced concrete panels 4 inches deep. The minimum 28-day compressive strength, f_c', is 5000 psi. The typical square panel is shown in Figure 2.3; the cross-section is shown in Figure 2.4. The typical panel is 8 feet long; the width of the panel varies depending on the spacing of the girders the PCP sits on, the top flange width of the girders, and the width of the bedding strip the panel sits on.

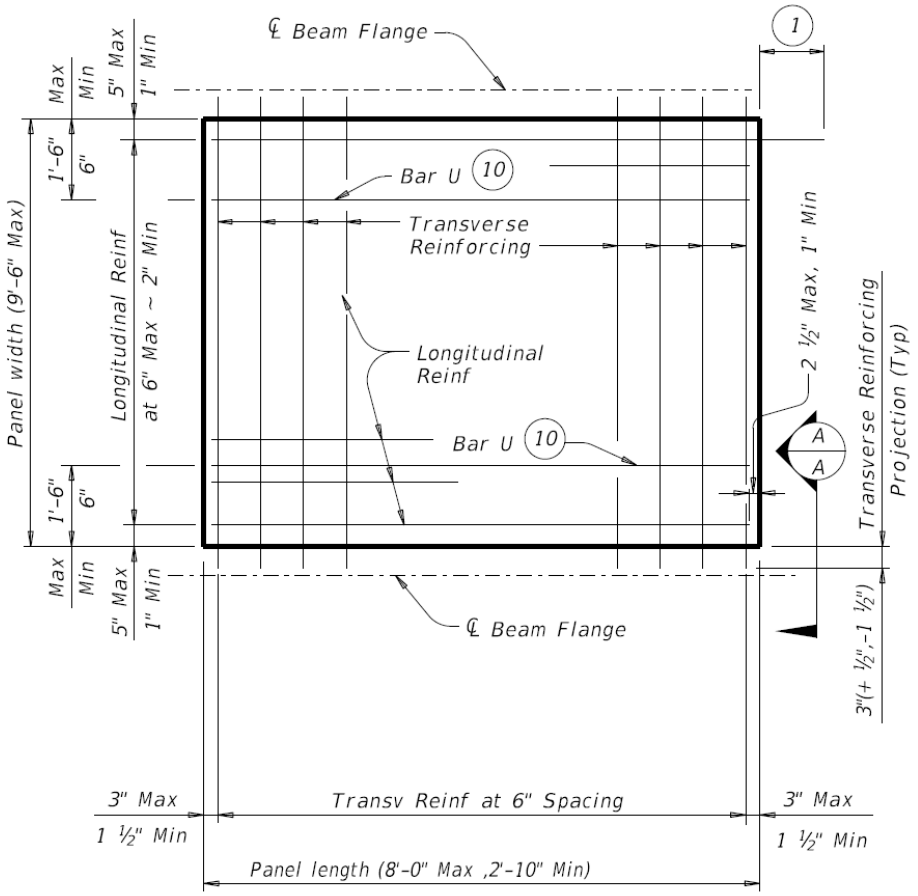

Figure 2.3: *Plan View of PCP (TxDOT, PCP-FAB, 2015)*

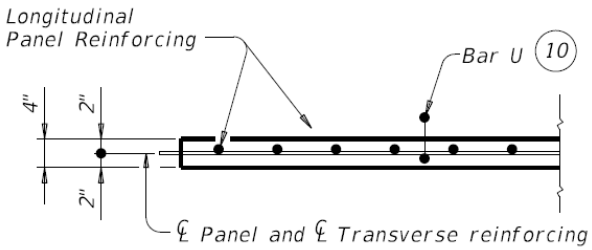

Figure 2.4: *Partial Cross-Section of PCP (TxDOT, PCP-FAB, 2015)*

The transverse reinforcement runs perpendicular to the beams that support the edge of the PCP. For panels with a width greater than 5 feet, this reinforcement is prestressed strand. It can be either ⅜-inch or ½-inch diameter grade 270 kip low-lax pre-stressing strand with each strand stressed to 14.4 kips. For panels with a width 5 feet or less but greater than 3'-6", the transverse reinforcement can either be pre-stressing strand or No. 4 grade 60 ksi reinforcing bars. For panels with a width 3'-6" or less, the transverse reinforcement is No. 4 grade 60 ksi reinforcing bars. The transverse reinforcement is placed at the center of the cross-section and extends 3 inches beyond the end of the PCP.

The longitudinal reinforcement runs parallel to the beams that support the PCPs. Panels can use No. 3 grade 60 ksi reinforcing bars spaced at a maximum of 6 inches, ⅜-inch diameter pre-stressing strand spaced at a maximum of 4 ½ inches, ½-inch diameter pre-stressing strand spaced at a maximum of 6 inches, or ASTM A1064 deformed welded wire reinforcing (WWR) providing 0.22 square inches per foot of panel. The largest wire allowed is a D11 wire; this limits the maximum spacing to 6 inches.

2.3.2 Using PCPs on Bridge Decks

In skewed bridges where the PCPs are taken to the edge of the span, a trapezoidal PCP can be used. In bridges where the PCPs are not taken to the end of the span, a

conventionally formed, full depth slab is usually cast. In some applications, permanent metal deck form sheets have been used in end regions; however the resulting aesthetics from below the bridge make this an unpopular choice.

The standard detail for placing the PCP is shown in Figure 2.5. The PCP is placed on a polystyrene board, called the bedding strip, which acts as a temporary support during construction. The bedding strips on either side of the PCP may be at different heights to account for differential camber of the adjacent beams, cross-slope of the deck, or placing the beam ends at the incorrect elevations. The PCP overhangs the bedding strip a minimum of 1 ½ inches and maintains a minimum clearance to the top of the beam of ½ inch. This clear space between the PCP and the top flange of the girder fills up with concrete grout when the slab topping is cast. The grout under the beam serves as the long-term support for the PCP.

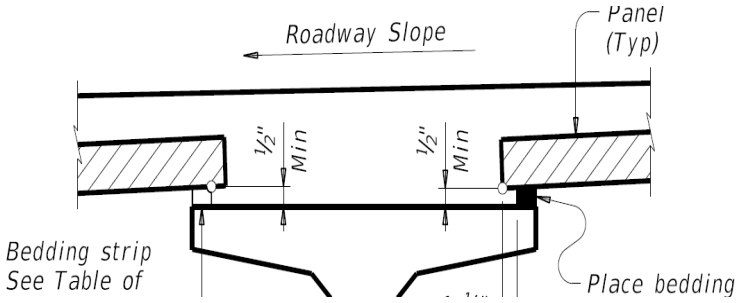

Figure 2.5: *Typical PCP to Girder Connection (TxDOT, PCP, 2015)*

The minimum width of the bedding strip is half its height, as seen in Table 2.1. The maximum height of the bedding strip is 4 inches; when more than 4 inches between the top flange and the PCP is needed, to bring the PCP to the correct elevation, a reinforced concrete leveling pad is poured on top of the beam, the full width of the beam as seen in Figure 2.6. This allows the use of shorter bedding strips.

Table 2.1: *Bedding Strip Dimensions (TxDOT, PCP, 2014)*

Width	Height	
	Min	Max
1" (Min)	½"	2"
1 ¼"	½"	2 ½"
1 ½"	½"	3"
1 ¾"	½"	3 ½"
2" (Max)	½"	4"

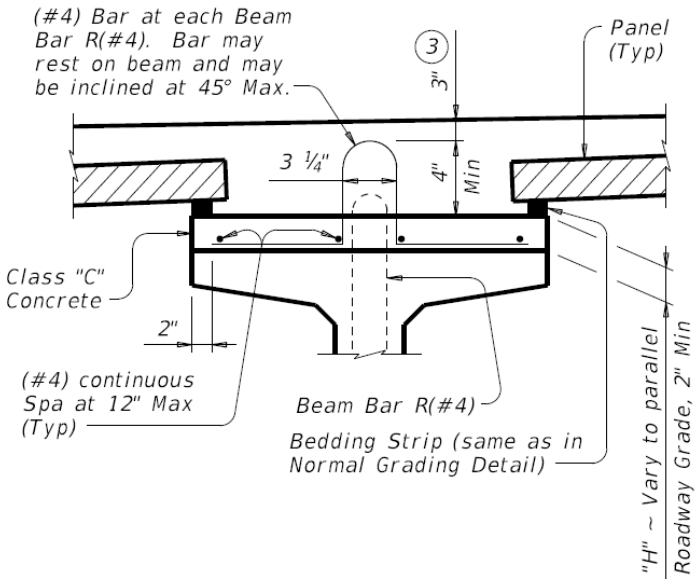

Figure 2.6: *PCP to Girder Connection with Excess Haunch (TxDOT, PCP, 2015)*

2.3.3 PCP Limitations

When the full width of the bridge is not constructed at the same time, longitudinal construction joints are present in the deck. TxDOT limits the clearance between the longitudinal construction joint and the PCP to a minimum of 3 inches, as shown in Figure 2.7.

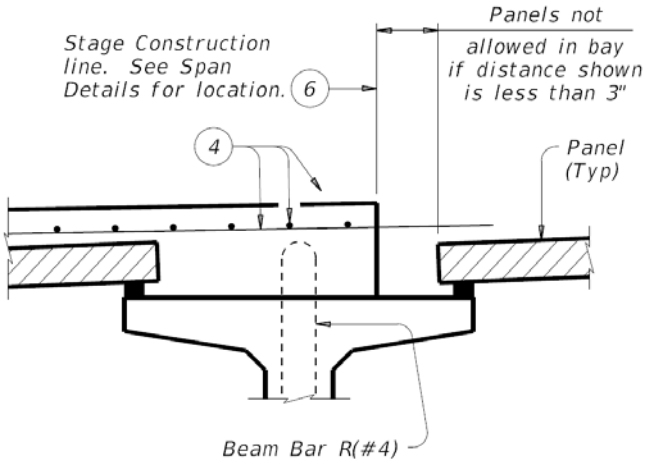

Figure 2.7: *PCP at a Phased Construction Joint (TxDOT, PCP, 2015)*

In widenings, PCPs are typically disallowed in the bay adjacent to the original structure because there is typically not sufficient room to set the PCP properly (Merrill, 2002).

Steel girders with top flanges less than 12 inches wide are prohibited from using PCPs because the PCP conflict with the shear studs (Merrill, 2002). The minimum clearance distance between the shear studs and a PCP is ⅝ inch (TxDOT, SGMD, 2015). PCPs are also disallowed over the tension flanges of steel beams (TxDOT, PCP, 2014).

PCPs are currently disallowed on curved steel bridges because of the complex interaction of the beams, slabs, and diaphragms (Merrill, 2002).

CHAPTER 3

Experimental Program

One of the primary goals of this study is to develop a simple and effective connection between the precast panels and the bridge girders and to measure the corresponding strength and stiffness of the PCP and its connection to in-plane shear forces. The shear characteristics of the panels are of interest since this is the primary deformational mode that is engaged if the panels are to provide bracing to a girder. The initial stage of testing was conducted to develop and evaluate different connection details between the panels and the girders. Therefore, data of interest in these tests were gathered to obtain a clear measure of the stiffness and ultimate strength of the PCP and the connections.

3.1 TEST FRAME

The test methodologies used in this research draw heavily from the work done by Currah (1993) and Eğilmez (2005) in testing the strength and stiffness of permanent metal deck forms (PMDF). The design of the test frame was based on the test frame used in Currah's research on the strength and stiffness of PMDF (1993). Because the expected strength of the PCPs is larger than the PMDF systems, the frame was designed and fabricated to withstand larger forces than the previous frames. Figure 3.1 shows a schematic of the testing frame and the corresponding deformations that were applied. As the applied frame load, P, is increased, the shear deformation, Δ, is measured. The shear strain, γ, and average shear stress, τ, can then be calculated based on the geometry of the test frame and test specimen. The two beams on the left and right of Figure 3.1 simulate the top flanges of two adjacent girders that might displace due to torsion in a curved

girder, lateral wind load, or even as a result of buckling deformations. The connection strap at the end of the frame joins the two beams and ensures that each beam experiences the same lateral deformation. The strap was adjustable so that different PCP spans could be accommodated.

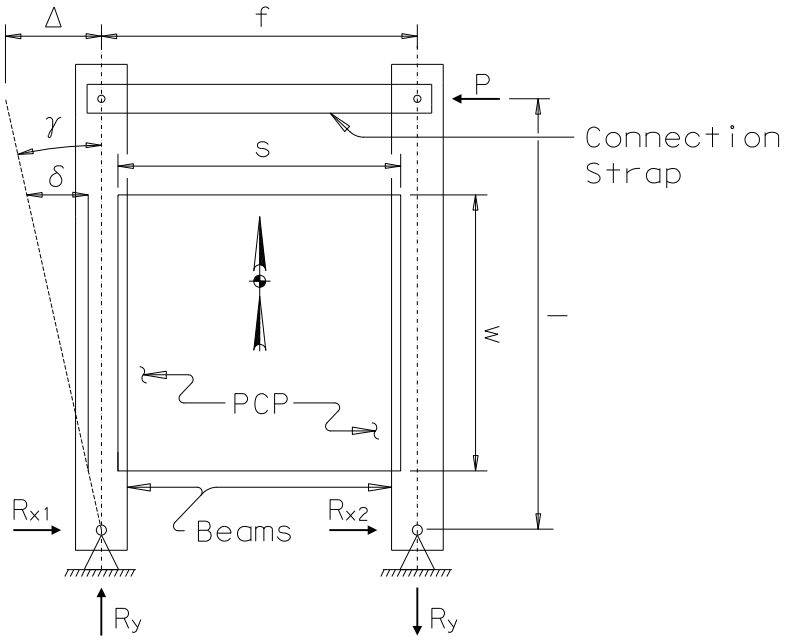

Figure 3.1: *Free Body Diagram of Test Frame*

The hydraulic actuator displaces the adjustable connection strap which moves the two beams an equal amount. The shear strain, γ, is the deflection, Δ, of the test frame divided by the distance from the deflection measurement to the fixed pins of the frame, *l*, as given in equation (3.1). The panel deformation, δ, is the deflection of the beam along the width of the panel, *w*.

$$\gamma = \frac{\Delta}{l} \qquad (3.1)$$

$$\delta = \gamma w = \frac{\Delta w}{l} \qquad (3.2)$$

Although the schematic in Figure 3.1 makes the frame appear to be relatively simple, in reality the details were more complicated due to the necessity of minimizing friction while also accommodating variable geometry to be the actual details of the testing frame are more complex. The system is internally complex, as shown by the free body diagram in Figure 3.2. The load, *P*, is applied to the east beam. The adjustable connection strap transfers a portion of the load, *F*, to the west beam. If the connection strap is sufficiently rigid the two beams will deflect the same amount.

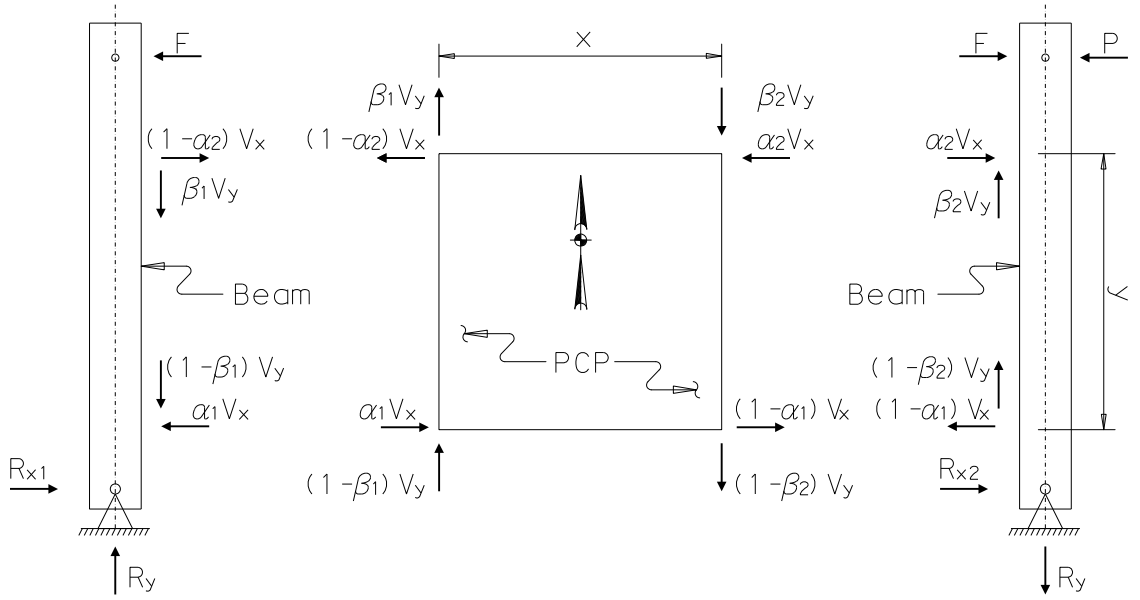

Figure 3.2: *Free Body Diagram of Beams and PCP*

Two of the PCP corners, the north-east and south-west corners, are in compression and two of the PCP corners, the north-west and south-east corners are in tension. If the PCP and its connections have the same stiffness in both compression and tension, the forces on all four corners will be the same magnitude. If the stiffness is different in compression than it is in tension, the force applied to each beam will be

different. If the compression stiffness is higher, more force will transfer to the east beam, where the lever arm to the reaction is larger. Conversely if the tensile stiffness if higher, more force will transfer to the west beam. Values of α_1, α_2, β_1, and β_2 are dependent on the relative stiffness of the panel and its connections in tension and compression.

The shear force on the PCP along the edge attached to the beam, V_y, is equal to the reaction force at the reaction block, R_y, which can be calculated from the equations of equilibrium; the equation for V_y is expressed by equation (3.3). The average shear force on the PCP along the edge attached to the beam, S_{avgY}, is expressed in equation (3.4). The effective shear modulus, G', can be expressed as the average shear stress divided by the shear strain. Substituting in equation (3.2) and (3.4), the effective shear modulus can be expressed as shown in equation (3.5).

$$V_y = \frac{P\,l}{f} \tag{3.3}$$

$$S_{avgY} = \frac{V_y}{w} = \frac{P\,l}{f\,w} \tag{3.4}$$

$$G' = \frac{S_{avgY}}{\gamma} = \frac{P\,l}{f\,w\,\gamma} = \frac{V_y}{\delta} \tag{3.5}$$

where

f = frame width, between the pins

P = applied load

w = width of the PCP

The shear force on the PCP in the direction transverse to the beam, V_x, can be found by treating the PCP as a simple shear element; as employed in equation (3.6). The average shear force on the PCP along the edge transverse to the beam, S_{avgX}, is expressed in equation (3.7).

$$V_x = \frac{V_y\,x}{y} = \frac{P\,l\,x}{f\,y} \tag{3.6}$$

$$S_{avgX} = \frac{V_x}{s} = \frac{P\,l\,x}{f\,y\,s} \tag{3.7}$$

where

s = span of the PCP

x = transverse distance between connections

y = longitudinal distance between connections

The shear force provided to each beam by the PCP, V, is expressed in equation (3.8). The rigidity of the PCP, Q, is expressed in equation (3.9).

$$V = S_{avgX}\,s_d = S_{avgY}\,\frac{w\,x}{y\,s}\,s_d = G'\,\gamma\,\frac{w\,x}{y\,s}\,s_d \tag{3.8}$$

$$Q = \frac{V_x}{\gamma} = G'\,\frac{w\,x}{y\,s}\,s_d \tag{3.9}$$

where

s_d = tributary span of the PCP for each beam

By making the simplifying assumptions that s is approximately equal to x and w is approximately equal to y, the equations 3.6 to 3.9 simplify to equations 3.10 to 3.13.

$$V_x = \frac{V_y\,s}{w} = \frac{P\,l\,s}{f\,w} \tag{3.10}$$

$$S_{avgX} = \frac{V_x}{s} = \frac{P\,l}{f\,y} \tag{3.11}$$

$$V = S_{avgX}\,s_d = S_{avgY}\,s_d = G'\,\gamma\,s_d \tag{3.12}$$

$$Q = \frac{V_x}{\gamma} = G'\,s_d \tag{3.13}$$

For a typical bridge with multiple bays, it can be assumed all the PCPs in the cross-section equally share their bracing shear force with all of the girders. In this case s_d is shown in equation (3.14). For the tests in the shear test frame there is only one PCP that is shared by the two beams; in this case the expression for s_d can be simplified to equation (3.15).

$$s_d = \left(S_g - b_{ft}\right)\frac{N_b - 1}{N_b} \qquad (3.14)$$

$$s_d = \frac{s}{2} \qquad (3.15)$$

where

b_{ft} = width of the top flange of the beam

N_b = number of beams or girders in the cross-section

S_g = beam or girder spacing

3.1.1 Test Frame Fabrication

The test frame was designed to apply a shear deformation into the PCP while minimizing the deflections of the frame by providing sufficient stiffness of the beams in the plane of the applied loads. Figure 3.3 shows an isometric view of the test setup. Figure 3.4 shows a plan view of the test setup.

Figure 3.3: *Isometric View of Test Frame*

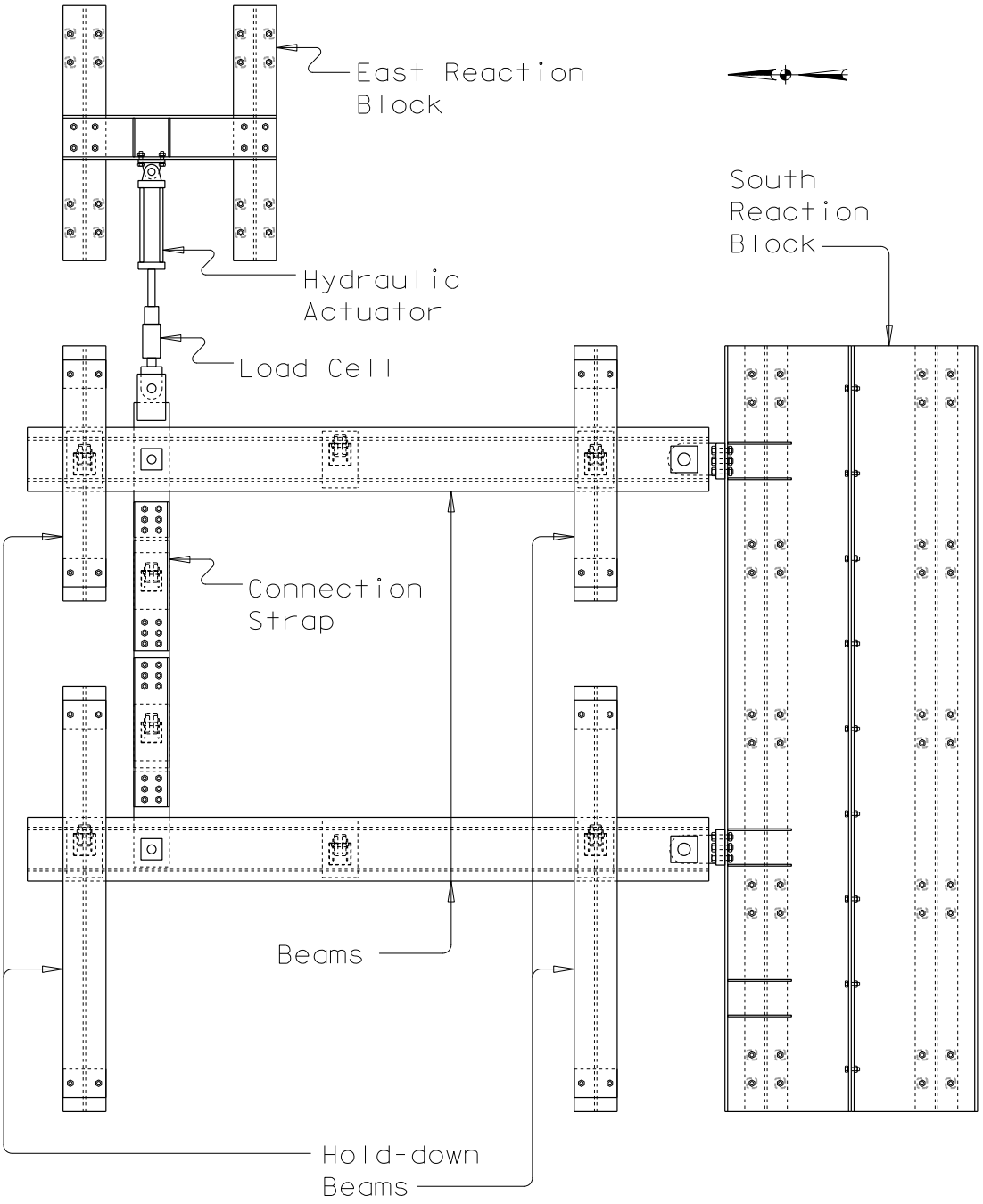

Figure 3.4: *Plan View of Test Frame*

The south reaction block is on the south side and the east reaction block is on the north-east side. Both the south reaction block and the east reaction block are anchored to the lab strong-floor via 1-inch diameter threaded rods. Forty threaded rods attach the south reaction block and sixteen threaded rods attach the east reaction block. Each threaded rod is post-tensioned to the strong-floor with a force of approximately 30 kips. The clamping force in the south reaction block is therefore approximately 1200 kips and the clamping force in the east reaction block is 420 kips. Assuming the coefficient of friction between the steel test frame components and the lab floor is 0.3, results in a lateral restraint of 360 kips in the south reaction block and 126 kips in the east reaction block. This lateral restraint is necessary to keep the reaction blocks from sliding or rotating under the applied load. A square HSS was welded between the flanges of the lower beam at each threaded bar to stiffen the flanges against the post-tensioning force.

The hydraulic actuator is mounted on the east reaction block. The hydraulic actuator is attached to the test frame with a clevis. A load cell is mounted on the hydraulic actuator to monitor the force that is applied to the frame. Pins with a diameter of 2 ½-inches were used at the corners of the frame as well as the connection to the actuator to accommodate the movements. The pins are threaded through two needle bearings that bear on the deck support beam and a 2 ½ inch plate in the adjustable connection strap. The beams are each attached to the reaction block with a 3 ½-inch pin that also was threaded through two needle bearings. To control the frame from potentially lifting up due to out of plane forces, four east-west running beams were used to clamp the frame down to the floor.

The adjustable connection strap is salvaged from Currah's (1993) test setup and is comprised of four C10x25 steel channels connected with 2 ½-inch thick plates that are 10 inches wide. The plates have bolt holes spaced at 3 inches which allows the pin-to-pin

length of the adjustable connection strap to vary from 9'-2" to 12'-8". Each of the bottom channels is supported on a heavy duty caster. The casters are pinned to a plate that is welded to the channel.

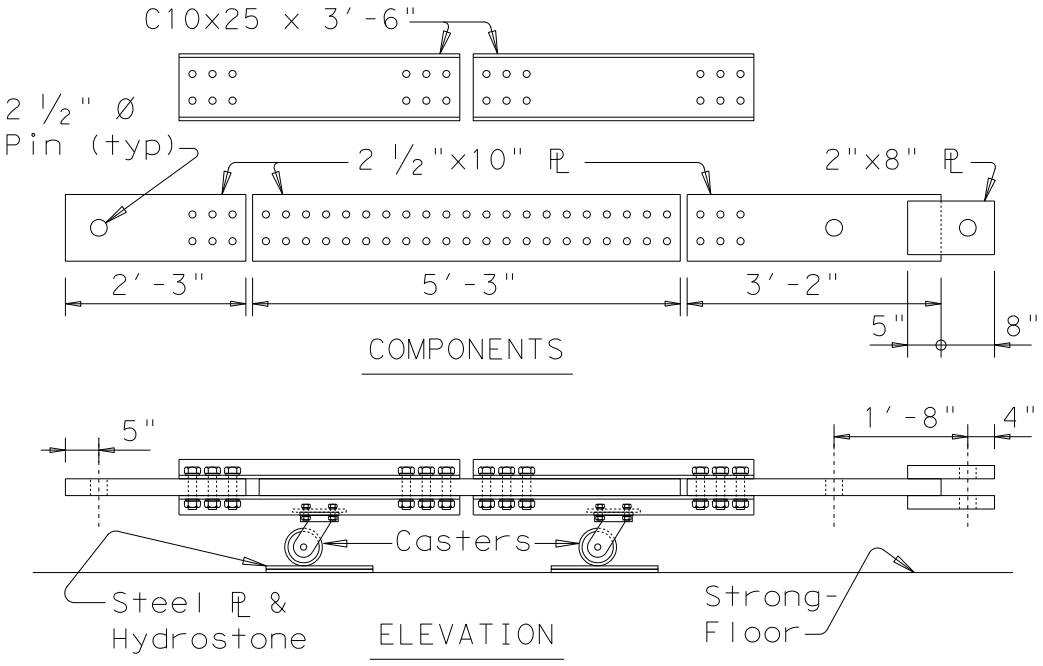

Figure 3.5: *Adjustable Connection Strap Detail*

The south reaction block is built with two 18-foot long W36x135 beams bolted together on their sides, which are supported by two W12x65 beams. The W36x135 and the W12x65 are post-tensioned to the strong floor. The W12x65 has pipe stiffeners welded to both flanges at the threaded rod locations. A clevis is attached to the reaction block where the beams frame in. Two stiffeners are welded to the W36x135 at each clevis attachment point. Two sets of stiffeners are welded to the west end of the south reaction block to allow the deck support beam to be mounted at the narrowest and widest distances that the adjustable connection strap can accommodate.

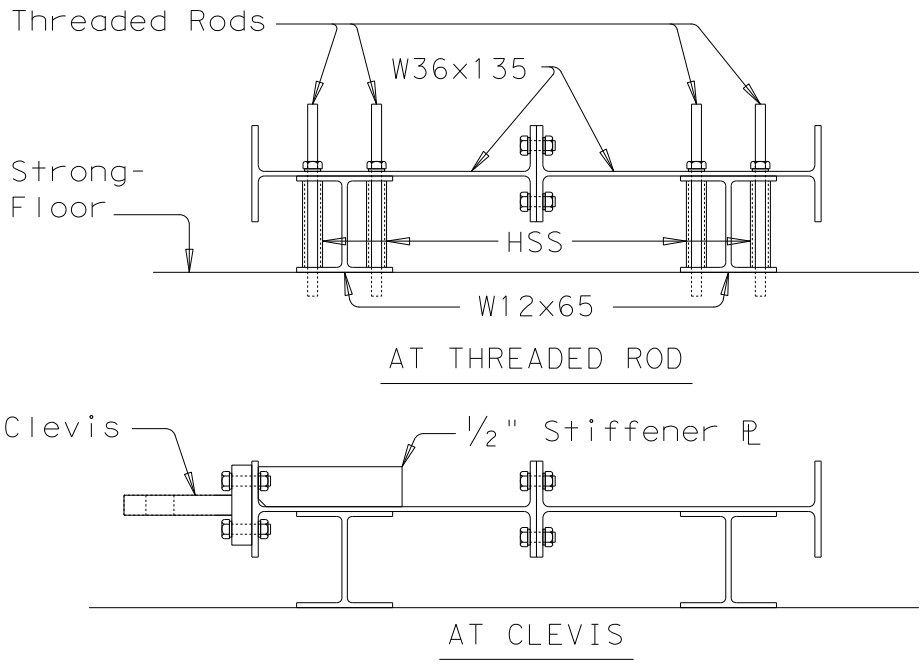

Figure 3.6: *Cross-Sections of Reaction Block*

The beams are each made of a W12x79 steel beam oriented in the weak axis configuration with a 1"x18" plate welded to the flanges of the W12x79. At the locations of the pins a ½-inch doubler plate is welded to the 1"x18" plate and a 1-inch doubler plate is welded to the web to increase the bearing area of the bearing housings. Two bearing housings were fabricated to accept the needle bearings for the pins are attached to the beam; one on the top plate and the other on the web. Steel-filled epoxy was used to fill the gap between the bearing housings and the holes in the beam. The bearing housings are bolted to the beam; the primary force transfer mechanism, however, is by bearing action through the steel filled epoxy. The beams are supported on three heavy duty casters. The casters were offset from the centerline of the beams, two in one direction, and the other in the opposite direction, to make the beams stable when not attached to the rest of the frame; this made assembling the frame easier. Access holes

were cut on the top flanges to allow the connection strap to connect to the pins. Access holes were cut on the bottom flanges to prevent the casters from hitting the flange edges.

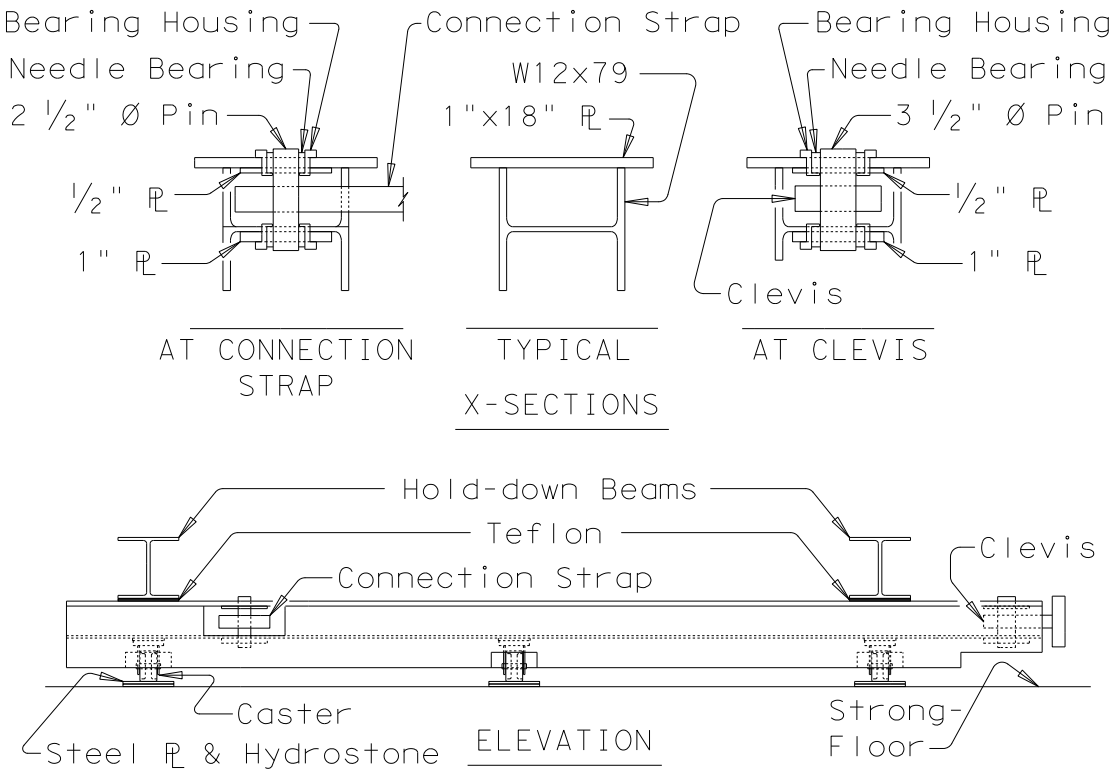

Figure 3.7: *Cross-Section and Elevation of the Beam*

The hold-down beams are fabricated from W12x65 steel beams. Teflon sheets with one side chemically etched to accommodate an epoxy adhesive to bond the Teflon to the beam and the bottom of the hold-down beam were used to reduce the friction in the system when the frame moves. Both the bottom surfaces of the tie-down beams and the top surfaces of the beams where they overlap are lined with Teflon sheets to allow easy movement of the test frame. The west hold-down beams are longer than the east hold-down beams to accommodate moving the loading beam to test a longer PCP specimen.

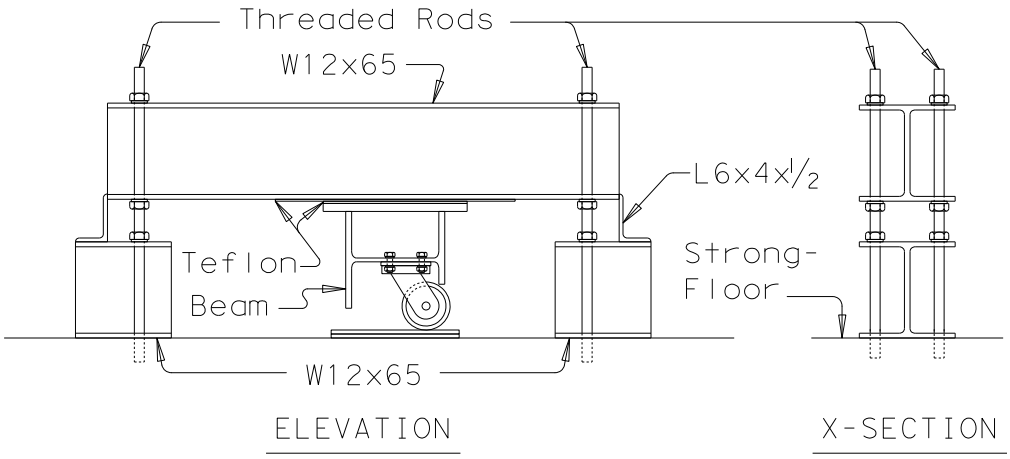

Figure 3.8: *Elevation of Hold-Down Beams and Cross-Section at Connection to Floor*

The east reaction block is constructed with two W12x65 steel beams that are post-tensioned to the strong-floor and a W12x79 that transfers the load from the hydraulic actuator to the W12x65 beams. Full depth ½-inch stiffeners are welded to the cross section on either side of where the hydraulic actuator attaches to the W12x79 transfer beam.

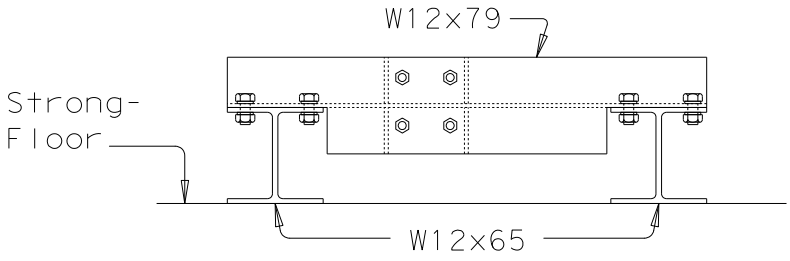

Figure 3.9: *Cross-Section of East Reaction Block*

A 100 kip Nopak double-acting hydraulic actuator with an 18-inch stroke is used to load the frame. The hydraulic actuator was installed at half stroke to allow the frame to be pushed nine inches in either direction. A variable speed hydraulic pump was used to pressure the hydraulic actuator. The hydraulic actuator is connected to the hydraulic

actuator connection block. A 100 kip Lebow load cell is attached between the hydraulic actuator and the frame to measure the force imposed.

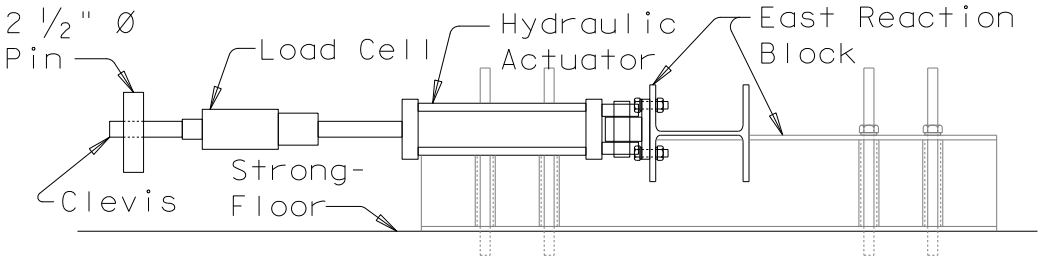

Figure 3.10: *Elevation View of Hydraulic Actuator Assembly*

3.1.2 Test Frame Assembly

To minimize the friction in the test frame, care was taken in the assembly of the test frame. First the south reaction block and the W12x65 beams of the east reaction block were assembled and post-tensioned to the floor. Then the slab support beams and adjustable connection straps were assembled. The pins and bearing housings were in place, but the bearing housings were not epoxied to the slab support beams. The hydraulic actuator assembly was attached to the frame and supported on blocks with the hydraulic actuator extended nine inches (half the stroke). The cross member of the hydraulic actuator assembly was attached to the W12x65 beams so the frame is square when the hydraulic actuator is at half stroke.

The beams were then leveled and placed on blocks. At this stage all of the casters were 1 to 1 ½ inches above the strong-floor. A ½-inch steel plate was placed under each caster and leveled using three leveling screws. Once the steel plates were touching the casters and were level in two orthogonal directions, hydrostone was cast under each plate and the bearing housings were epoxied in place. Once the hydrostone set, the blocks

were removed from the test setup and the hold-down beams were placed on top of the loading beams.

The hydraulic actuator assembly was detached from the frame so that a measure of the frictional resistance and the test frame could be obtained. Although the frame weighs in excess of 5 kips; the needle bearings, heavy duty casters, and Teflon lined surfaces significantly reduce the friction in the test setup. The frame moved with a minimal hand-applied force that was estimated at approximately 25 lbs. Due to the small force required to move the test frame, the determination was made that no correction for friction was needed when analyzing the results from the panel tests.

3.2 TEST SPECIMENS

As of the writing of this thesis, three connection details have been investigated in this research. The first connection investigated was the current connection method used by TxDOT; this is designated as the traditional method. The second connection was where the PCP is bolted to the shear studs on the top of the beam; this is designated as the shear stud connection. The third connection investigated was where the PCP has an embedded plate that is welded to a tee or angle that is then welded to the top flange of the beam; this is designated as the embedded angle connection.

All the PCPs used in this research were fabricated in-house using mild reinforcement. Typical PCPs used on bridges are prestressed in the direction spanning from beam to beam. Although subsequent tests will be carried out on prestressed panels, the use of prestressed panels was deemed impractical during the development stage of the connection methods because this would require the development of complex prestressing resources or the involvement of industry members at a very early stage in the study.

Therefore, the early tests were carried out on simple reinforced concrete panels. The results from these early studies are presented in this thesis.

All the PCPs in this research are 4-inches thick and 8-feet wide. The length of the PCPs varied based on what was necessary for the connections being tested. A summary of the tests performed is tabulated in Table 3.1.

Table 3.1: *Summary of Panel Tests*

Test Designation	Connection Type	Panel		Bedding Strip	
		Width	Length	Height	Width
1	T	8'-0"	8'-3"	2"	1"
2	T	8'-0"	8'-3"	3"	1.5"
3	T	8'-0"	8'-3"	4"	2"
4	SS	8'-0"	8'-0"	0"	~
5	EA	8'-0"	8'-3"	0"	~
6	EA	8'-0"	8'-3"	4"	2"
7	EA	8'-0"	8'-3"	2"	1"
8	EA	8'-0"	8'-3"	4"	2"

T = Traditional Connection
SS = Shear Stud Connection
EA = Embedded Angle

The concrete strengths and reinforcing schemes for the panels in Tests 4 through 8 are given in Table 3.2. The concrete strength and reinforcement information for tests 1 through 3 are not provided because the panels in these tests were not positively connected to the test frame and therefore were not engaged structurally.

Table 3.2: *Summary of Concrete Strengths and Reinforcing Details for Panel Tests*

Test Designation	Concrete Strength	Reinforcement Details		
		Transverse	Longitudinal	Strength
4	3.0 ksi	WWR 4x4 4.0		60 ksi
5	6.1 ksi	A	B	40 ksi
6	6.5 ksi	A	B	40 ksi
7	5.1 ksi	A	D	40 ksi
8	5.1 ksi	A	A	40 ksi

A = No. 4 at 6" o.c.

B = No. 4 at 6" o.c. with 3 ~ No. 4 180^{o} hooks 4" wide 8" o.c. at the edge

C = No. 4 at 6" o.c. with 6 ~ No. 4 at 4" o.c. at the edge

D = B in the NE & SW corners, C in the NW & SE corners

3.2.2 Traditional Connection

The current practice in Texas is to epoxy a bedding strip to the top flange of the beam then set the PCP on the bedding strip. When the bedding strip exceeds 2 ½ inches in height the bedding strip may also be epoxied to the bottom of the PCP. The PCPs overhang the bedding strips a minimum of 1 ½ inches. The concrete from the C-I-P topping flows under the overhang of the PCP while the deck is being cast forming a concrete ledge under the ends of the PCP. This ledge of concrete is the long-term vertical support for the PCP. The height of the bedding strip is also referred to as the haunch, or the distance from the top of the beam to the bottom soffit of the slab.

This connection does not resist in-plane shear, but it was of interest to test at what shear deformation the panels become unstable and fall. The heights and widths of the bedding strips that were tested are tabulated in Table 3.1. The internal reinforcing details and concrete strength of the PCP are not important because no in-plane force flows through the panel and therefore are not presented.

The PCP tested was eight feet wide and 8'-3" long. The bedding strip was located at the edge of the beam. Figure 3.11 and Figure 3.12 show the plan view of the test setup and cross-section of the panel to beam connection. The bedding strip ran the full width of the PCP.

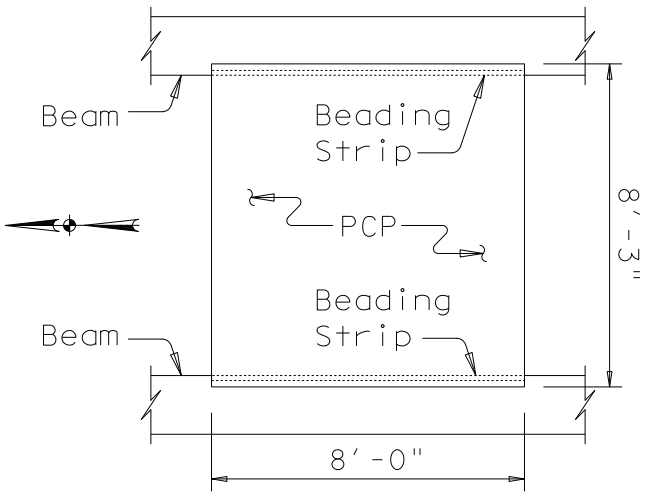

Figure 3.11: *Plan View of Traditional Connection PCP Specimen*

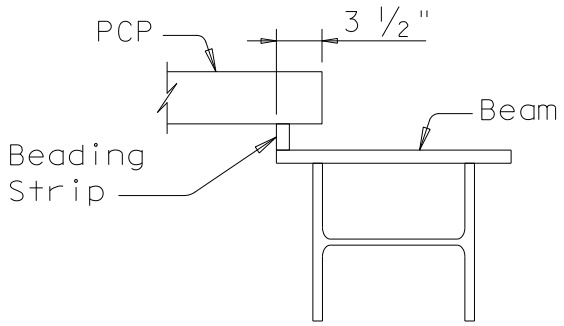

Figure 3.12: *Cross-Section of Traditional Connection PCP Specimen*

3.2.3 Shear Stud Connection

To take advantage of the shear studs on steel beams or the interface reinforcing bars on concrete beams, this connection was considered. Threaded rods were cast into the PCP. A steel channel was used to clamp the threaded rod to the shear studs by placing a U-bolt around the shear studs.

The shear studs were placed as close as they could be welded to give an upper bound stiffness of this connection. Figure 3.13 and Figure 3.14 show the plan view of the test setup and cross-section of the panel to beam connection. Figure 3.15 shows a partial elevation of the connection viewed from the edge of the beam. This PCP sits directly on the beam to establish an upper-bound estimation of the stiffness.

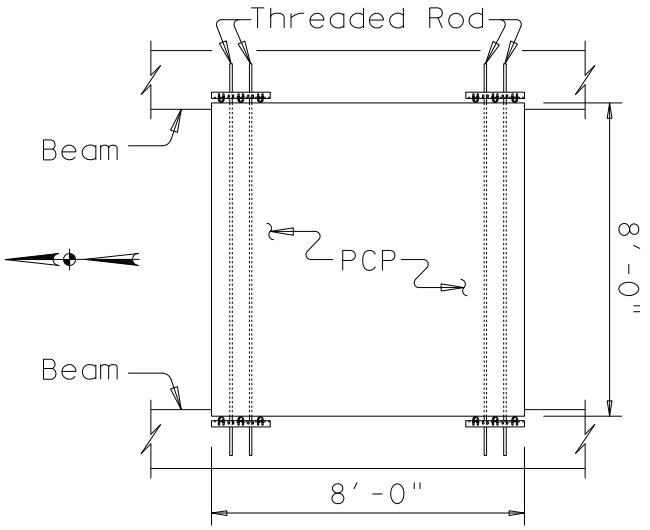

Figure 3.13: *Plan View of Shear Stud Connection PCP Specimen*

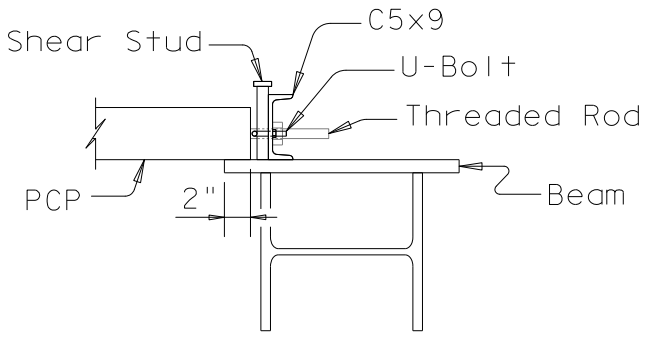

Figure 3.14: *Cross-Section of Shear Stud Connection PCP Specimen*

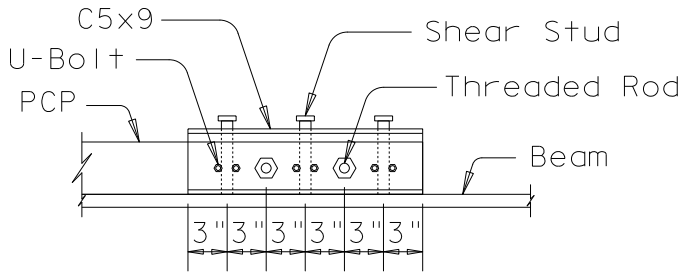

Figure 3.15: *Partial Elevation of Shear Stud Connection PCP Specimen*

The channel was threaded through the threaded rods that were embedded in the PCP and placed in contact with the shear studs. U-bolts were placed around the back side of the shear studs and threaded through the channel. The bolts and the threaded rods were secured to the channel with A490 heavy hex nuts. The bolts were tightened using the turn of the nut method. The U-bolt was a ⅜-inch diameter by ½-inch long zinc plated U-bolt. The shear studs were ⅞-inch diameter by 6 inches long.

The PCP used in this test was 8-feet long and the concrete strength at the time of testing was 3.0 ksi. The mild steel used to reinforce this PCP consisted of two layers of welded wire reinforcement. Each layer of welded wire reinforcing was made of 0.04 square inch wires spaced at 4 inches on center resulting in 0.24 square inches per foot of

reinforcing steel in each direction. This closely resembles the transverse reinforcement in the standard Texas PCPs, which consists of 0.22 square inches per foot. The welded wire reinforcement was ASTM A615, grade 60 steel. The two layers of welded wire reinforcement sandwiched the threaded rod which were positioned at mid-height of the panel. The threaded rod was ¾-inch diameter ASTM A307 Grade A Steel. The threaded rod was continuous from the connections on the east side of the panel to the connections on the west side. The reinforcing is shown in the formwork in Figure 3.16.

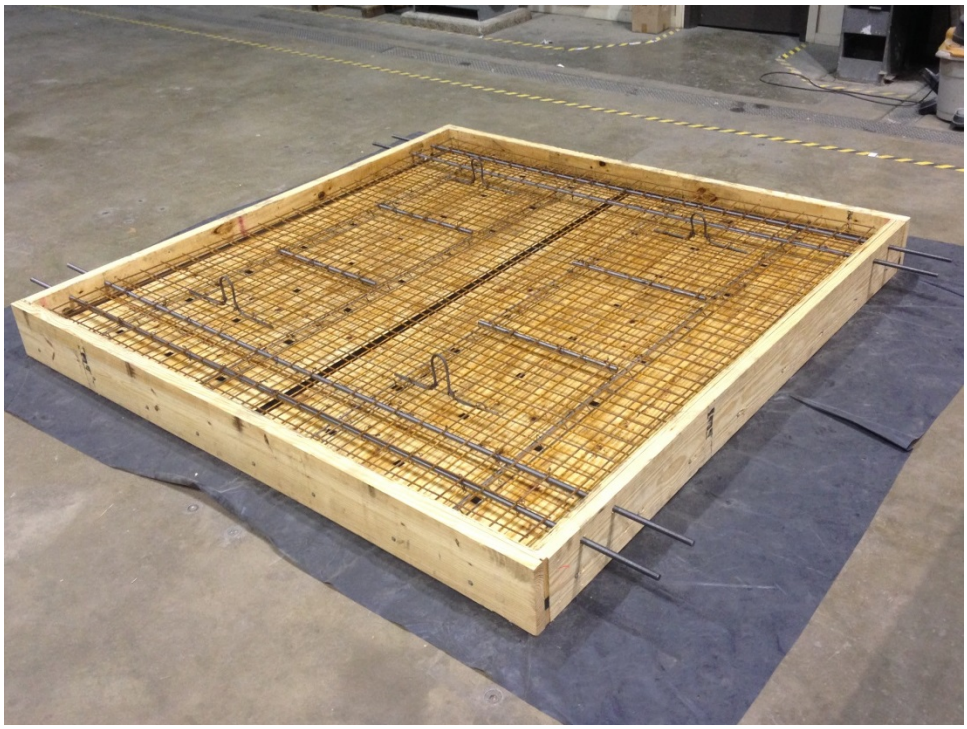

Figure 3.16: *Plan View of Reinforcement in PCP for Test 4*

3.2.4 Embedded Angle Connection

For the embedded angle connection, a steel angle welded to anchors was cast into the transverse edge of the PCP. This embedded angle was then welded to a steel shape,

designated the “connection member.” The connection member was welded to the top flange of the beam.

The PCPs tested were eight feet wide and 8’-3” long. Figure 3.17 shows the plan view of the connection. Figure 3.18 shows a partial elevation of the connection viewed from the edge of the beam.

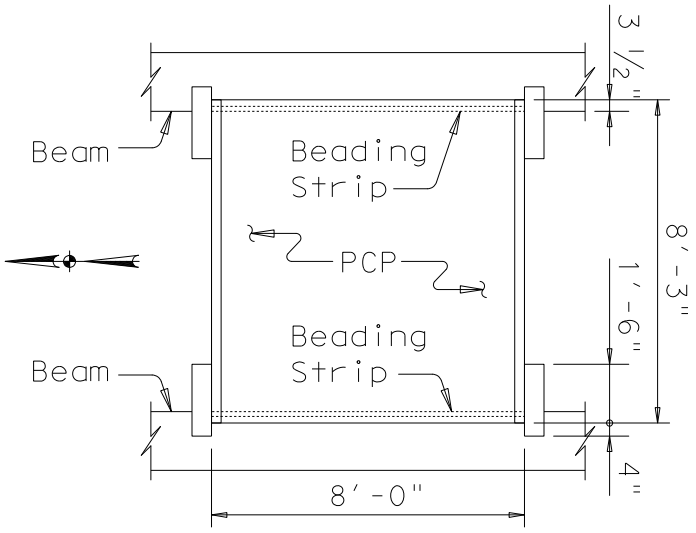

Figure 3.17: *Plan View of Embedded Angle Connection PCP Specimen*

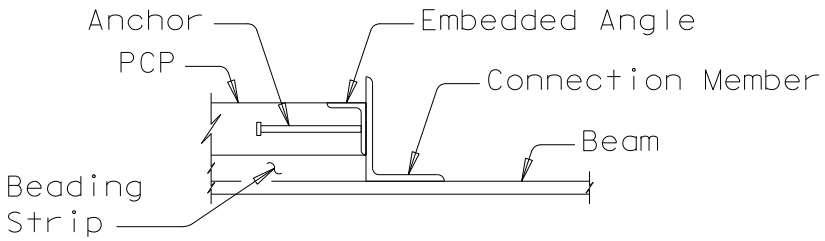

Figure 3.18: *Partial Elevation of Embedded Angle Connection PCP Specimen*

The PCP in Test 5 sat directly on the beam to get an upper-bound estimation of the stiffness. The PCPs in Tests 6 through 8 were elevated on bedding strips to allow for

a non-zero haunch. The connection member used in the tests was either an angle or a tee section. It was necessary to use an angle for the connection member with the PCP without a haunch. The longest leg commercially available on a rolled structural angle is eight inches. The eight inch leg does not protrude enough from the top of a four inch panel sitting on a four inch bedding strip to accommodate a weld to the embedded angle. Therefore, a steel tee section was used as the connection member for the PCP on a four inch bedding strip. Table 3.3 details the connection members and anchor schemes used in each corner of each test.

Table 3.3: *Embedded Angle Connection Details at Each Corner*

Test Designation	Connection Member		Anchors	
	NE & SW	NW & SE	NE & SW	NW & SE
5	L 6x6x½		A	
6	WT 9x35.5		A	
7	L 8x6x½	L 8x6x¾	A	B
8	WT 9x35.5		C	

A = 3 ½" x ½" Studs at 6" o.c. typ. with 4 ~ 8" x ½" Studs at 8" o.c. at the edge
B = 3 ½" x ½" Studs at 6" o.c. typ. with 4 ~ 3 ½" x ½" Studs at 8" o.c. at the edge
C = 6 ~ 18" x ½" deformed bars at 6" o.c. at each edge

The connection member was welded to the beam in a C-shaped weld. The embedded angle in the PCP was welded to the connection member.

The PCPs used in these tests were 8'-3" long. The mild steel used to reinforce these PCPs was No. 4 mild grade 40 reinforcement. The transverse reinforcement, spanning between the beams, for all the panels was No. 4 reinforcing bars spaced at 6 inches on center.

The longitudinal reinforcement, parallel to the beams, in Tests 5 and 6 was No. 4 reinforcing bars at 6 inches on center in the middle with three U-shaped bars spaced 8 inches on center at each edge. These legs of the U-bars were spaced 4 inches center-to-center and lapped a full lap length with the U-bars on the other side of the panel. Four ½" diameter studs, eight inches long were welded to the embedded angle so they would be placed between each U-bar. ½" diameter studs, three inches long were spaced at six inches on center between the eight-inch-long studs, falling between the longitudinal reinforcing bars. An additional No. 4 bar was placed on top of the eight-inch studs. Figure 3.19 shows the reinforcement for Tests 5 and 6. Figure 3.20 shows a closer view of the U-bars and shear studs at the edges of the PCP.

Figure 3.19: *Reinforcing in PCP for Test 5 and Test 6*

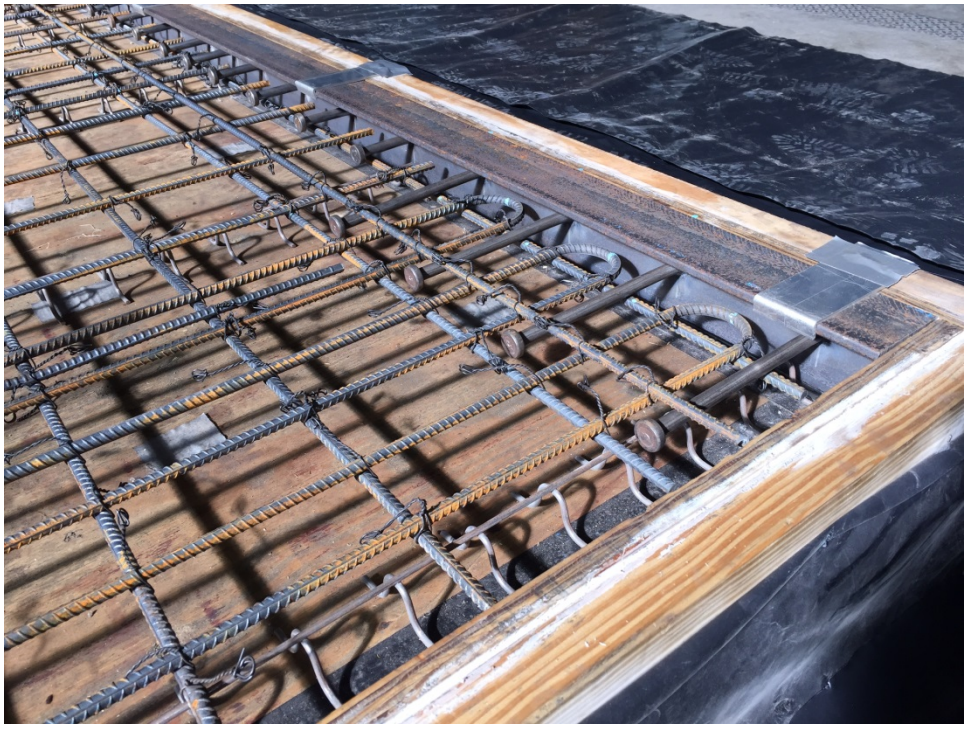

Figure 3.20: *Detail of Corner Reinforcing in PCP for Test 5 and Test 6*

Opposite diagonal corners, North-East and South-West for Test 7 had the same reinforcing as Tests 5 and 6. In the North-West and South-East corners straight No. 4 bars were used instead of the U-bars and three-inch-long studs were used instead of the eight-inch-long studs. Figure 3.21 shows the reinforcement for Test 7. Figure 3.22 shows a closer view of the reinforcement in the two types of corners.

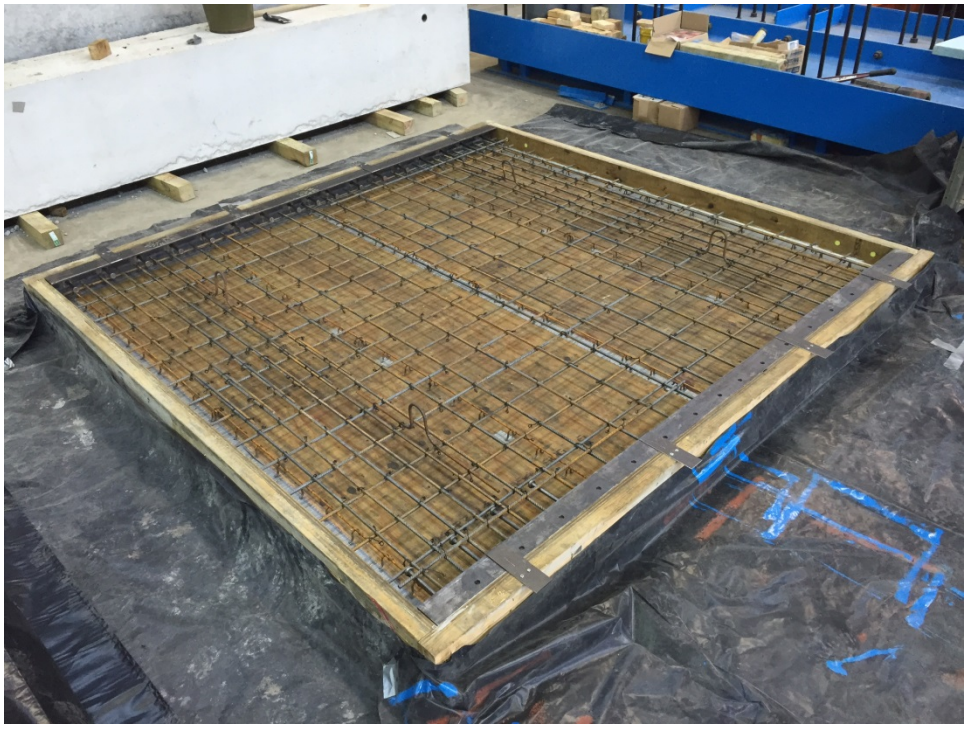

Figure 3.21: *Reinforcing in PCP for Test 7*

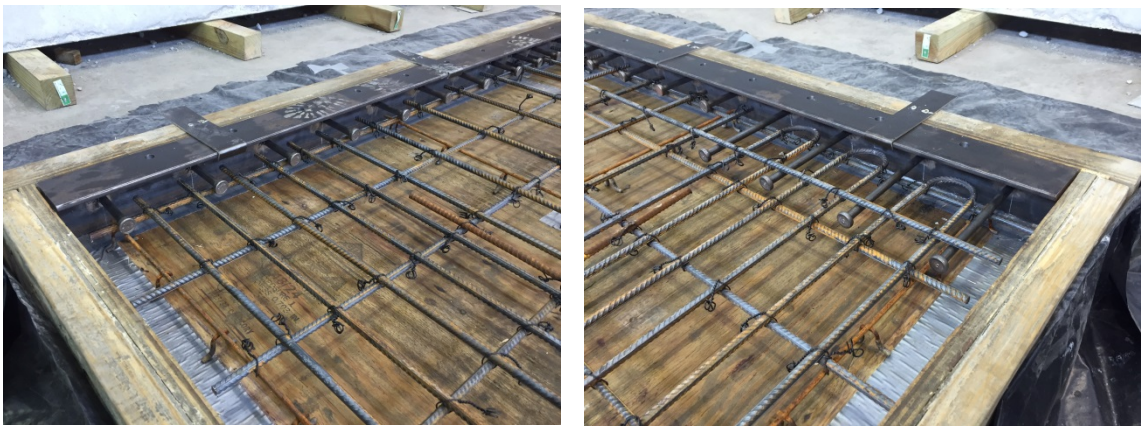

Figure 3.22: *Detail of Corner Reinforcing in PCP for Test 7 at the North-West (left) and North- East (right) Corners*

The longitudinal reinforcement in Test 8 was No. 4 reinforcing bars at 6 inches on center along the full length of the panel. Six ½"-diameter deformed anchors, eighteen

inches long were welded to the embedded angle so they would lap with the outside No. 4 bars. Figure 3.23 shows a sketch of the reinforcement used in this PCP.

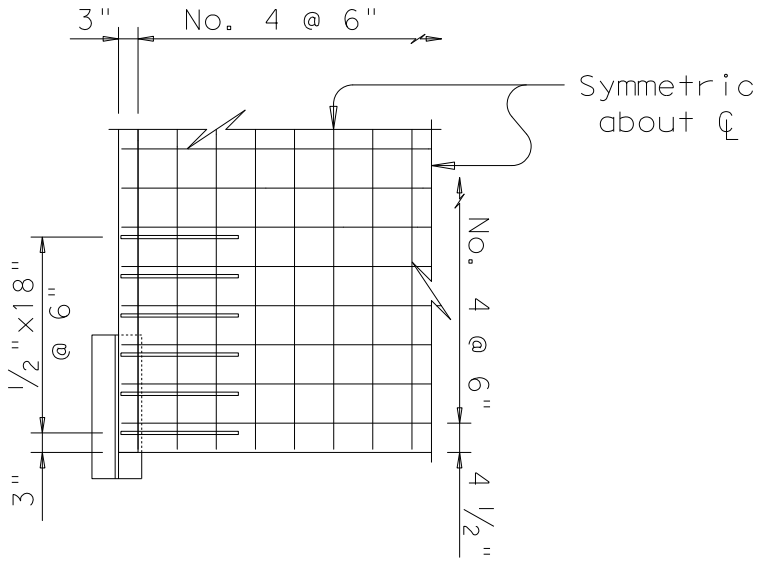

Figure 3.23: *Reinforcing in PCP for Test 8*

3.3 INSTRUMENTATION

In all the tests a load cell was used to capture the force applied by the hydraulic actuator to the connection strap. Linear potentiometers (L-pots) and string-potentiometers (S-pots) were used to capture the displacements. One-inch, two-inch, four-inch, and six-inch L-pots and ten-inch S-pots were used.

3.3.1 Instrumentation Calibration

All the linear potentiometers were calibrated using a series of calibration blocks of known length. Each block was used to displace the potentiometer's slider a known distance, and the resulting voltage output was recorded. LabView was used to capture the readings from the potentiometers.

The measured voltage output was plotted against the known displacements. A linear regression was performed on the data to calculate a linear equation for the relationship of the measured data to the displacement of the linear potentiometer. The slope of the linear equation was used as the calibration factor for processing the voltage changes of the potentiometers into displacements.

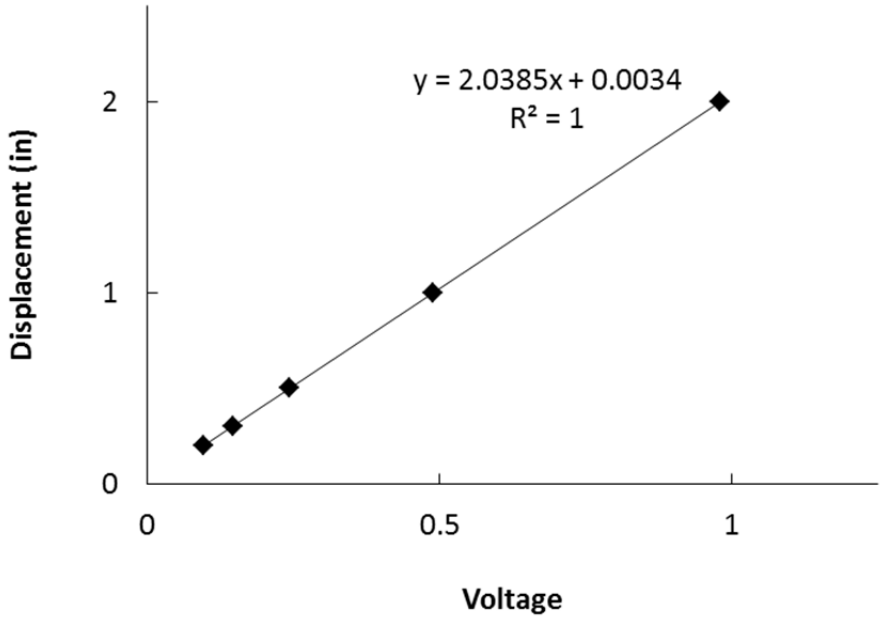

Figure 3.24: *Example L-pot Calibration Plot*

3.3.2 Instrumentation Plan

Tests 1, 2, and 3 were conducted to determine at what shear strain the PCP would drop off the bedding strips. The panel was expected to undergo large movements and drop out of plane. String potentiometers were used to capture the relative movement of the PCP to the beams. A six-inch L-pot captured the frame movement. When the frame moved in excess of six inches, the L-pot was moved and re-zeroed. A plan view of the instrumentation is shown in Figure 3.25.

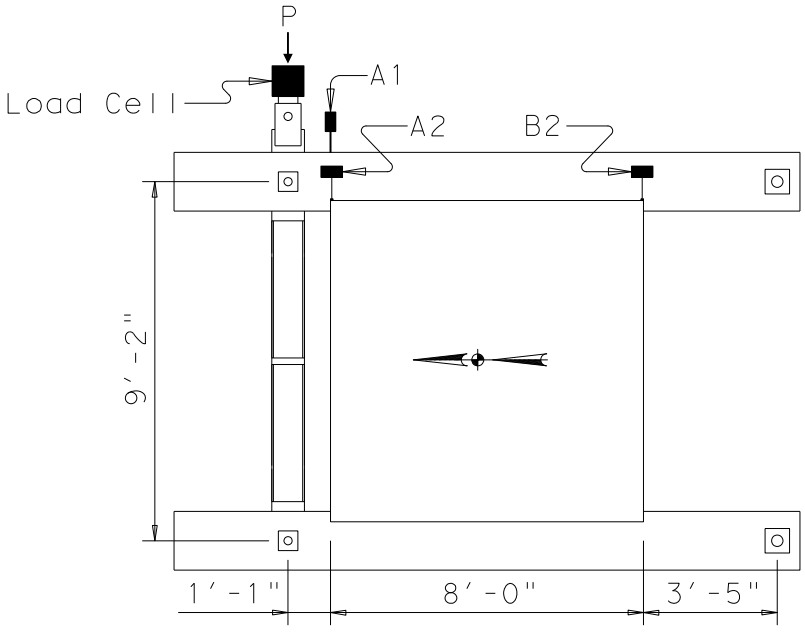

Figure 3.25: *Plan View of Instrumentation for Tests 1 through 3*

L-pot stands were fabricated for this test. Two L-pots were attached to the stand; one at the elevation of the top flange of the loading beam and one on the web of the loading beam at ten inches below the upper L-pot. This allowed the twist of the loading beams to be measured. For tests 1 thru 3 very little force was required since the PCP was not positively connected to the loading beam; the twist of the loading beam was not of any concern so only the top L-pot was monitored for these tests.

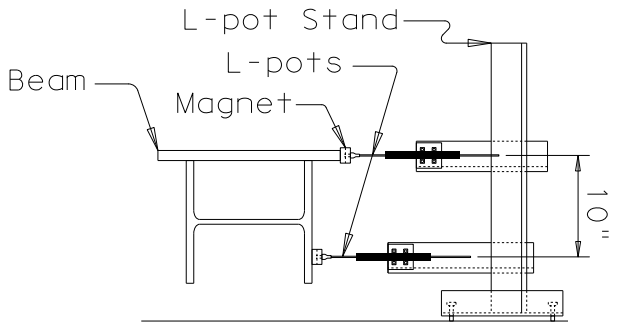

Figure 3.26: *Elevation of L-pot Stand for Frame*

The six-inch L-pots were used to capture the lateral deflection of the frame. These L-pots do not have an internal spring; to make sure the L-pots would pick up the deflections of the frame in either direction, the L-pot slider was threaded into a strong magnet that would stay attached to the steel frame. Before each test the L-pots on the stand were given a three inch extension, leveled, squared to the frame, and a spacer was used at either side of the slider to ensure they were 10 inches apart.

Figure 3.27 shows the locations, designations, and lengths of the L-pots for Test 4. Each L-pot is given a unique designation in the format "X#", where "X" is a letter that designates the corner where the L-pot is attached and "#" is a number. All L-pots with the same "X" are at the same corner. All L-pots with the same "#" measure the same displacement at the different corners. L-pot A1 refers to the specific L-pot in the North-East corner in position 1; L-pot X1 refers to the L-pots in all four corners in position 1.

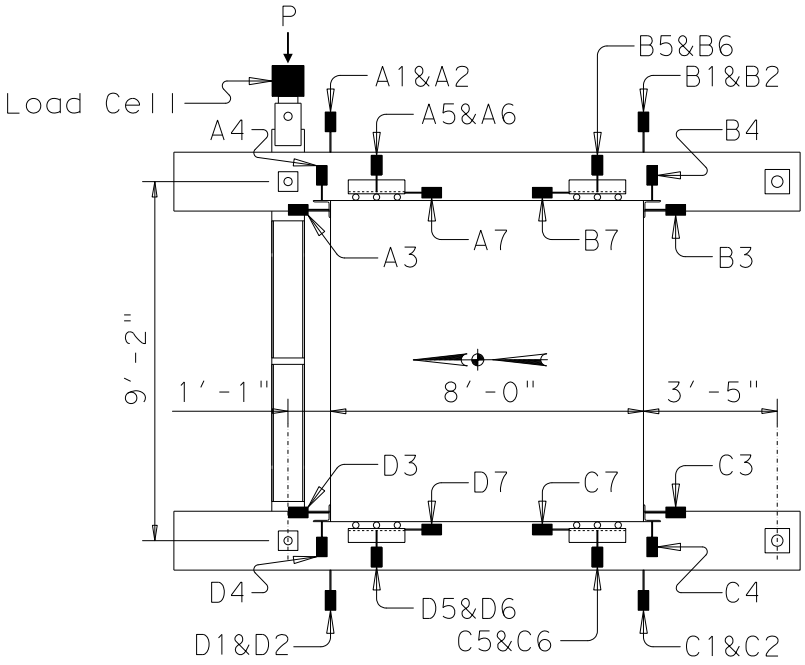

Figure 3.27: *Plan View of Instrumentation for Test 4*

Care was taken in Test 4 to ensure the test frame was adequately stiff in the plane of the applied load. The lateral deflection of the frame was measured at two points along each loading beam to capture lateral bending that might affect the measured stiffness. Two L-pots were placed at each of these locations, X1 and X2, spaced vertically ten inches from each other to measure any twist in the loading beams. The movement of the panel in the North-South direction and the East-West direction relative to the loading beam was measured by the L-pots X3 and X4, respectively. Two L-pots, X5 and X6, were placed on the channel spaced vertically 2 ½ inches to measure the East-West movement of the channel relative to the loading beam and to capture any twisting in this member. Lateral slip of the channel, in the North-South direction, was captured by L-pot X7.

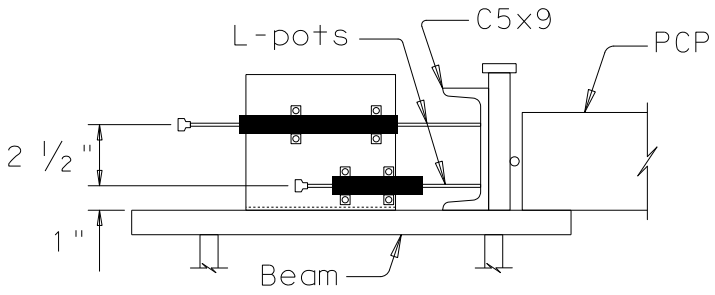

Figure 3.28: *Elevation of L-pots on Chanel for Test 4*

In Tests 5 through 8 the lateral deflection of the frame was measured at only one point along each loading beam. Two L-pots were placed at each of these locations, X4 and X5, spaced vertically ten inches from each other to measure any twist in the loading beams. The movement of the panel in the East-West direction was measured by the L-pot X3. Two L-pots, X1 and X2, were placed on the connection member spaced vertically 2 ½ inches to measure the North-South movement of the channel relative to the loading beam and to capture significant twisting in this member that might affect the accuracy of the measurements.

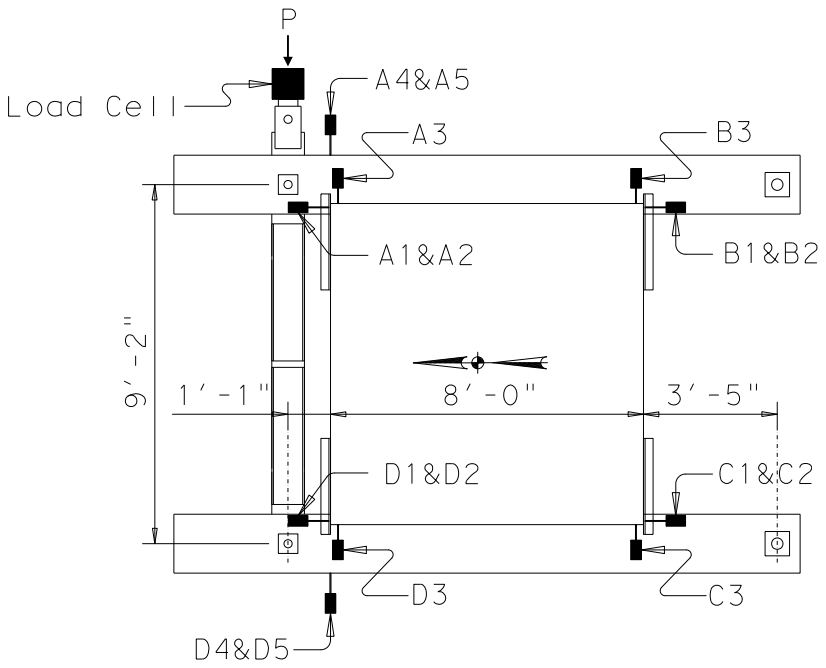

Figure 3.29: *Plan View of Instrumentation for Tests 5 through 8*

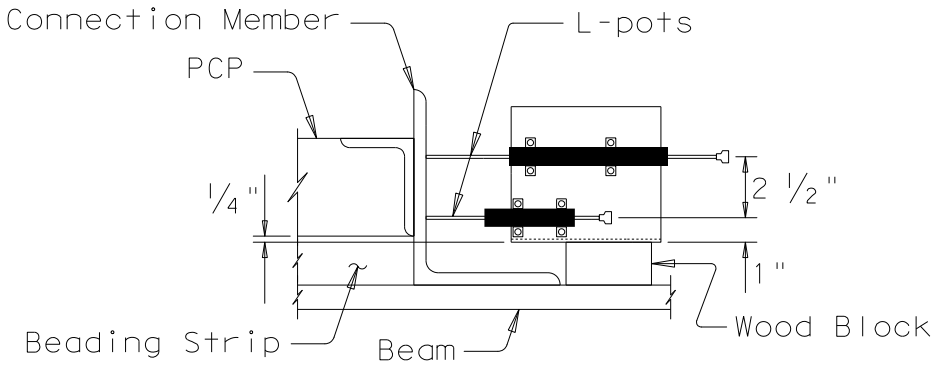

Figure 3.30: *Elevation of L-pots on Connection Member for Tests 5-8*

3.4 TEST PROCEDURE

3.4.1 Test Setup

Before running each test the specimen and the instrumentation was inspected and adjusted accordingly. The instrumentation was then checked to make sure there were no problems with the data capturing system. The setup procedure is as follows:

1. Square the test frame.
2. Install test specimen.
3. Install instrumentation.
4. Setup the configuration for the data capture system. Each data channel was identified and calibration factors for each L-pot were entered. Each pod had an excitation channel that all the L-pots and S-pots attached to that pod used. LabView was used to capture the data.
5. Zero the instrumentation.
6. Test all L-pots and S-pots. Displace each potentiometer a known amount and verify the readings are in agreement with the displacements applied. Document the direction of the positive direction.

If errors were found on one channel, that sensor was moved to a different channel. When errors were found on multiple channels in a pod, the pod was either reset or replaced. After replacing or resetting a pod, the test setup returned to step 4 and proceeded until no errors were found in the system.

3.4.2 Test 1-3 Procedure

The test procedure for Tests 1 through 3 is as follows:

1. Orient the casters to move in the west direction.
2. Zero the instrumentation. Begin recording.

3. Load the test frame by applying a displacement using the hydraulic actuator in the west direction. Load at a rate of 0.5 to 1 inch of panel displacement per minute.
4. If the L-pot measuring the frame movement approaches 5 inches, hold the displacements and reset the L-pot.
5. Re-zero the reading for the moved L-pot.
6. Continue with step 3 until ultimate capacity is reached.

3.4.3 Test 4 Procedure

The test procedure for Test 4 is as follows:

1. Orient the casters to move in the west direction.
2. Zero the instrumentation. Begin recording.
3. Load the test frame by applying a displacement using the hydraulic actuator in the west direction. Load at a rate of 0.25 to 0.50 inches of panel displacement per minute.
4. Once the displacement cycle goal is achieved, hold the displacements and mark cracks.
5. Reorient the casters in the east direction of travel.
6. Release the force in the hydraulic actuator.
7. Load the test frame in the east direction. Continue loading till the same displacement cycle goal is achieved in the opposite direction.
8. Hold the displacements and mark cracks.
9. Reorient the casters in the west direction of travel. Continue with step 3.

Table 3.4 lists the deflections at which each cycle of the test was stopped. Each displacement level was repeated twice in each direction. For example, in cycle 1 the

panel was first displaced 0.25 inches in the west direction, returned to zero inches of displacement, then displaced 0.25 inches in the east direction. Then in cycle 2 the panel was again displaced 0.25 inches in the west direction, returned to zero displacement, then displaced 0.25 inches in the east direction. The panel was only loaded to failure in the west direction.

Table 3.4: *Test 4 Cycle Goals*

Cycle Number	L-Pot A1	Panel Movement
1 & 2	0.25”	0.18”
3 & 4	0.5”	0.35”
5 & 6	0.75”	0.53”
7 & 8	1.0”	0.70”
9 & 10	1.25”	0.88”
11 & 12	1.5”	1.05”
13	To Failure	

3.4.4 Test 5-8 Procedure

The test procedure for Test 5-8 is as follows:

1. Orient the casters in the west direction of travel.
2. Zero the instrumentation. Begin recording.
3. Apply a westward displacement of the test frame by lengthening the hydraulic actuator. Load at a rate of approximately 0.10 to 0.20 inches of panel displacement per minute.
4. Once the goal loading for this cycle is achieved, hold the displacements and mark cracks.
5. Continue with step 3 until ultimate capacity is reached.
6. Hold the displacements and mark cracks.

7. Reorient the casters in the opposite direction.
8. Release the force in the hydraulic actuator.
9. Apply an eastward displacement of the test frame by shortening the hydraulic actuator.
10. Once the goal loading for this cycle is achieved, hold the displacements and mark cracks.
11. Continue with step 8 until ultimate capacity is reached.

The test was stopped at multiples of the values recorded in Table 3.5, then continued. Tests were run first in one direction, then in the opposite direction.

Table 3.5: *Test 5-8 Stopping Increments*

Test Designation	Load Cell P	Reaction V_y
5	5.0 kip	6.23 kip
6	8.03 kip	10.0 kip
7	8.03 kip	10.0 kip
8	8.03 kip	10.0 kip

3.5 SUMMARY

This chapter provided an overview of the setup that was used to obtain a measure of the shear properties of the PCPs. A summary of the basic geometry of the test frame was provided as well as an overview of the assembly method that was used to ensure a high quality testing apparatus. In addition to discussing the basic frame geometry, an overview of the specimens that were tested as part of this thesis was provided. The testing protocol that was used in each test was provided. The next chapter of this thesis focuses on the experimental results obtained in the initial testing phase of the project.

CHAPTER 4

Experimental Results

4.1 OVERVIEW

Results of the in-plane shear tests are presented in this chapter. The results that are reported include the shear deflection capacity, shear strength, shear stiffness, and the load-deflection curves.

4.1.1 Shear Deflection Capacity

For the cases in which the PCPs had traditional support methods, the panel rotated about a point close to its center, which was evidenced by observations that the deflections of the panel relative to the frame were approximately equal and opposite. The panel continued to rotate until one end of the bedding strip tipped over. The panel then shifted in one direction, as shown by the horizontal lines at the top of the graphs in Figure 4.1.

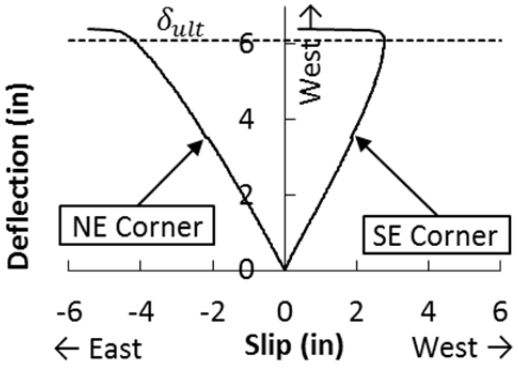

Figure 4.1: *Panel Slip vs. Panel Deflection*

The shear deflection capacity, δ_{ult}, is the maximum lateral deflection of the beams over the length of the panel with the bedding strips remaining stable. The shear

deflection capacity was calculated by plotting the slip of the panel with respect to the beam versus the lateral deflection of the beams over the length of the panel. The shear deflection capacity is the panel deflection at which one of the two corners begins to move back in the opposite direction from which it was first moving, signifying the beginning of the collapse of the bedding strip.

The panel deflection, δ, is the transverse, east-west, distance the beam racks along the eight foot panel width, as given in equation (4.1). The slip is the transverse (east-west) distance the corner of the panel moved with respect to the girder. This value was directly measured with the string potentiometers.

$$\delta = \frac{\Delta w}{l} \qquad (4.1)$$

where

Δ = frame deflection measured by L-pot A1

l = 137 inches = distance from L-pot A1 to the center of the pin at the south reaction block

w = 96 inches = width of the PCP

4.1.2 Load Deflection Curves

The load deflection curves plot the panel deflection, δ, versus the panel shear, V_y, as shown in Figure 4.2. The panel deflection is given in equation (4.1) with the exception that the frame deflection measured by averaging readings from L-pots A1, A2, D1, and D2 for Test 4 and averaging readings from L-pots A4, A5, D4, and D5 for Tests 5-8. The panel shear is given in equation (4.2).

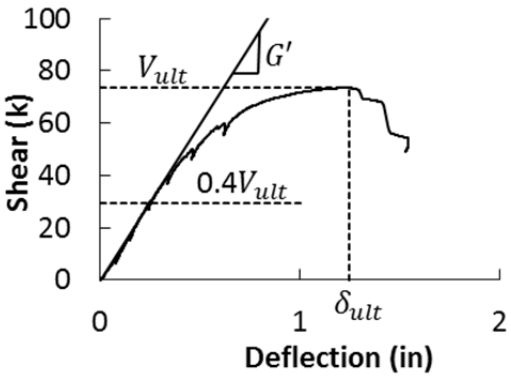

Figure 4.2: *Load Deflection Curve*

$$V_y = \frac{P\,l}{f} \qquad (4.2)$$

where

f = 110 inches = frame width, between the pins

P = applied load

Load-deflection curves were gathered for thirteen cycles in test 4; the last of which was taken to the ultimate capacity. All load deflection curves from the tests are provided in the appendix.

4.1.3 Shear Strength

The shear strength, V_u, is the maximum panel shear, V_y, the PCP resisted before it started to lose capacity.

4.1.4 Shear Stiffness

The effective shear stiffness, G', was calculated based on the tangent stiffness of the load deflection curve at 40% of the shear strength using equation (4.3).

$$G' = \frac{V_y}{\delta} \qquad (4.3)$$

In the reverse loading direction the effective shear stiffness based on the 40% of the shear strength, G'_{40}, was excessively high due to the lag that occurs where the panel

reorients itself before picking up more load. Effective shear stiffness based on the 60% of the shear strength, G'_{60}, was also calculated.

4.2 TRADITIONAL CONNECTION TEST RESULTS

The behavior of the PCP attached to the loading beam using a traditional connection and displaced laterally is depicted in Figure 4.3 through Figure 4.5. Figure 4.3 shows the connection of the panel before any displacement is applied. This figure shows the four-inch tall bedding strip; this bedding strip was epoxied to both the loading beam and the PCP. The three-inch tall bedding strip was also epoxied to both the beam and the PCP, while the two-inch bedding strip was only epoxied to the beam, not the PCP.

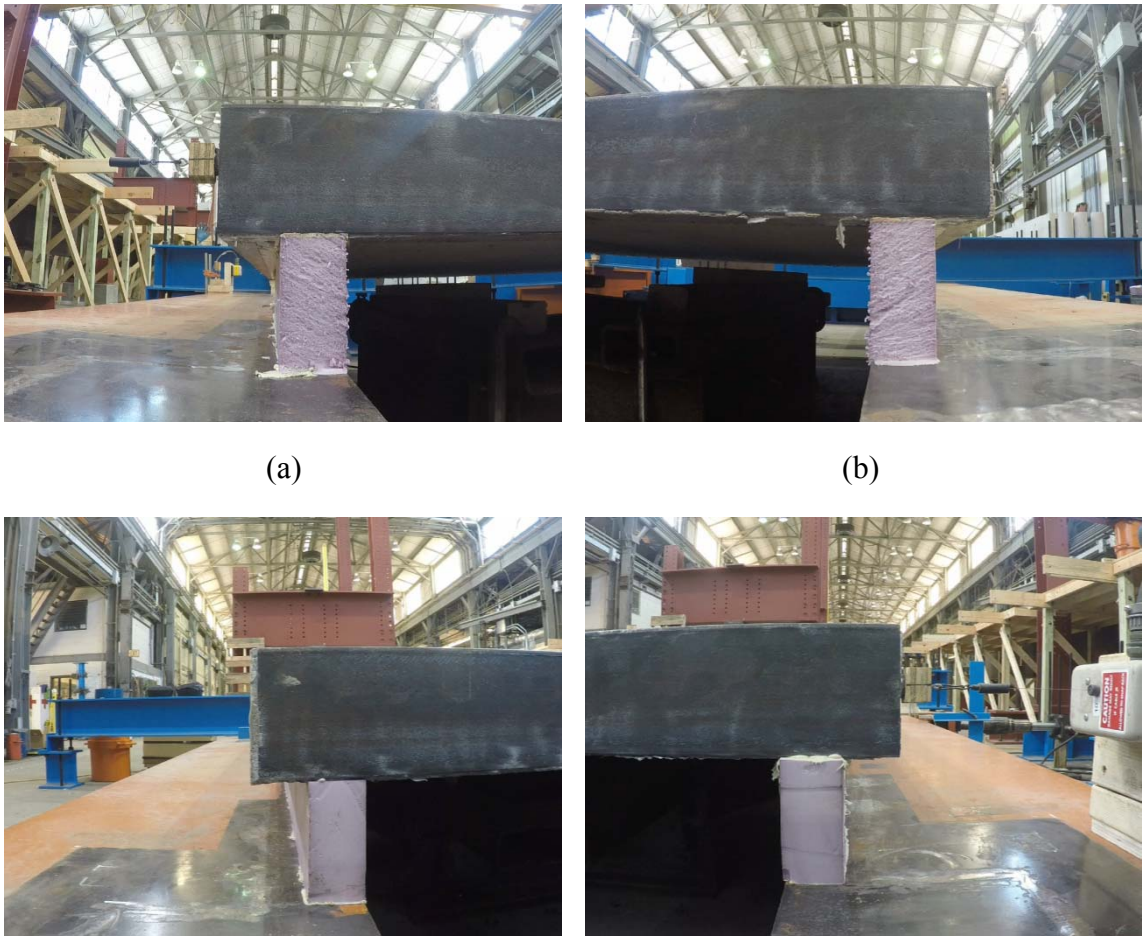

(a) (b)

(c) (d)

Figure 4.3: *PCP with a 4" Bedding Strip with 0" of Panel Movement at the North-East (a), North-West (b), South-West (c), and the South-East (d) PCP Corners*

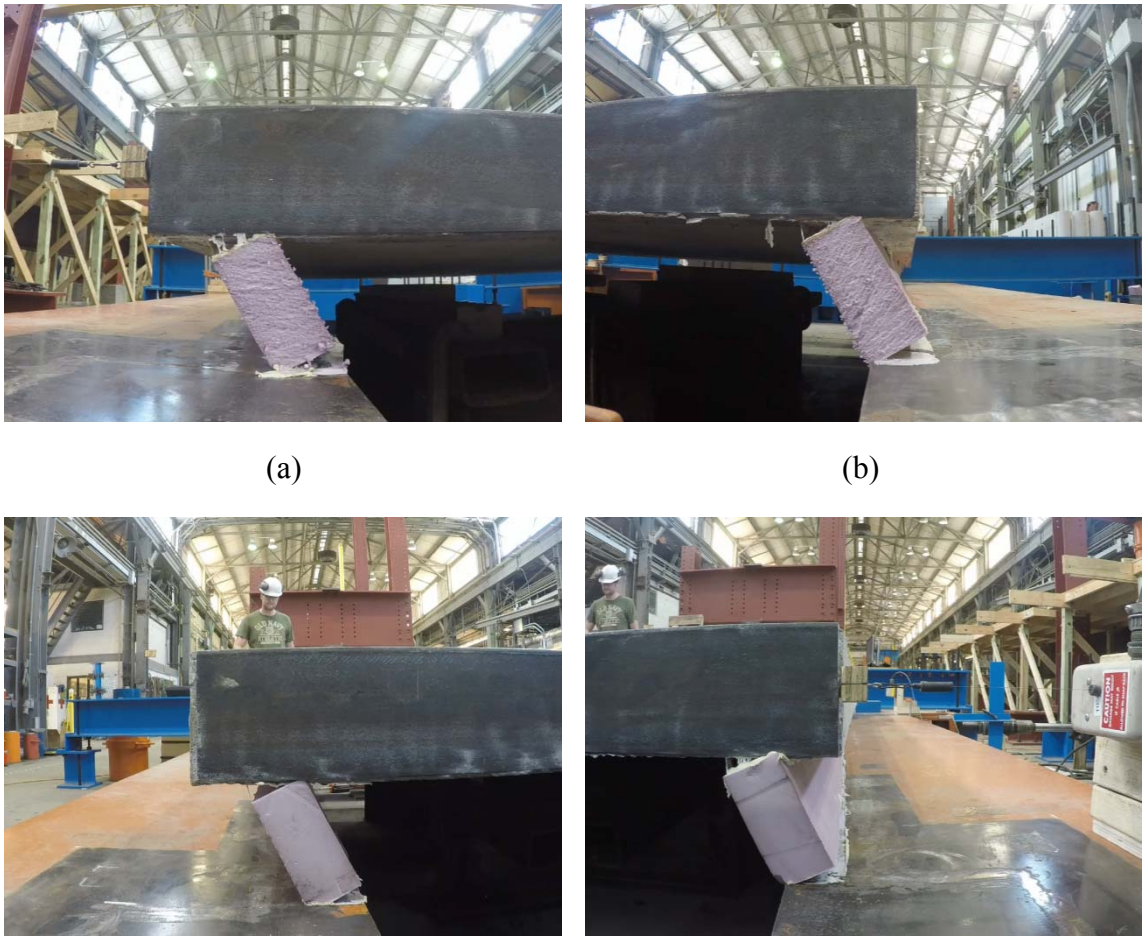

(a) (b)

(c) (d)

Figure 4.4: *PCP with a 4" Bedding Strip with 3.5" of Panel Movement at the North-East (a), North-West (b), South-West (c), and the South-East (d) PCP Corners*

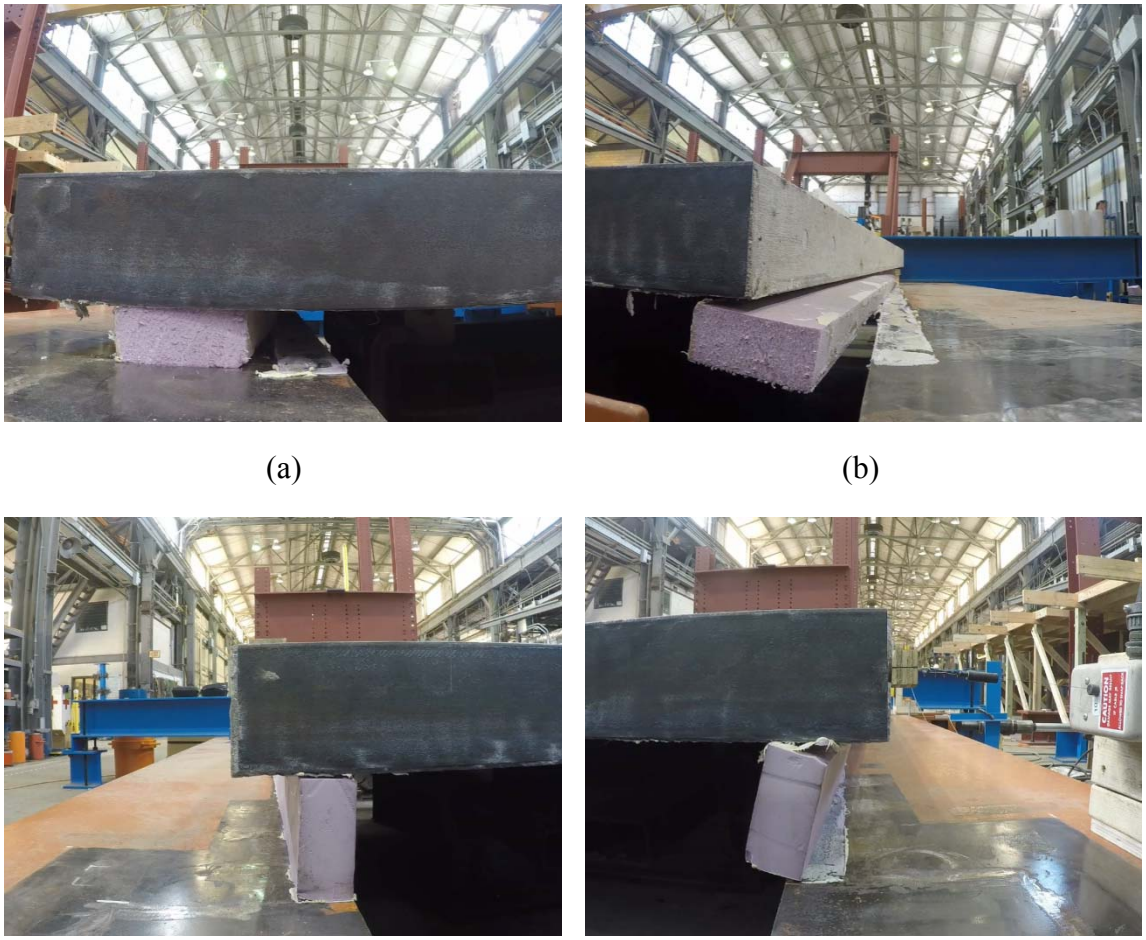

(a) (b)

(c) (d)

Figure 4.5: *PCP with a 4" Bedding Strip with 6.4" of Panel Movement at the North-East (a), North-West (b), South-West (c), and the South-East (d) PCP Corners*

As the frame was racked laterally, the panel shifted with respect to the frame. The North end of the frame racked to the East. The north corners of the panel moved east with respect to the frame and the south corners of the panel moved to the west with respect to the frame. These movements caused the bedding strip to twist under the panel, which can be seen in Figure 4.4. Figure 4.6 and Figure 4.7 show this behavior for the two-inch and three-inch tall bedding strip tests.

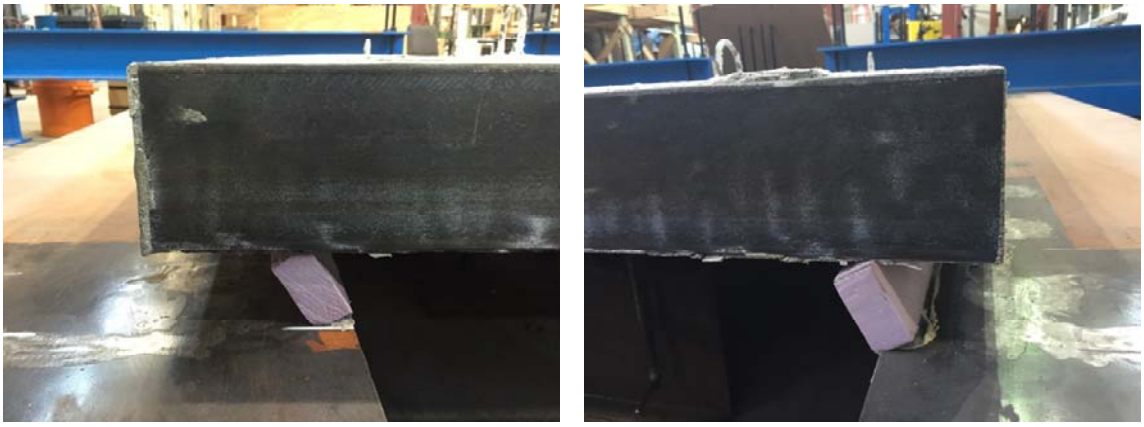

Figure 4.6: *PCP with a 2" Bedding Strip with 2" of Panel Movement at the South-West (left) and North-West (right) PCP Corners*

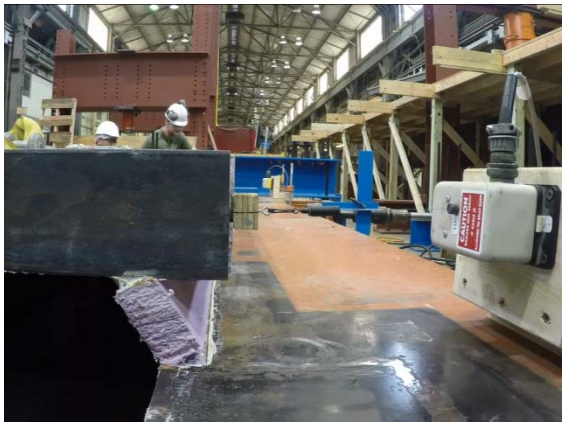

Figure 4.7: *PCP with a 3" Bedding Strip with 3" of Panel Movement at the South-East PCP Corner*

When the bedding strip reached the limit of its stability, the whole panel shifted in one direction, as seen in Figure 4.8, causing the bedding strip on one side to fall over. One of these corners fell toward the center of the girder, as seen in the right picture of Figure 4.9, and the other corner fell off the girder, as seen in the left picture of Figure 4.10.

Figure 4.8: *Isometric View of PCP with a 4” Bedding Strip with 6.4” of Panel Movement*

Figure 4.9: *PCP with a 2” Bedding Strip with 2.7” of Panel Movement at the North-West (left) and South-West (right) PCP Corners*

Figure 4.10: *Top View of PCP with a 4" Bedding Strip with 6.4" of Panel Movement at the North-West (left) and South-West (right) PCP Corners*

Slipping of the panel with respect to the beam versus the lateral deflections is graphed in Figure 4.11. The ultimate panel movement is the panel movement at which one of the two corners began to move back in the opposite direction from which it was first moving, signifying the beginning of the collapse of the bedding strip.

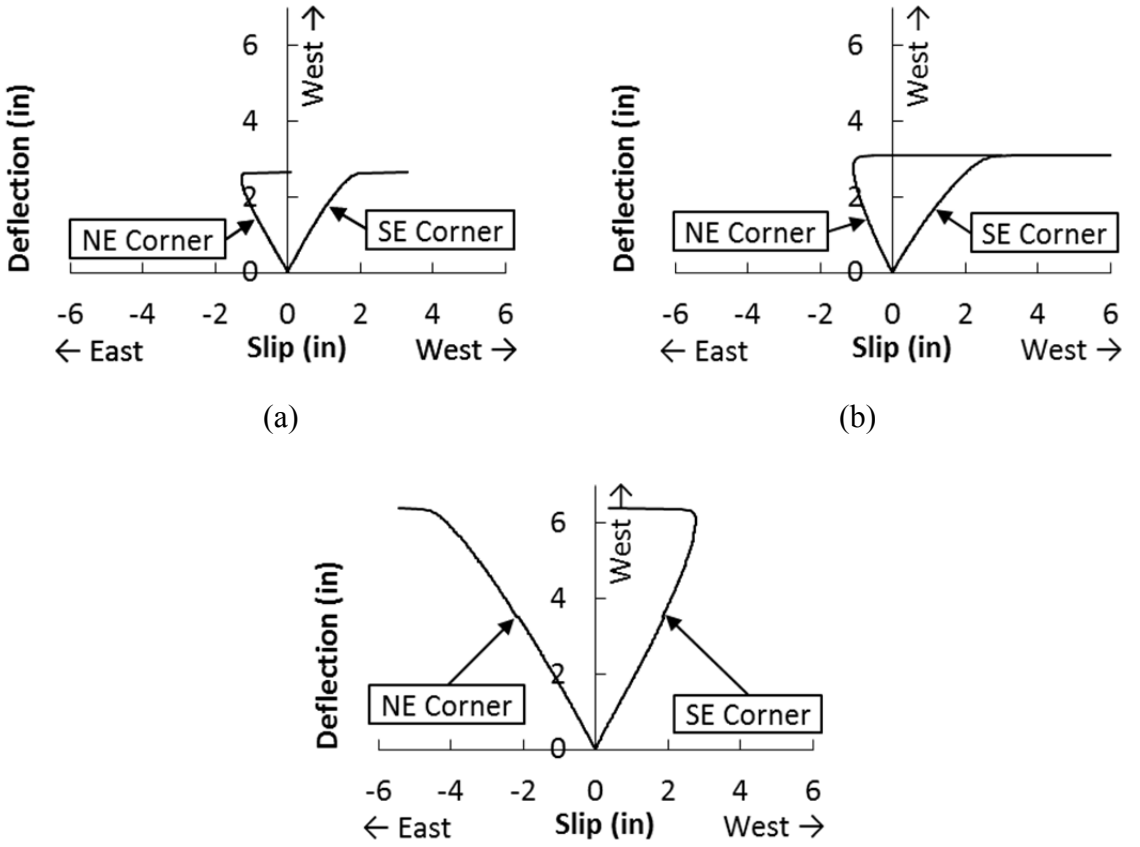

Figure 4.11: *Panel Slip vs. Panel Deflection for 2" Bedding Strip (a), 3" Bedding Strip (b), and 4" Bedding Strip (c).*

4.3 SHEAR STUD CONNECTION TEST RESULTS

The behavior of the PCP attached to the loading beam using the shear stud connection when the loading beam was racked laterally is depicted in Figure 4.12. As the frame was racked laterally, the panel shifted with respect to the frame. As the North end of the frame was racked to the East, the North-East and South-West corners were in tension and the North-West and South-East connections were in compression. Both the tension and compression corners also transferred a small amount of shear.

As the displacement increased, the panel rotated, pulling the tension corners apart from one another. At higher displacements the threaded rod in the compression corners slipped through the holes in the channel. This slipping of the threaded rods in the channel caused the panel to rotate more with respect to the girders. This rotation resulted in a lateral displacement of the panel at the compression corners. This lateral displacement bent the threaded rods at the compression corners. The racking of the beams also added a lateral displacement to the system. The slipping of the threaded rods continued until the U-bolts clamping the channel to the shear studs bore on the PCP. The bearing of the U-bolts on the PCP caused local crushing of the concrete. The bending of the threaded rod from the lateral movement at the compression corner, as seen in the left picture of Figure 4.12, localized at the face of the PCP, caused local crushing of the concrete that propagated in a crack, as seen in Figure 4.13.

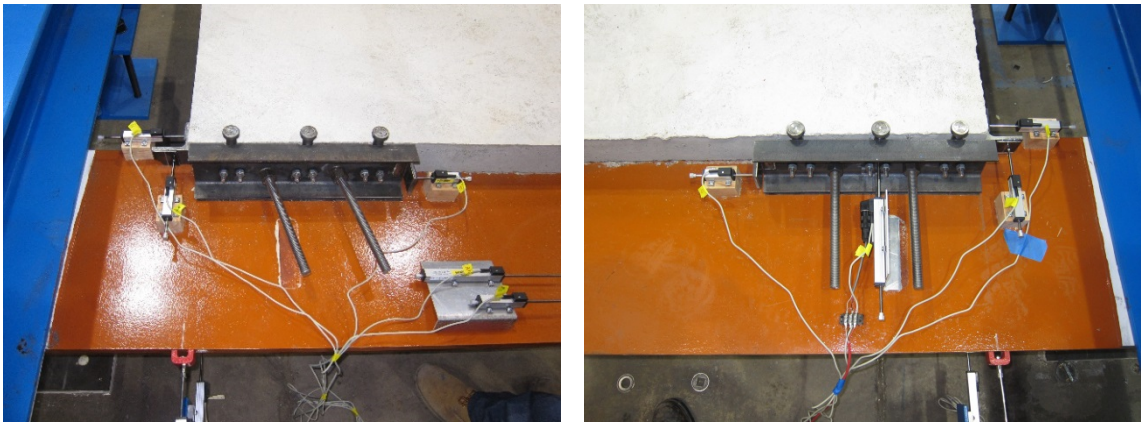

Figure 4.12: *PCP with Shear Stud Connection at 1.1" of Panel Movement at the Compression Corner (left) and the Tension Corner (right)*

Figure 4.13: *Crack at Embedded Threaded Rod*

As the load was reversed, the threaded rods that were previously at the compression corners were now at tension corners. These threaded rods slipped back out until the nut bore on the channel, and the threaded rods in the new compression corners began to slip. The back-and forth bending of the threaded rods exacerbated the crushing of the concrete at the face of the PCP. The failure on Test 1 occurred at the south-east corner, seen in Figure 4.14. This corner was in tension at the time of failure.

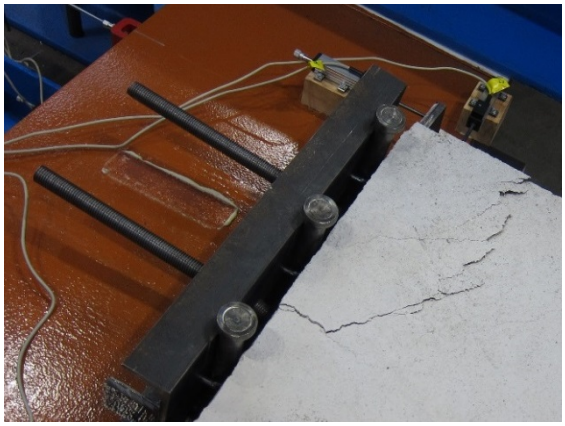

Figure 4.14: *PCP with Shear Stud Connection Nodal Failure*

The cracks were localized at the nodal regions, as depicted in Figure 4.15. There was no global shear cracking in this panel. The failure was due to a nodal failure at the tension node where the threaded rod entered the panel.

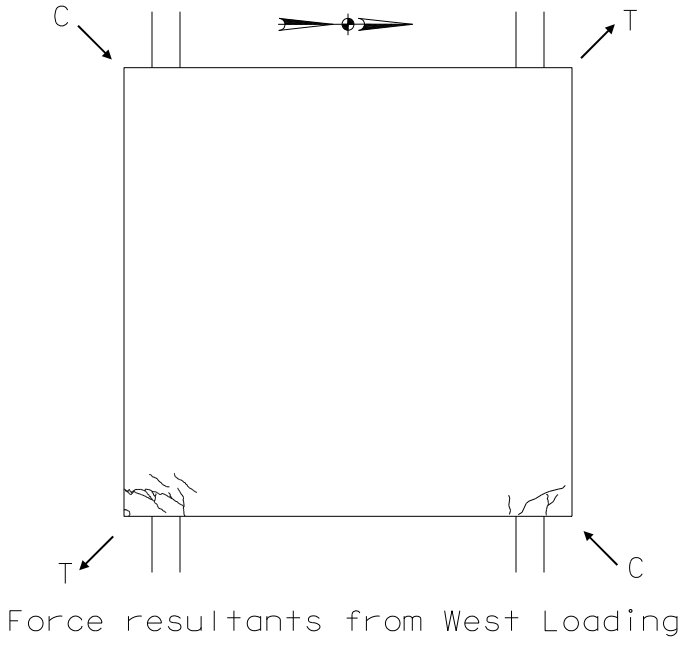

Figure 4.15: *Crack Patterns from Test 4*

A graph of the panel shear versus the panel deflection is shown in Figure 4.16 through Figure 4.18. The initial loading of the PCP was relatively stiff. The unloading response was stiff as the PCP relaxed in place. At low levels of load in the reverse direction, around one to two kips of panel shear; the response softened as the PCP rotated to pull out the previously rotated threaded rods to load them in tension. The response stiffened up once the threaded rods had straightened out, providing a main load path of a tension strut between the two tension corners. At higher load levels, around 7 or 8 kip, the response flattened out again as the threaded rod slipped through the channel. The stiffness picked up again as the U-bolts bearing on the PCP added a compression strut to the already existing tension strut.

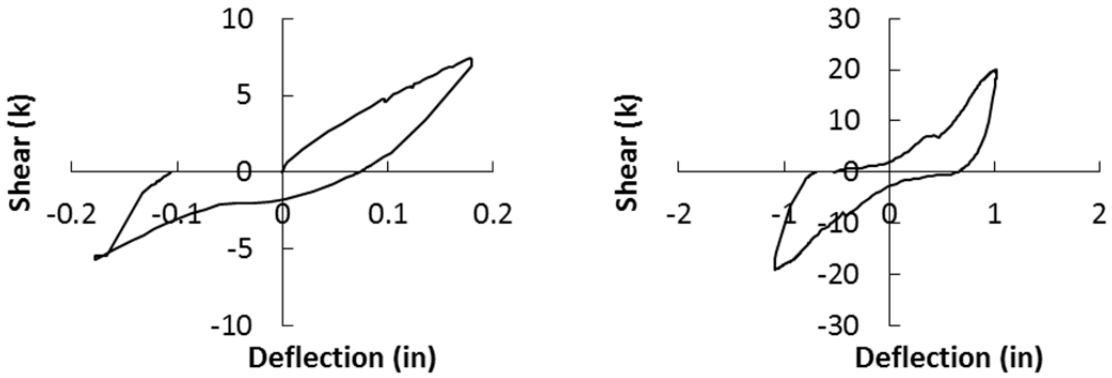

Figure 4.16: *Panel Shear vs. Panel Deflections for Cycle 1 (left) and Cycle 11 (right) for Test 4*

A graph of all the cycles is shown in Figure 4.17. For comparison with the other tests a back bone curve was created using the data from the first loop in the first cycle of each deflection, as shown on the left side of Figure 4.18.

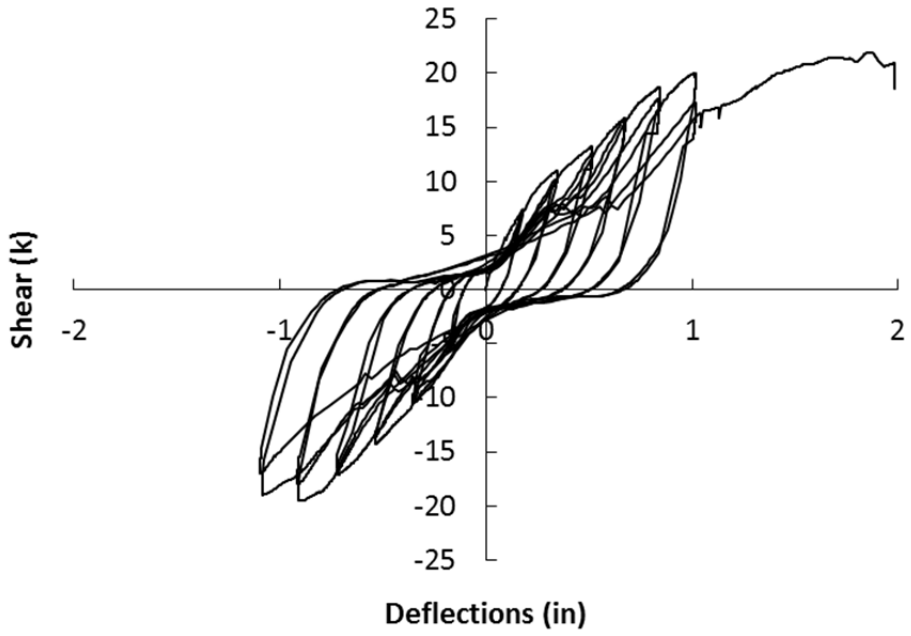

Figure 4.17: *Panel Shear vs. Panel Deflections for All Displacement Cycles of Test 4*

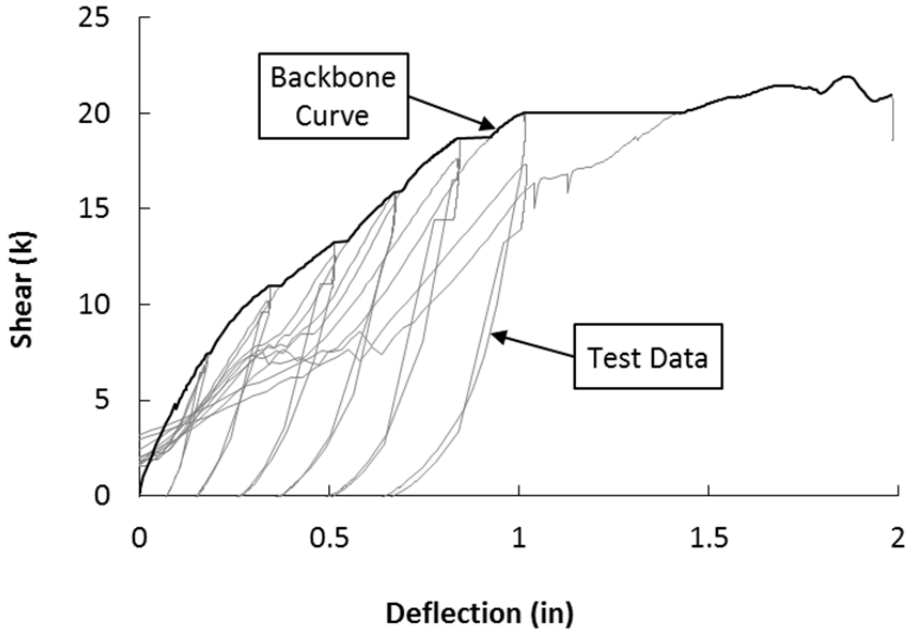

Figure 4.18: *Backbone Curve of Panel Shear vs. Panel Deflections for Test 4*

The panel deflections and panel movements for both halves of both cycles is tabulated in Table 4.1. The panel deflections, shears, and stiffnesses tabulated are based on the maximum panel shear in that cycle. Following 12 cycles of loading, the panel was taken to failure on the 13th cycle.

Table 4.1: *Maximum Panel Shears and Corresponding Panel Movement for Test 4*

Cycle Number	Panel Deflection	Panel Shear	Panel Stiffness
1	0.18"	7.4 k	41 k/in
	-0.18"	-5.7 k	32 k/in
2	0.17"	6.8 k	40 k/in
	-0.18"	-5.5 k	31 k/in
3	0.34"	11 k	32 k/in
	-0.36"	-10.6 k	29 k/in
4	0.34"	10.2 k	30 k/in
	-0.35"	-10.2 k	29 k/in
5	0.51"	13.2 k	26 k/in
	-0.53"	-14.2 k	27 k/in
6	0.51"	12.6 k	25 k/in
	-0.54"	-13.7 k	25 k/in
7	0.67"	15.9 k	24 k/in
	-0.72"	-17.2 k	24 k/in
8	0.67"	15.9 k	24 k/in
	-0.72"	-16.5 k	23 k/in
9	0.84"	18.7 k	22 k/in
	-0.89"	-19.5 k	22 k/in
10	0.84"	17.6 k	21 k/in
	-0.91"	-17.9 k	20 k/in
11	1.01"	20 k	20 k/in
	-1.09"	-19 k	17 k/in
12	1.02"	17.3 k	17 k/in
	-1.1"	-17 k	15 k/in
13	1.87"	21.9 k	12 k/in

Initially the panel was stiffer when loaded in the westward loading direction, but by the third cycle the behavior in the two directions became similar.

Adding a nut to the threaded rod at the back-side of the channel would likely keep the PCP closer to its original location, but the load path would change, as there would be no contribution to the capacity from the bearing of the U-bolts on the PCP. The compression through the threaded rod would be limited to its buckling capacity. This may be a more desired configuration to allow concrete to flow between the shear studs and the PCP. The capacity of this double-nut configuration would be dependent on the buckling capacity of the threaded rods.

4.4 EMBEDDED ANGLE CONNECTION TEST RESULTS

Four PCPs with the embedded angle connections were tested in the load frame. As the frame was racked laterally, the connection member welded to the beam was pulled along with the beam and in turn pulled on the embedded angle in the PCP. One set of diagonal corners was in compression and the other set was in tension. This member was connected eccentrically to the PCP and the flow of stresses also applied a moment to the ends of the PCP. This is most noticeable was the tension corner where a gap between the tee or angle and the embedded angle was opened up as shown in picture (a) of Figure 4.20. The bottom of the connection member was more rigid than the top; once the connection member deformed significantly, the differential stiffness also resulted in a moment to the edge of the PCP as seen in picture (b) of Figure 4.20.

As the North end of the frame was racked to the East, the North-East and South-West corners were in tension and the North-West and South-East connections were in compression.

For tests with no haunch, the effects of the eccentric connection were less pronounced in the tension corners under relatively light loads. The effects of the veritable stiffness of the connecting members on the compression corners were more pronounced in the test with no haunch.

4.4.1 Test 5: 8-Inch Studs with No Bedding Strips

The PCP in Test 5 had 8-inch shear studs developing U-bars in the panel and no haunch. The panel was first loaded in the westward direction, causing the north-west and south-east corners to be in tension and the north-east and south-west corners to be in compression. The first cracks appeared at the tension corners at 25 kips of panel shear. The angle started to peel away from the PCP at the tension corners at 31 kips of panel shear and separation continued to grow in length and width as the load increased. There was some mild cracking around the embedded angle to PCP interface on the compression corners around 47 kips of panel shear. At 87 kips of panel shear the first global shear crack was observed. At 112 kips a second global shear crack was apparent. The compression corner of the panel deflected more at the top of the panel than the bottom of the panel, as evidenced by a ¼-inch gap between the bottom of the panel and the top flange of the loading beam at 118 kips of shear.

Just prior to the ultimate shear at 118 kips of panel shear, as seen in Figure 4.19, the embedded angle on the tension side, south-east, had begun to pull away from the connection member and the concrete of the PCP. The compression side, north-east, began to distort the connection member. At this time there was one global shear crack in the panel, a moderate amount of cracking at the top of the PCP at the tension corners, and no visible distress at the compression corners.

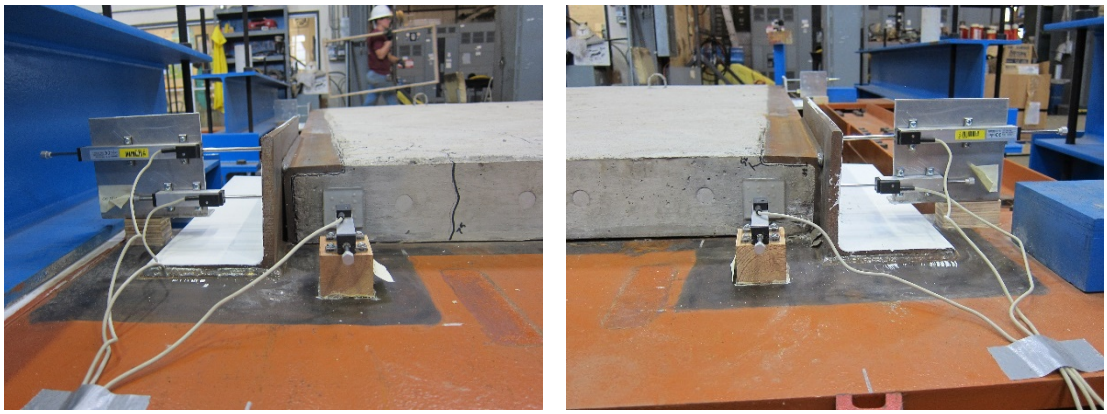

(a) (b)

Figure 4.19: *Elevation View at the South-East (a) and the South-West (b) Corners of Test 5 PCP at 1.1" of Panel Movement*

At the ultimate load the connection members on the compression side began to yield. The ultimate capacity of the panel was 135 kips, which was reached at a displacement of 1.20 inches. The peak capacity occurred just prior to the global crushing of the concrete at the north-east corner.

At 0.2 inches of panel displacement beyond ultimate, as seen in Figure 4.20, the connection member on the compression corner had significantly distorted, adding moment to the end of the panel. The top of the embedded angle on the compression corners pulled away from the PCP and the concrete on the north-east corner crushed.

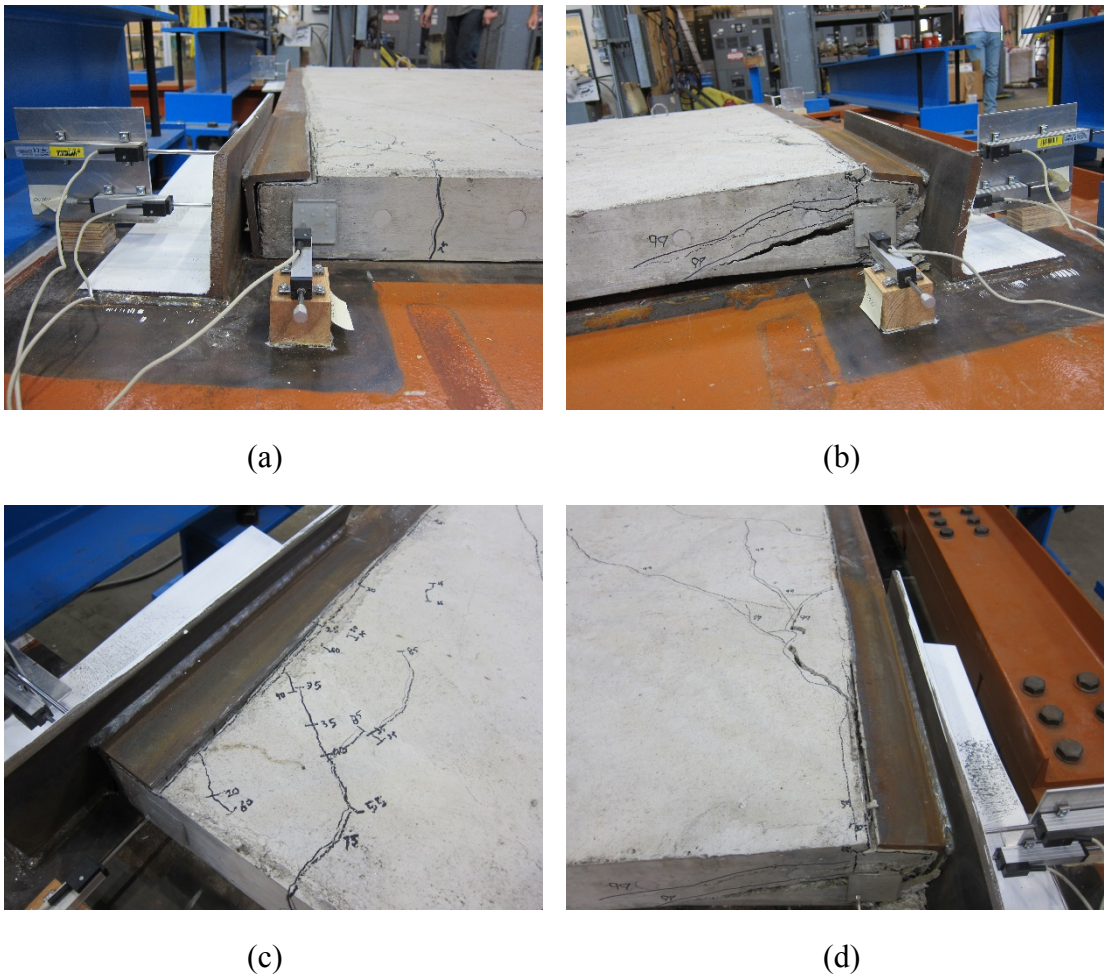

(a) (b)

(c) (d)

Figure 4.20: *Elevation View at the South-East (a) and the South-West (b) Corners and Plan View at the South-East (c) and the South-West (d) Corners of Test 5 PCP at 1.4" of Panel Movement*

After the ultimate strength was achieved loading in the westward direction, the force in the hydraulic actuator was released and the panel was loaded in the eastward direction, causing the north-west and south-east corners to be in compression and the north-east and south-west corners to be in tension. Most of the cracks closed up when the panel was loaded, with the exception of the cracks from the bending and crushing at the compression corners. It was hard to tell when the angles started to pull away because there was significant residual damage from the test in the other direction.

The first cracks appeared at the tension corners at -25 kips of panel shear. The cracks at the corner that previously crushed were relatively wide cracks. The cracks appeared at the other tension corners at -50 kips of panel shear. At -112 kips the first two global shear cracks occurred. There was some localized crushing at the bottom of the panel at the south-east corner at -112 kips. The panel lifted off the beam near the compression corner.

Just prior to the ultimate capacity of -112 kips of panel shear, as seen in Figure 4.21, there were two global shear cracks in the panel, the north-east tension corner was damaged due to the previous test while the south-west tension corner had a moderate amount of cracking at the top of the PCP, the south-east compression corner had a moderate amount of crushing, and the north-west compression corner had no visible distress.

(a) (b)

Figure 4.21: *View at the South-East (a) and the South-West (b) Corners of Test 5 PCP at -0.9" of Panel Movement*

At the ultimate load the connection members on the compression side began to yield. The peak capacity occurred just prior to the global crushing of the concrete at the

south-east corner. The capacity of the panel was -126 kips, which was reached at a displacement of -0.88 inches. At 0.5 inches of panel displacement beyond ultimate, as seen in Figure 4.22, the connection member on the compression corner had significantly distorted. The top of the embedded angle on the compression corners had pulled away from the PCP and the concrete in this corner had crushed.

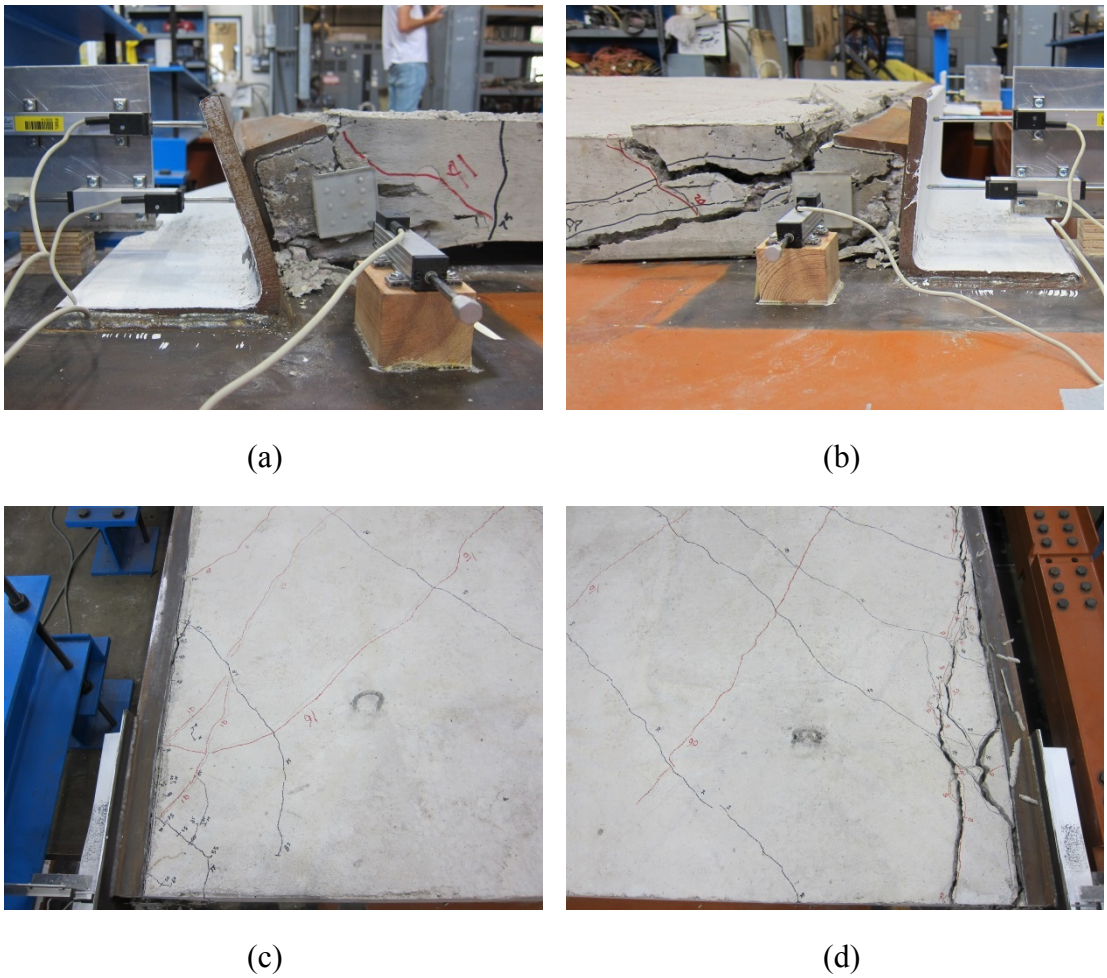

(a) (b)

(c) (d)

Figure 4.22: *Elevation View at the South-East (a) and the South-West (b) Corners and Plan View at the South-East (c) and the South-West (d) Corners of Test 5 PCP at -1.4" of Panel Movement*

The final crack patterns are depicted in Figure 4.23. This panel predominantly acted in in-plane shear, but the capacity was reached when the corners crushed under the combined compressive reaction and bending of the edge of the panel.

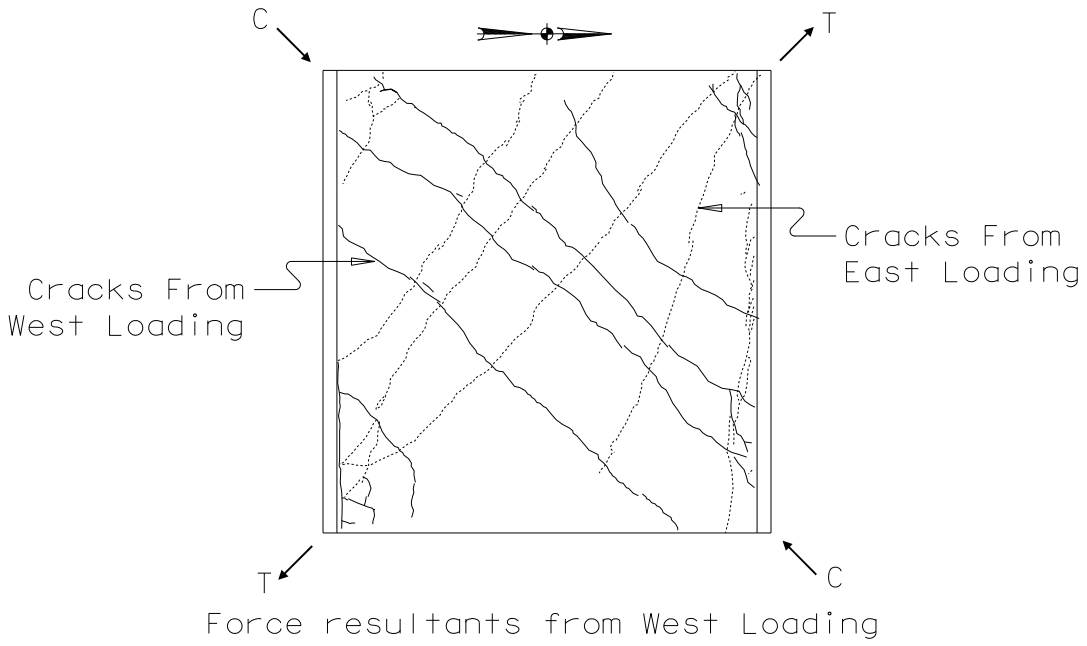

Figure 4.23: *Crack Patterns from Test 5*

4.4.2 Test 6: 8-Inch Studs with 4-Inch Bedding Strips

The PCP in Test 6 included 8-inch shear studs developing U-bars in the panel and a 4-inch haunch. The PCP was connected to the beam with a steel tee connection member. The panel was first loaded in the westward direction, causing the north-west and south-east corners to be in tension and the north-east and south-west corners to be in compression. The first cracks appeared at the tension corners at 30 kips of panel shear followed by cracking at the compression corners at 40 kips of panel shear. The gap at the bottom of the embedded angles and the connection member on the tension corners and the rotation of the embedded angle at the compression corners was noticeable by 60 kips, which was when the first global shear crack occurred.

Just prior to the ultimate shear at 70 kips of panel shear, as seen in Figure 4.24, the embedded angle on the tension side, south-east, had begun to pull away from the connection member. The compression side, north-east, was beginning to distort the connection member. At this time there was one global shear crack in the panel, a moderate amount of cracking at the top of the PCP at the tension corners and compression corners. There was localized crushing at the bottom of the panel at the compression corners, and the panel had lifted up from the beam near the compression corners.

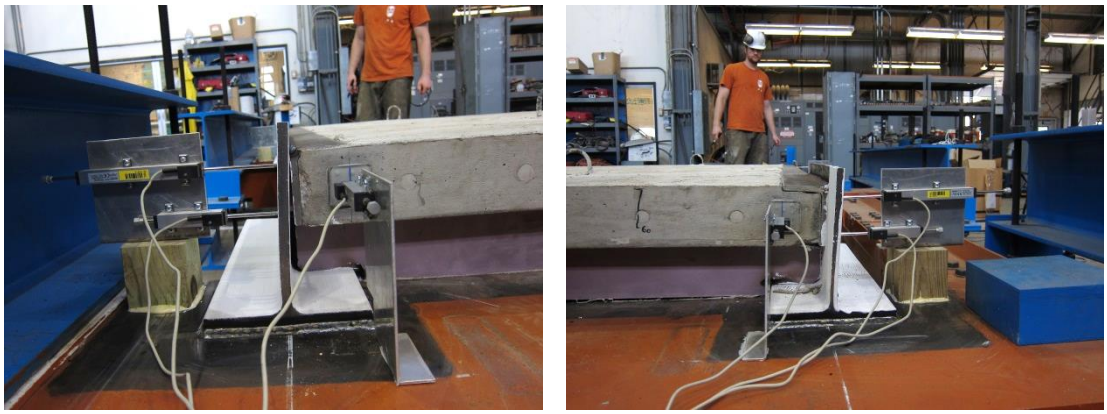

(a) (b)

(c) (d)

Figure 4.24: *Elevation View at the South-East (a) and the South-West (b) Corners and Plan View at the South-East (c) and the South-West (d) Corners of Test 6 PCP at 1.0" of Panel Movement*

At the ultimate load the connection members on the compression side began to yield. The capacity of the panel was 74 kips, which was reached at a displacement of 1.39 inches. The peak capacity occurred just prior to the global crushing of the concrete at both corners.

At 0.2 inches of panel displacement beyond ultimate, as seen in Figure 4.25, the connection member on the compression corner had distorted adding moment to the end of the panel. There were flexural cracks at the top of the panel at the compression corners.

The top of the embedded angle on the compression corners pulled away from the PCP and the concrete at both corners had crushed.

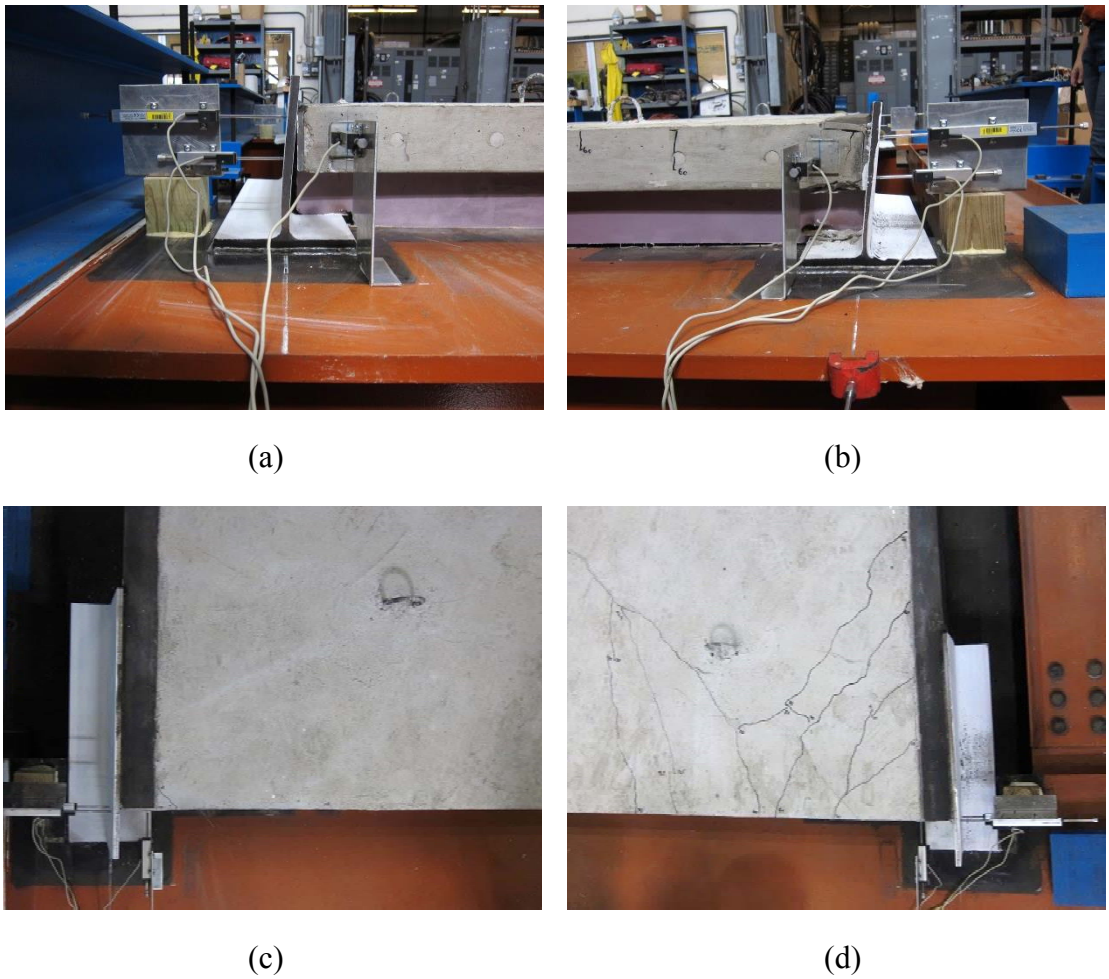

(a) (b)

(c) (d)

Figure 4.25: *Elevation View at the South-East (a) and the South-West (b) Corners and Plan View at the South-East (c) and the South-West (d) Corners of Test 6 PCP at 1.6" of Panel Movement*

After the ultimate strength was achieved loading in the westward direction, the force in the hydraulic actuator was released and the panel was loaded in the eastward direction, causing the north-west and south-east corners to be in compression and the north-east and south-west corners to be in tension. Most of the cracks closed up when the

panel was loaded, with the exception of the cracks from the bending and crushing at the compression corners. By -10 kips of panel shear the PCP was solidly bearing on the bedding strip again. By -20 kips the south-east embedded angle was in full contact with the connection member; by -30 kips the north-west embedded angle was in full contact with the connection member. It was hard to tell when the angles started to pull away because there was so much residual damage from the test in the opposite direction.

The first cracks appeared at the compression corners at -30 kips of panel shear. Bending cracks appeared in the top of the PCP at the compression corners at -50 kips. The cracks appeared at the other tension corners at -50 kips of panel shear. At -60 kips the first global shear crack occurred.

Just prior to the ultimate shear at -70 kips of panel shear, as seen in Figure 4.26, there were two global shear cracks in the panel, the south-west tension corner was damaged due to the previous test, the north-east tension corner had a moderate amount of cracking at the top of the PCP, and both compression corners had a moderate amount of crushing at the bottom of the panel. The panel had lifted off the beam near the compression corners.

(a) (b)

(c) (d)

Figure 4.26: *Elevation View at the South-East (a) and the South-West (b) Corners and Plan View at the South-East (c) and the South-West (d) Corners of Test 6 PCP at -1.0" of Panel Movement*

At the ultimate load the connection members on the compression side began to yield. The peak capacity occurred just prior to the global crushing of the concrete at the south-east corner. The capacity of the panel was -72 kips, which was reached at a displacement of -1.10 inches. At 0.6 inches of panel displacement beyond ultimate, as seen in Figure 4.27, the connection member on the compression corner had significantly distorted. The top of the embedded angle on the compression corners had pulled away from the PCP and the concrete in the north-west corner had crushed.

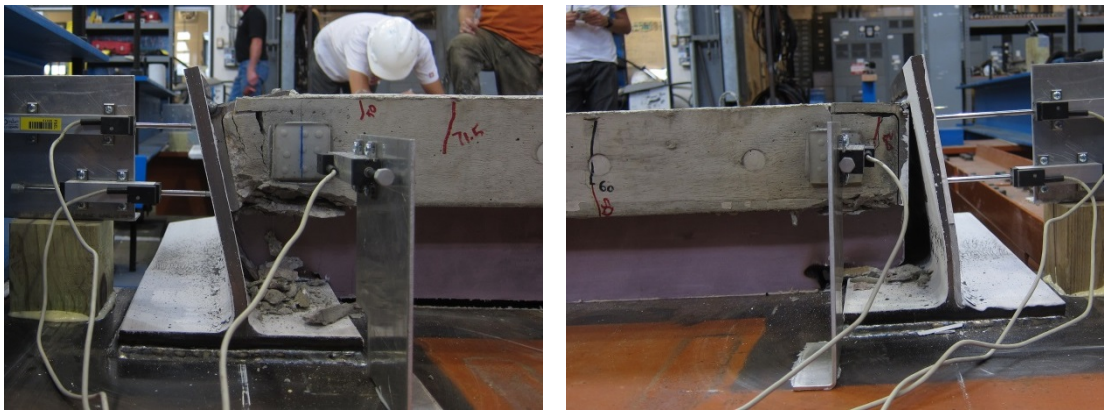

(a) (b)

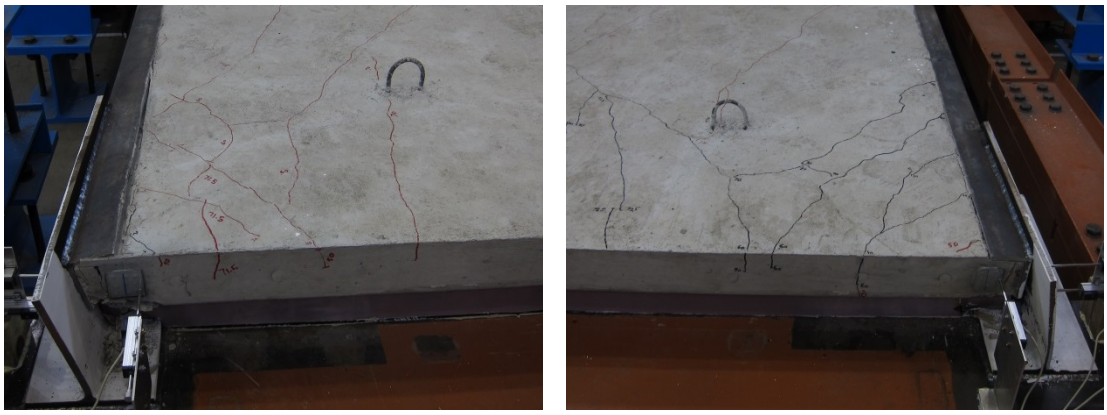

(c) (d)

Figure 4.27: *Elevation View at the South-East (a) and the South-West (b) Corners and Plan View at the South-East (c) and the South-West (d) Corners of Test 6 PCP at -1.6" of Panel Movement*

The final crack patterns can be seen in Figure 4.28. This panel acted in a combination of out-of-plane bending and in-plane shear. The capacity was reached when the corners crushed under the combined compressive reaction and bending of the edge of the panel.

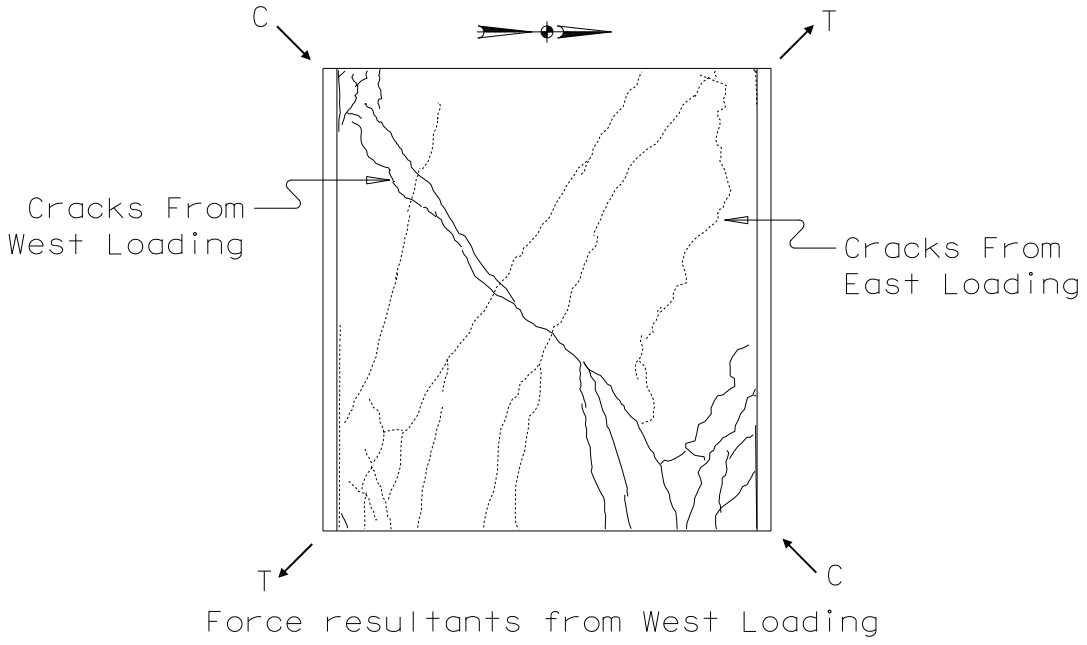

Figure 4.28: *Crack Patterns from Test 6*

4.4.3 Test 7: 8- and 3-Inch Studs with 2-Inch Bedding Strips

The PCP in Test 7 had 8-inch shear studs developing U-bars in the panel in the north-east and south-west corners, the corners that see compression in the first stage of loading. These corners had the lighter angle connection member, an L 8x6x½. The PCP had 3-inch shear studs between straight in the north-west and south-east corners, the corners that see tension in the first stage of loading. These corners had the stiffer angle connection member, an L 8x6x¾. This panel had 2 inches of haunch. The panel was first loaded in the westward direction, causing the north-west and south-east corners to be in tension and the north-east and south-west corners to be in compression.

The first cracks appeared at the tension corners at 20 kips of panel shear. At 30 kips the cracks at the tension corners are the full depth of the panels; they continue to widen as the load increases. These are the corners with the 3-inch shear studs. Cracks appeared at the compression corners at 50 kips of panel shear. At 70 kips of panel shear the first global shear crack occurred.

Just prior to the ultimate shear at 70 kips of panel shear, as seen in Figure 4.29, the concrete on the tension side had cracked through the full depth of the panel. There was no evident distress to the connection members on the tension corners, nor was the embedded angle pulling away from the connection member. The compression side, north-east, began to distort the connection member. There was localized crushing at the compression corners. At this time there was one global shear crack in the panel, a moderate amount of cracking at the top of the PCP at the compression corners and a full-depth crack at the tension corners.

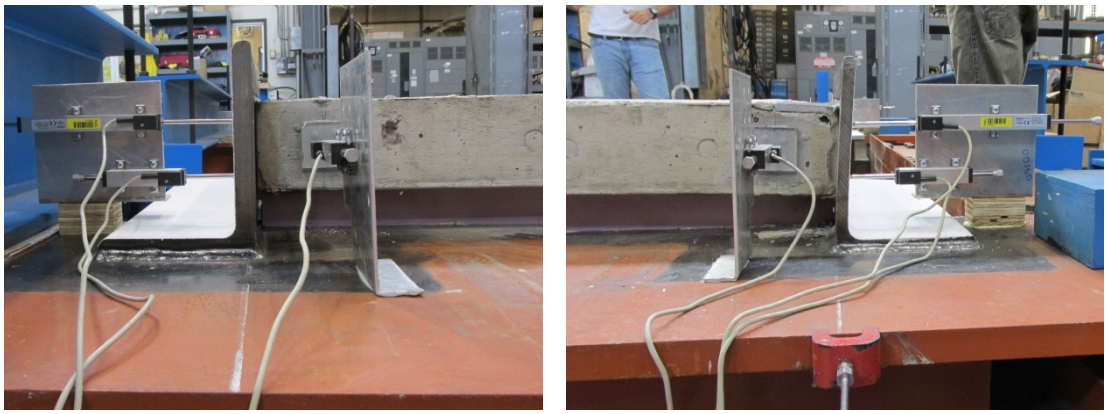

(a) (b)

(c) (d)

Figure 4.29: *Elevation View at the South-East (a) and the South-West (b) Corners and Plan View at the South-East (c) and the South-West (d) Corners of Test 7 PCP at 0.8" of Panel Movement*

At the ultimate load the connection members on the compression side began to yield. The capacity of the panel was 71 kips, which was reached at a displacement of 0.82 inches. The peak capacity occurred just prior to the global crushing of the concrete at the north-east corner.

At 0.3 inches of panel displacement beyond ultimate, as seen in Figure 4.30, the connection member on the compression corner had significantly distorted, adding moment to the end of the panel. The top of the embedded angle on the north-east

compression corner pulled away from the PCP. The vertical crack at the tension corners had propagated along the edge of the panel partially ripping the embedded angle off the PCP.

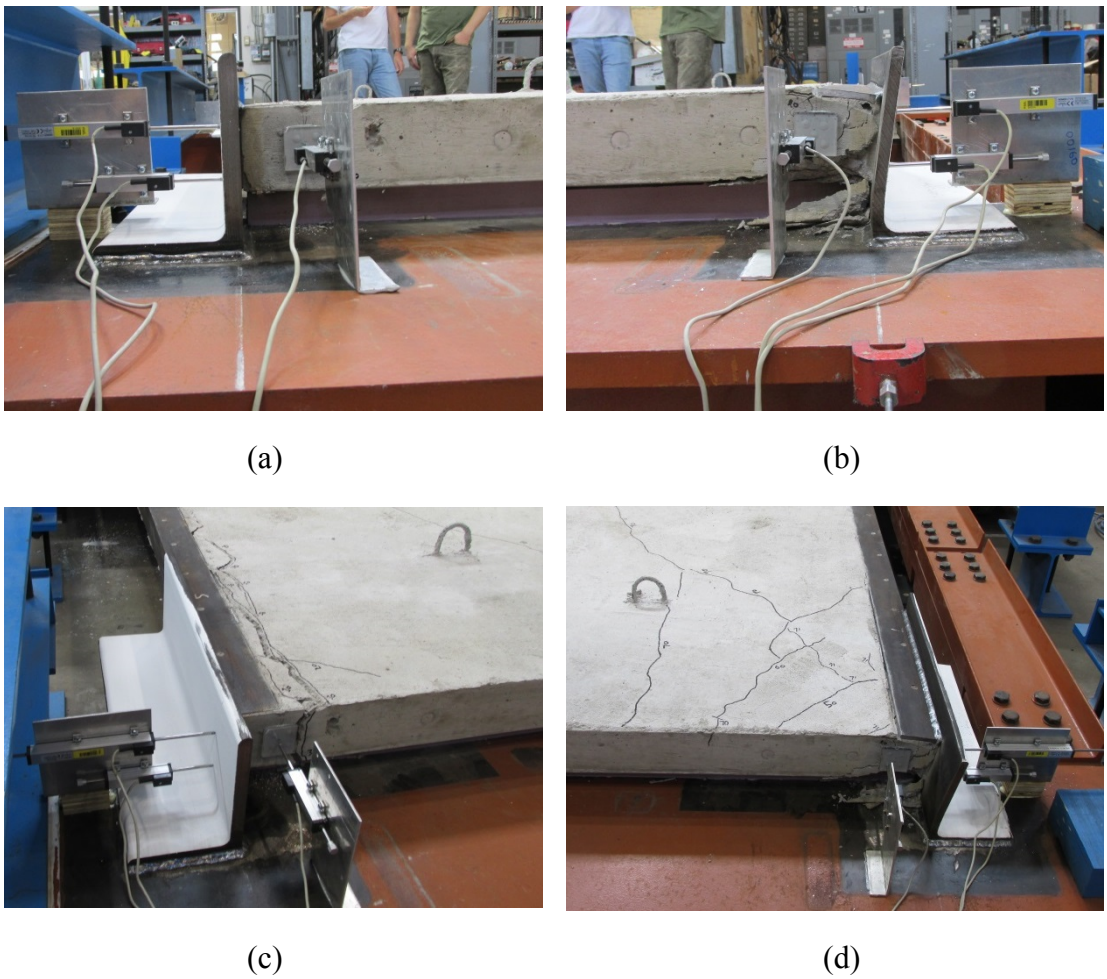

(a) (b)

(c) (d)

Figure 4.30: *Elevation View at the South-East (a) and the South-West (b) Corners and Plan View at the South-East (c) and the South-West (d) Corners of Test 7 PCP at 1.1" of Panel Movement*

After the ultimate strength was achieved loading in the westward direction, the force in the hydraulic actuator was released and the panel was loaded in the eastward direction, causing the north-west and south-east corners to be in compression and the

north-east and south-west corners to be in tension. Most of the cracks closed up when the panel was loaded, including the large vertical cracks at the north-west and south-east corners. The cracks at the north-west corner were closed by -20 kips of panel shear. The cracks at the south-east corner were substantially closed by -30 kips. It was hard to tell when the angles started to pull away in the north-east corner because there was so much residual damage from the test in the other direction. At -60 kips the first global shear crack occurred.

Just prior to the ultimate shear at -70 kips of panel shear, as seen in Figure 4.31, there was one global shear crack in the panel, the north-east tension corner was damaged due to the previous test, and there was no other obvious signs of distress.

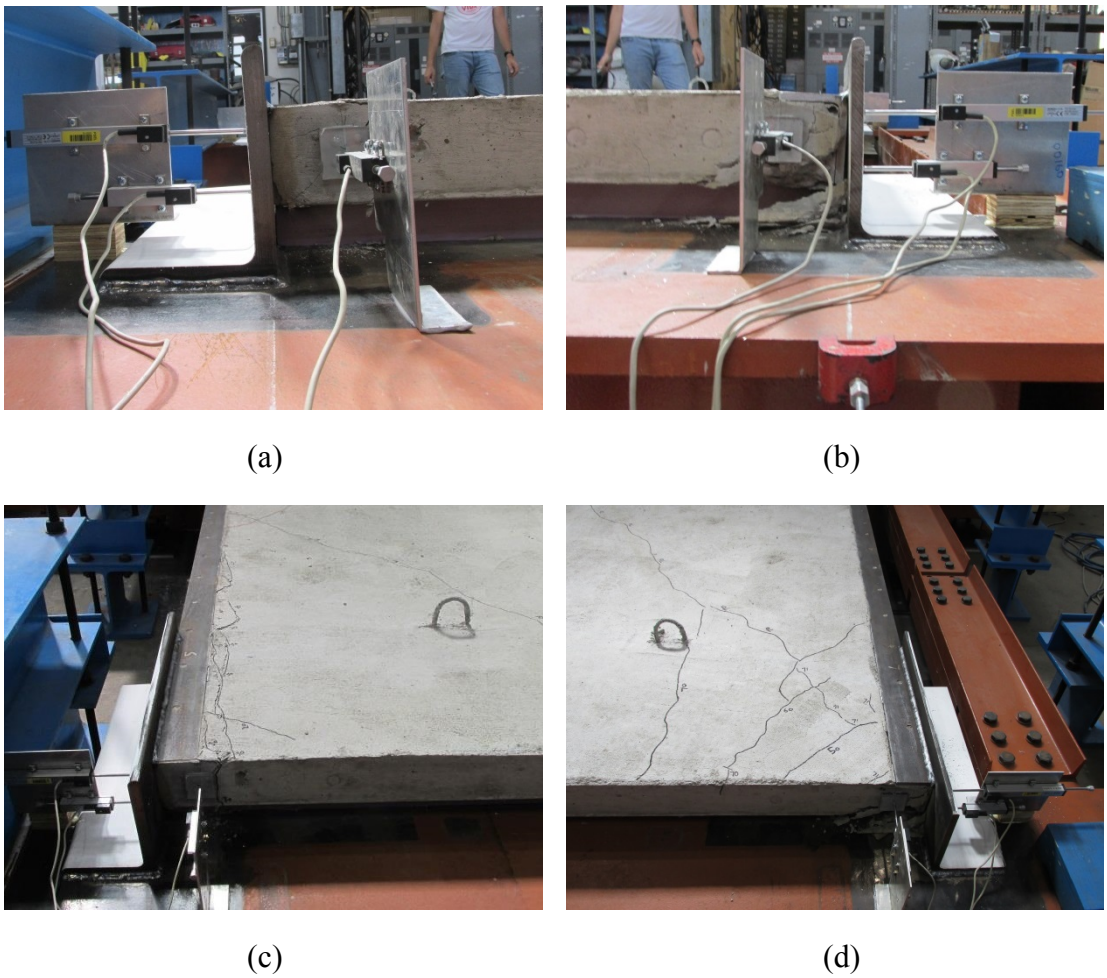

(a) (b)

(c) (d)

Figure 4.31: *Elevation View at the South-East (a) and the South-West (b) Corners and Plan View at the South-East (c) and the South-West (d) Corners of Test 7 PCP at -0.5" of Panel Movement*

The peak capacity occurred just prior to the crushing of concrete at the south-east corner. The capacity of the panel was -81 kips, which was reached at a displacement of -0.83 inches. At 0.6 inches of panel displacement beyond ultimate, as seen in Figure 4.32, the weld from the connection member to the beam failed at the south-east corner. The weld failed at 1.4 inches of panel displacement.

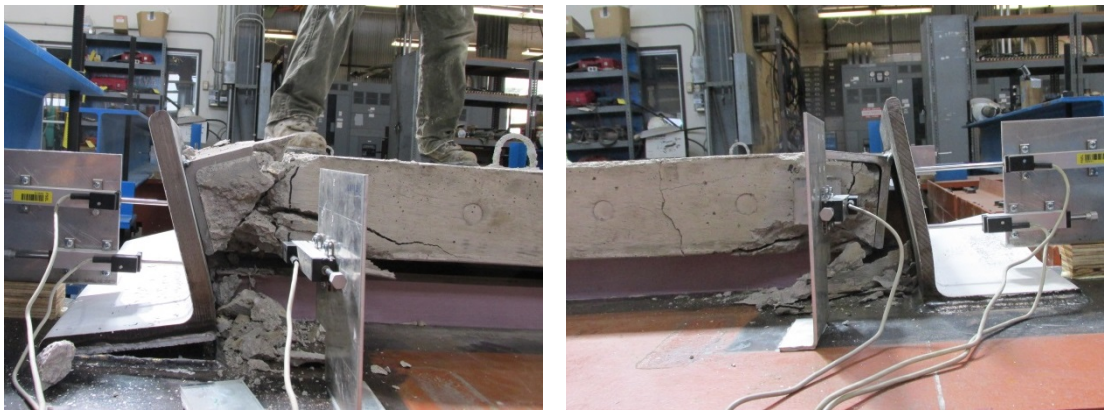

(a) (b)

(c) (d)

Figure 4.32: *Elevation View at the South-East (a) and the South-West (b) Corners and Plan View at the South-East (c) and the South-West (d) Corners of Test 7 PCP at -1.4" of Panel Movement*

The final crack patterns can be seen in Figure 4.33. For westward loading this panel predominantly acted in compression; the tension force was lost early from the splitting of the PCP at the tension corners. For eastward loading this panel predominantly acted in shear. The capacity for westward loading was reached when the corners crushed under the combined compressive reaction and bending of the edge of the panel. The capacity for eastward loading was reached when the already damaged corner crushed under the compressive force.

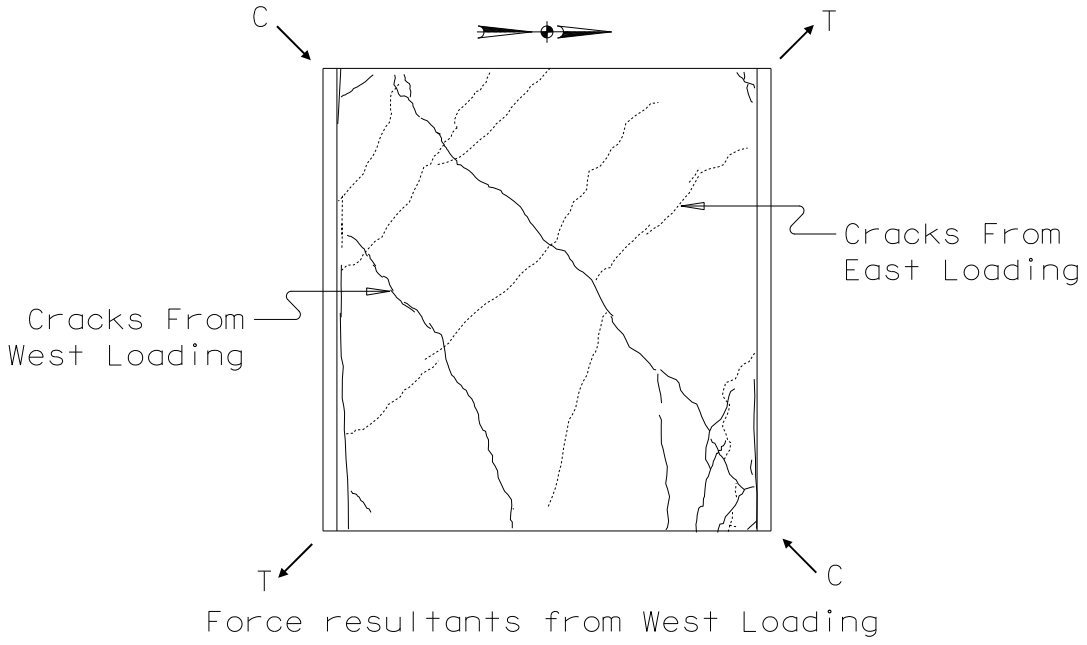

Figure 4.33: *Crack Patterns from Test 7*

4.4.4 Test 8: 15-Inch Deformed Anchors with 4-Inch Bedding Strips

The PCP in Test 8 had 18-inch deformed anchors lapped with the longitudinal reinforcing in the panel and a 4-inch haunch. The PCP was connected to the beam with a steel tee connection member. The panel was first loaded in the westward direction, causing the north-west and south-east corners to be in tension and the north-east and south-west corners to be in compression. The first cracks appeared at the compression corners at 50 kips of panel shear and the embedded angle began to separate from the PCP as the connection member began to distort. Cracks appeared in the tension corners and the first global shear crack occurred at 60 kips of panel shear.

Just prior to the ultimate shear at 60 kips of panel shear, as seen in Figure 4.34, the embedded angle on the tension side, south-east, had begun to pull away from the connection member. The compression side, north-east, began to distort the connection member. The panel had deflected up away from the beam near the north-east compression corner. At this time there was one global shear crack in the panel, a moderate amount of cracking at the top of the PCP at the compression corners, and minor cracking at the tension corners.

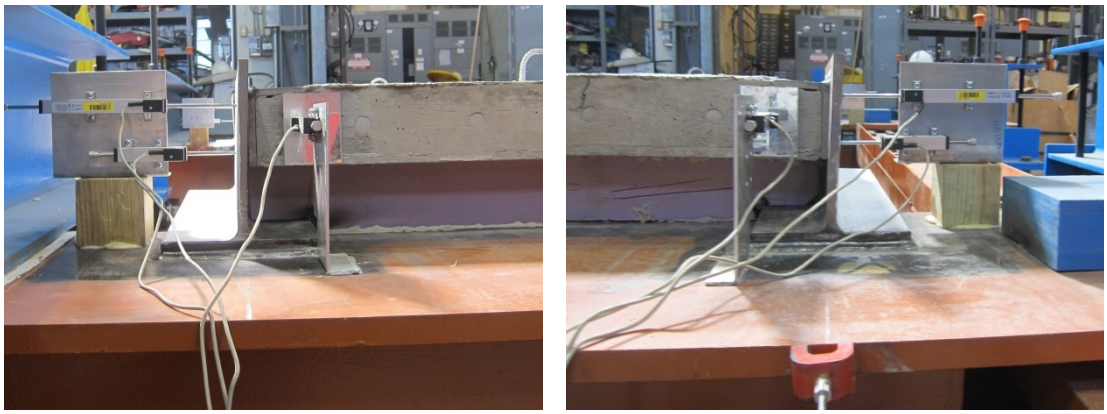

(a) (b)

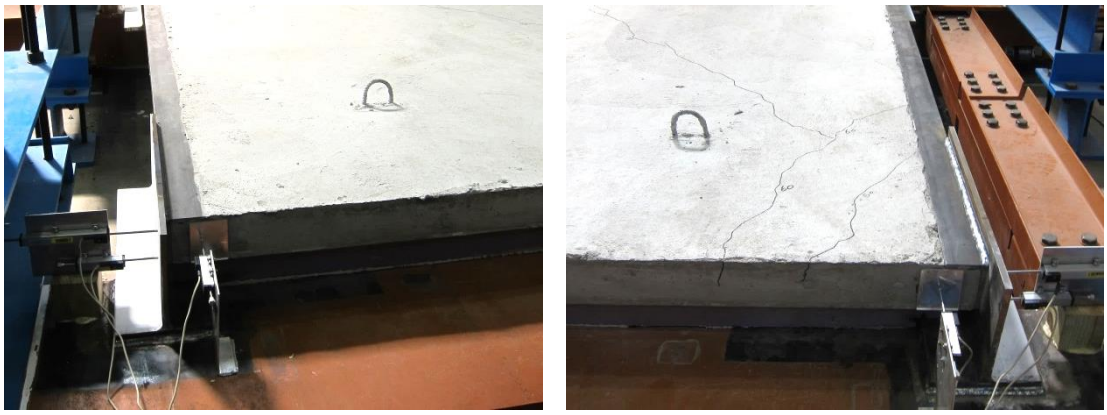

(c) (d)

Figure 4.34: *Elevation View at the South-East (a) and the South-West (b) Corners and Plan View at the South-East (c) and the South-West (d) Corners of Test 8 PCP at 0.6" of Panel Movement*

At the ultimate load the connection members on the compression side began to yield. The capacity of the panel was 73 kips, which was reached at a displacement of 1.25 inches. The peak capacity occurred just prior to the global crushing of the concrete at the north-east corner.

At 0.25 inches of panel displacement beyond ultimate, as seen in Figure 4.35, the connection member on the compression corner had distorted, adding moment to the end of the panel. There were flexural cracks at the top of the panel at the compression

corners. The top of the embedded angle on the compression corners pulled away from the PCP and the concrete at both corners has crushed. The connection member on the tension corners warped significantly, allowing that corner of the PCP to move.

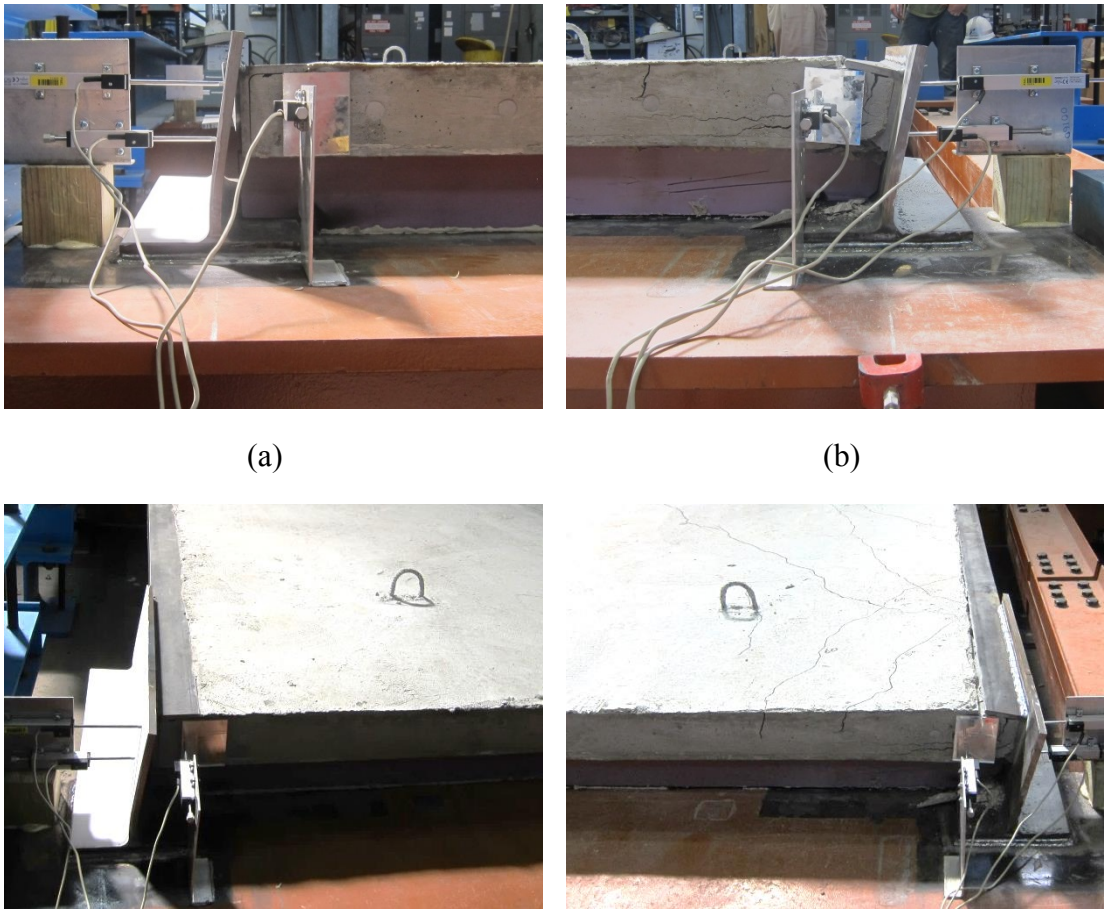

(a) (b)

(c) (d)

Figure 4.35: *Elevation View at the South-East (a) and the South-West (b) Corners and Plan View at the South-East (c) and the South-West (d) Corners of Test 8 PCP at 1.5" of Panel Movement*

After the ultimate strength was achieved loading in the westward direction, the force in the hydraulic actuator was released and the panel was loaded in the eastward direction, causing the north-west and south-east corners to be in compression and the

north-east and south-west corners to be in tension. Most of the cracks closed up when the panel was loaded, with the exception of the cracks from the bending and crushing at the compression corners. By -10 kips of panel shear the PCP solidly bore on the bedding strip. By -30 kips the north-west embedded angle was in full contact with the connection member; by -40 kips the south-east embedded angle was in full contact with the connection member. It was hard to tell when the angles started to pull away because there was so much residual damage from the test in the other direction.

The first cracks appeared at the tension and compression corners on the east side of the PCP at -50 kips of panel shear. At -60 kips the first global shear crack occurred.

Just prior to the ultimate shear at -60 kips of panel shear, as seen in Figure 4.36, there was one global shear crack in the panel, the north-east tension corner was damaged due to the previous test, the west tension and compression corners had no cracking from this direction of loading, the east corners had minor cracking at the top of the PCP, and there were no other obvious signs of distress.

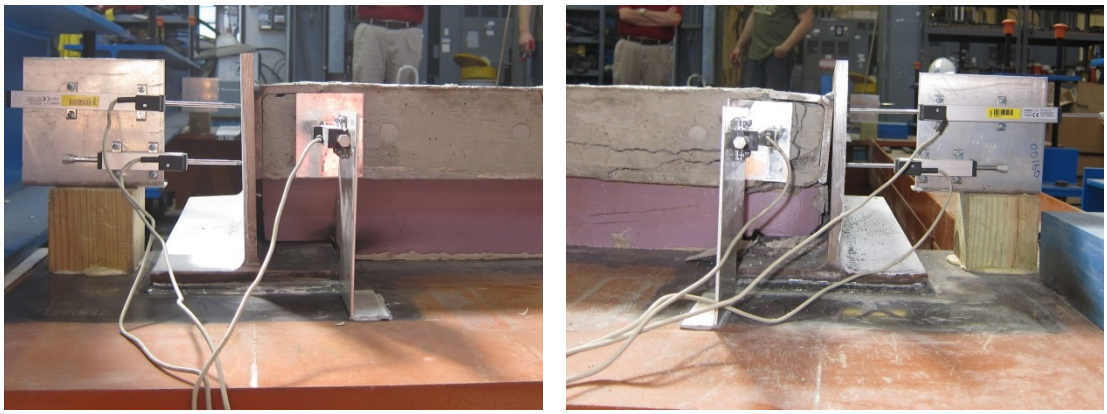

(a) (b)

(c) (d)

Figure 4.36: *Elevation View at the South-East (a) and the South-West (b) Corners and Plan View at the South-East (c) and the South-West (d) Corners of Test 8 PCP at -0.5" of Panel Movement*

At the ultimate load the connection members on the compression side began to yield. The peak capacity occurred just prior to the global crushing of the concrete at the south-east corner. The capacity of the panel was -73 kips, which was reached at a displacement of -0.94 inches. At 0.6 inches of panel displacement beyond ultimate, as seen in Figure 4.37, the connection member on the compression corner had significantly distorted. The top of the embedded angle on the compression corners had pulled away from the PCP and the concrete in the south-east corner had crushed.

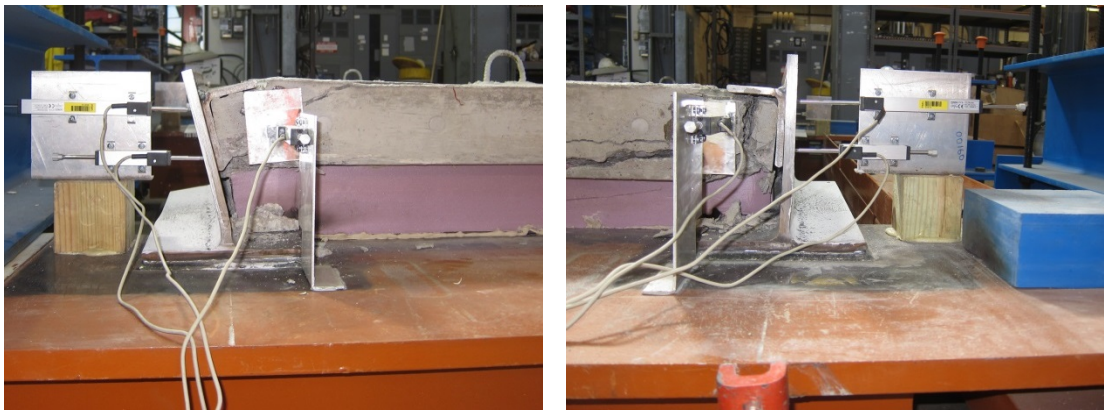

(a) (b)

(c) (d)

Figure 4.37: *Elevation View at the South-East (a) and the South-West (b) Corners and Plan View at the South-East (c) and the South-West (d) Corners of Test 8 PCP at -1.5" of Panel Movement*

The final crack patterns can be seen in Figure 4.38. This panel acted in a combination of out-of-plane bending and in-plane shear. The capacity was reached when the corners crushed under the combined compressive reaction and bending of the edge of the panel.

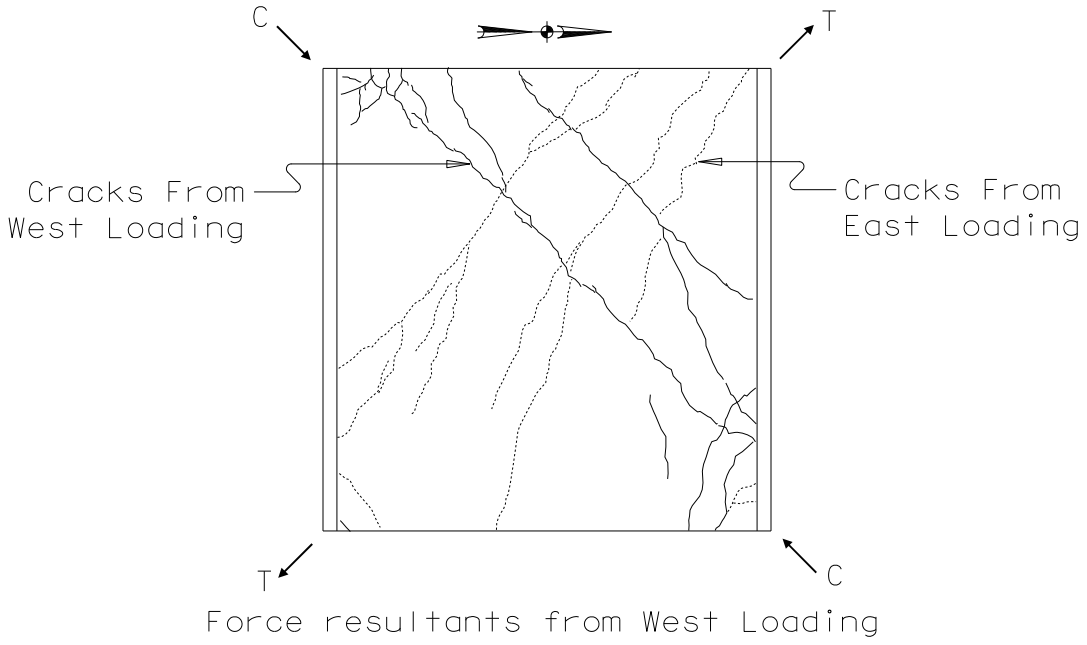

Figure 4.38: *Crack Patterns from Test 8*

4.5 SUMMARY OF EXPERIMENTAL RESULTS

A table summarizing the panel deflections is given in Table 4.2. A general trend that was observed as the bedding strip height increases, the movement it can withstand increases. It is likely that shorter bedding strips would not be able to withstand as much deflection as the 2" tall bedding strips.

Table 4.2: *Summary of Traditional Connection Panel Tests*

Test Designation	Bedding Strip Height	Bedding Strip Width	Shear Deflection Capacity
1	2"	1"	2.5"
2	3"	1.5"	2.8"
3	4"	2"	6.1"

A table summarizing the shear strength, the corresponding panel deflections, and values of the effective shear stiffness at 40% and 60% of the shear strength is given in

Table 4.3. In general, the capacities of the panels are similar in both directions given the same details, but the deflections that correspond to the capacities are not. Stiffness data for the eastward loading half of the curve is not a good comparison to the stiffness data on the westward loading half of the curve.

Table 4.3: *Maximum Panel Shears and Corresponding Panel Movement for Tests 5-8*

Test Designation	δ_{ult}	V_{ult}	$G'_{0.4Vu}$	$G'_{0.6Vu}$
4	1.87"	21.9 k	39 k/in	26 k/in
5	1.20"	135.4 k	166 k/in	149 k/in
	-0.88"	-126.0 k	1279 k/in	287 k/in
6	1.39"	73.5 k	99 k/in	99 k/in
	-1.10"	-71.9 k	417 k/in	155 k/in
7	0.82"	71.0 k	98 k/in	105 k/in
	-0.83"	-80.7 k	431 k/in	198 k/in
8	1.25"	73.4 k	118 k/in	112 k/in
	-0.94"	-72.6 k	-345 k/in	156 k/in

CHAPTER 5

Discussion and Comparison

5.1 TRADITIONAL CONNECTION

The maximum panel shear experienced by any of these panels was less than one kip. The assumption that the concrete strength and reinforcing details are not important to the shear performance of this connection type was verified.

The shear deflection capacity for all of these tests is between 0.9 and 1.5 times the bedding strip height. Assuming the panel rotates about its center, half of that deflection would be seen at either end of the bedding strip.

The shorter bedding strips have the smallest shear deflection capacity. The minimum bedding strip height of ½ inch would be the most critical. Additional tests should be done to investigate this height of bedding strip. With the additional tests, the limiting shear deflection capacity can be found.

Finite element analysis should be performed to calculate the shear deflection demand for bridges with different radii of curvature. This data in conjunction with the limiting shear deflection capacity will help limit the radii of curvature for which the traditional connection is viable.

5.2 OTHER CONNECTIONS

The load-deflection curves for these tests are found in Figure 5.1.

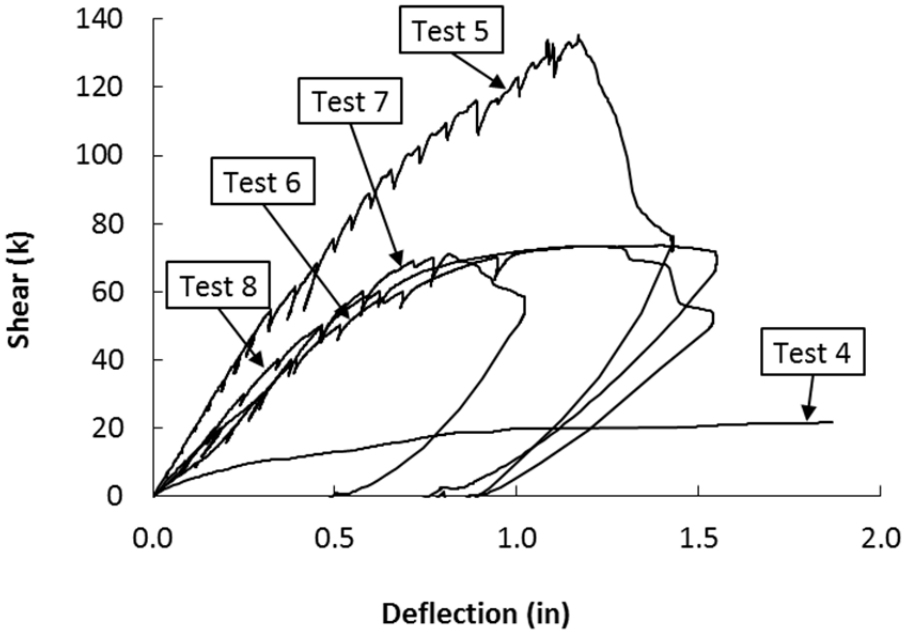

Figure 5.1: *Load-Deflection Curves for Tests 4-8*

Test 5, the PCP with the embedded angle connection and no haunch, had the highest stiffness. The connection in this test was very stiff; the base of the PCP bore against the horizontal leg of the connecting member angle. This connection was stiffer than any connection that would be used in the field, because the PCP must be at least ½ inch above the flange of the beam. Because this connection is so stiff, it can be assumed that this test represents the stiffness of the panel and large deviations from this stiffness are due to the stiffness of the connections. This test is the upper bound of what a connection can achieve with either stiffness or strength.

There is no appreciable difference in the response from the panel with 8-inch shear studs and 180-degree hooked longitudinal bars in Test 6 to the panel with 18-inch deformed anchors and straight longitudinal bars in Test 8. The 18-inch deformed anchors can be used with the current reinforcing retail. The 8-inch studs require the standard reinforcing to be modified by adding the 180-degree hooks at the edges of the panels.

The behavior in Test 7, with 3-inch shear studs on the tension corner has a similar capacity as Tests 6 and 8, but the deflection at the shear capacity is significantly lower. This panel had significant damage at relatively low loads.

The shear stud connection in Test 4 had significantly lower strength and stiffness than any of the other tests, but the ductility was much greater. This connection could be used where only a small stiffness is required. One of the cons of this connection is the relative location of the studs to the threaded rod must be known before punching holes in the channel for the U-bolt connection. One improvement that might be made to this connection is using a double nut on the channel to threaded rod connection, one nut on either side of the channel. Using a double nut would prevent the threaded rod from slipping through the channel.

The pre-stressing strands require a 3-inch strand extension; panels are typically cast 6 inches apart from one another to maximize the use of the pre-stressing bed. The required extension of the threaded rod is dependent on the distance between the panels and the shear studs. These rods parallel the pre-stressing strands; the required spacing of the PCPs in the prestressing bed will be variable.

5.3 CONCLUSIONS

Additional tests of the traditional connection are needed to determine if this connection can be used on curved girder systems.

The connection that provides the greatest bracing force is the embedded angle connection. The 18-inch long deformed ½-inch diameter anchors have the best performance with the least impact on the standard PCP reinforcing.

CHAPTER 6

Summary and Conclusions

The primary objective of this project is to determine feasible connection details that can resist in-plane shear and to determine the in-plane shear strength and stiffness of the various connections tested.

An additional investigation into the stability of the current bedding strip detail to shear movement was also performed.

6.1 CONCLUSIONS

6.1.1 Traditional Connection

The traditional connection where the PCP is set on a bedding strip without positively attaching it to the girder was tested with three different bedding strip heights.

It is the opinion of the author that meaningful conclusions cannot be drawn with the current data set. From the tests performed, the shorter bedding strips appear to be more critical; however, further testing is required to verify this conclusion for bedding strips less than 2" in height."

6.1.2 Other Connections

Tests were conducted on two different connection types. The shear-stud connection was tested in reverse loading cycles. Variations of the embedded angle connection were tested including: different bedding strip heights, different anchorages for the embedded angle, and different reinforcing in the PCP.

The in-plane shear strength and stiffnesses are presented in Table 4.3.

The shear stud connection was the more flexible connection; it can withstand a greater amount of shear deformation, but this connection also provides the least bracing stiffness and strength.

The loads induced in the PCP from the weld from the connection member to the embedded angle were a combination of out-of-plane bending as-well-as in-plane shear.

It is the opinion of the author that the anchors of the embedded angle should extend past the development location of the panel reinforcing. The embedded angle with short headed studs developed a tensile crack the full depth of the panel that unzipped along the embedded angle as the shear deformations increased.

6.2 FUTURE WORK

The work contained in this thesis documents the first phase of the testing with a significant amount of testing to be carried out over the next few years. In addition to the work contained in this thesis, there will be in-plane shear testing of prestressed PCPs and large-scale testing of PCPs attached to beams.

6.2.1 Traditional Connection

The author suggests two additional tests be performed with the bedding strip heights of 1 inch and ½ inch.

6.2.2 Pre-Cast Prestressed Panel Tests

The tests contained in this thesis were on conventionally reinforced PCPs. Tests of prestressed PCPs will supplement this research. Prestressed PCPs are used on typical bridges; conventionally reinforced PCPs are only used on bridges when the PCP spans short distances, when the girders are closely spaced.

6.2.3 Twin I-Beam / Steel Tub / Concrete U-Beam Tests

Large scale testing of PCPs attached to beams will also be conducted. These beams will be loaded eccentrically to simulate the loading on a curved girder. There will be three suites of test: PCPs on twin steel I-beams, PCPs on a steel tub beam, and PCPs on a concrete U-beam. The loading of these panels will be more complex than the loading contained in this thesis. The PCPs will be loaded in in-plane shear as the beams' cross-sections warp and out-of-plane bending as the beams torsionally rotate. This will more closely represent the forces the PCPs will encounter on a curved bridge.

Appendix A

Test Results

This appendix contains additional test results.

A.1 Panel Slip of the Traditional Connection

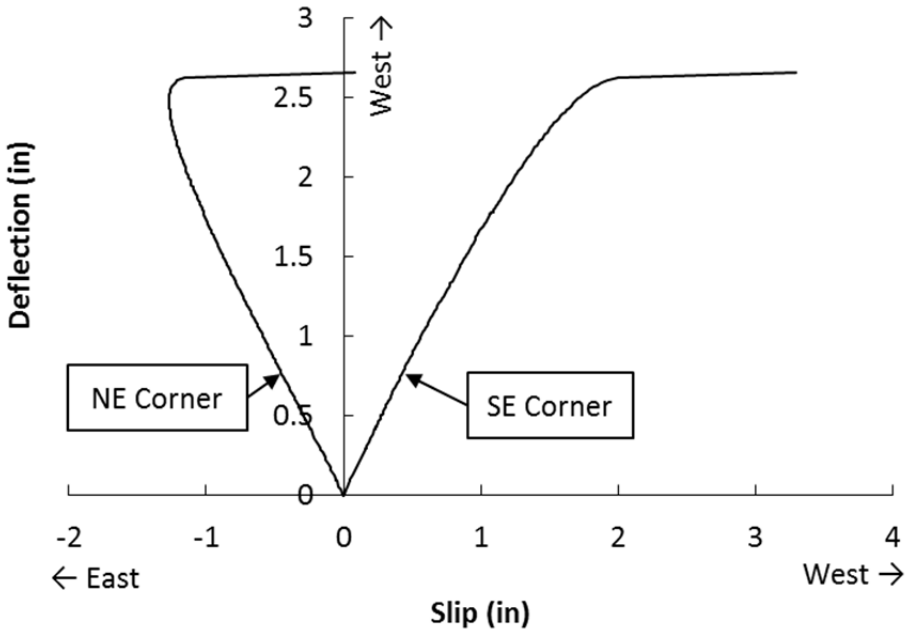

Figure A.1: *Panel Slip vs. Panel Deflection for Test 1 with a 2" Bedding Strip*

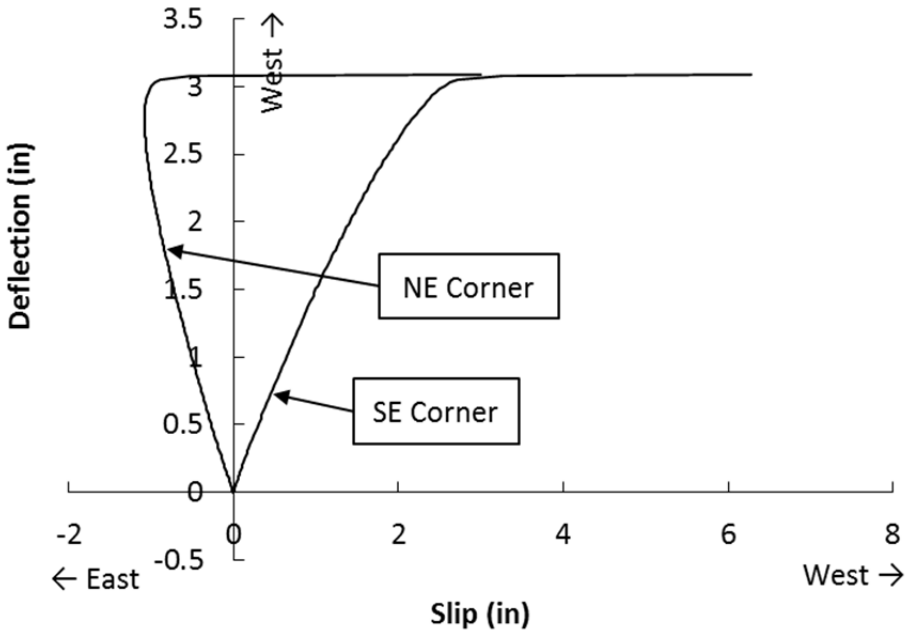

Figure A.2: *Panel Slip vs. Panel Deflection for Test 2 with a 3" Bedding Strip*

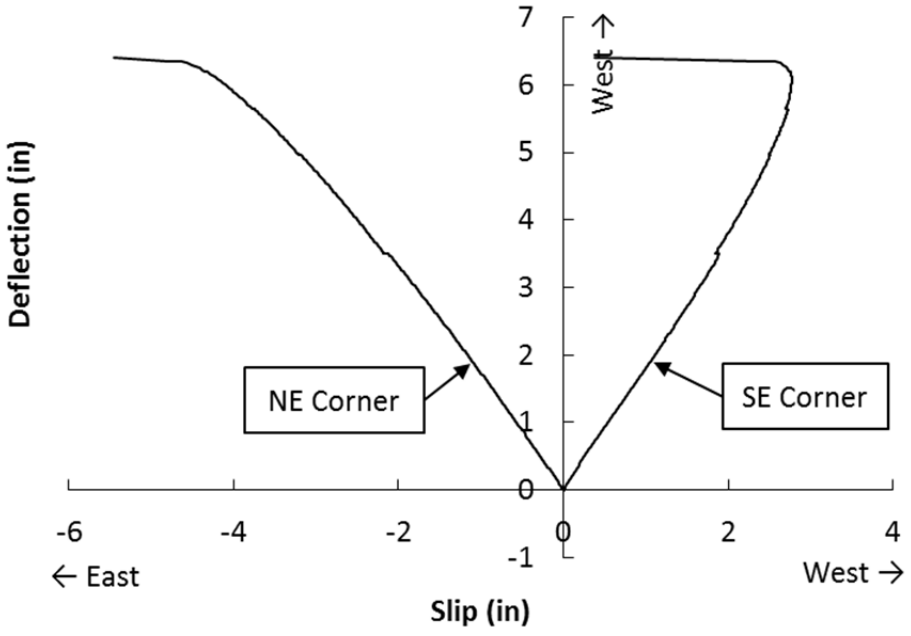

Figure A.3: *Panel Slip vs. Panel Deflection for Test 3 with a 4" Bedding Strip*

A.2 LOAD DEFLECTION CURVES

A.2.1 Traditional Connection

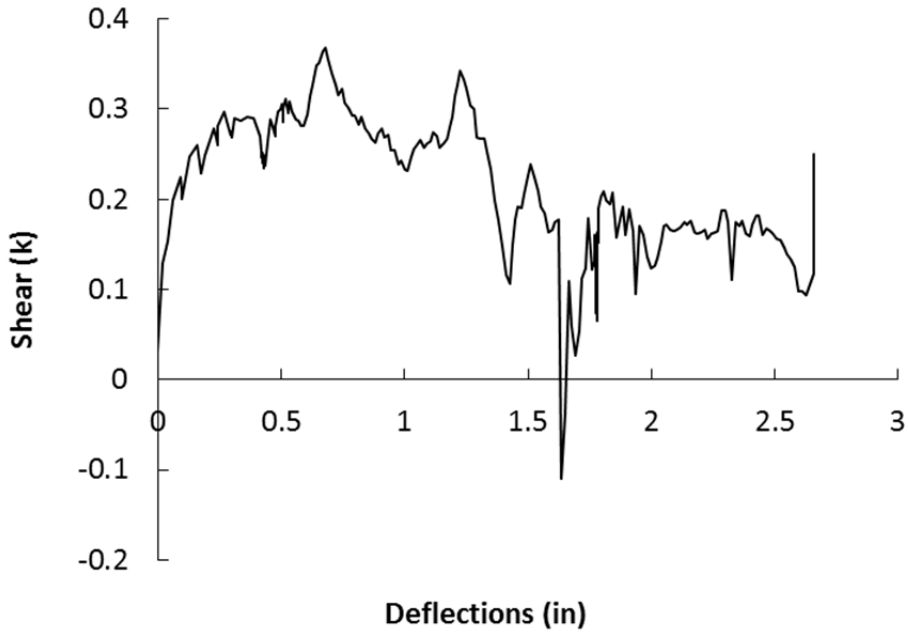

Figure A.4: *Panel Shear vs. Panel Deflections for Test 1*

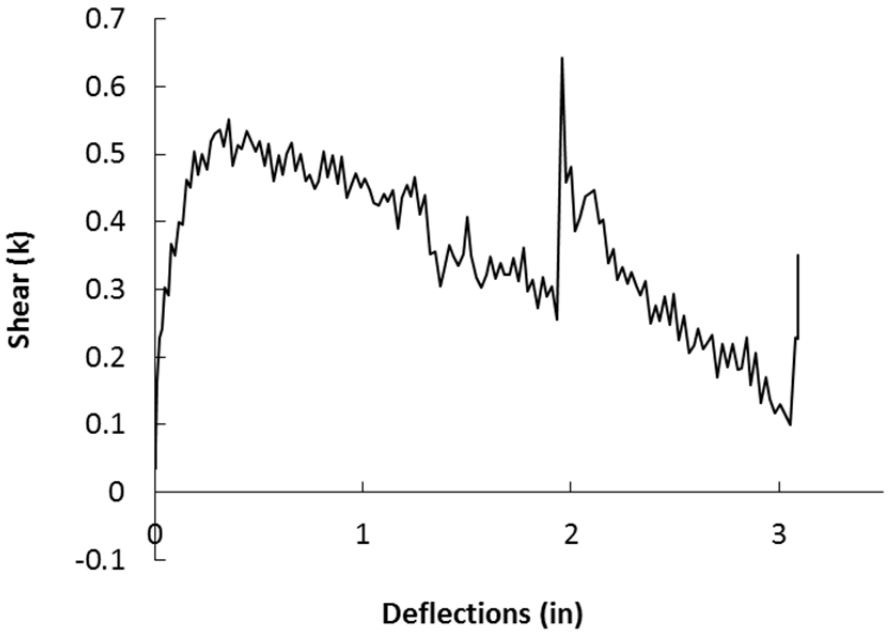

Figure A.5: *Panel Shear vs. Panel Deflections for Test 2*

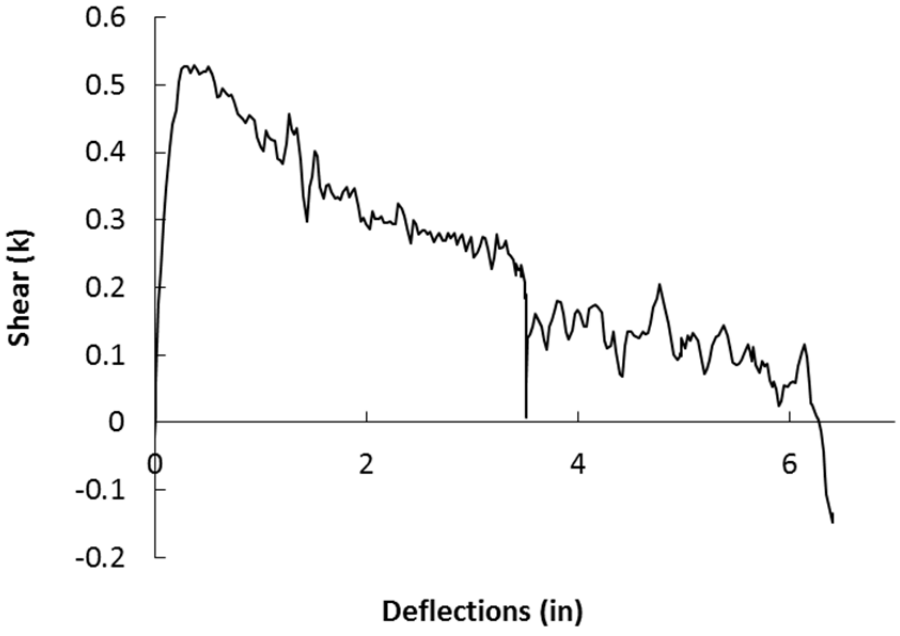

Figure A.6: *Panel Shear vs. Panel Deflections for Test 3*

A.2.2 Shear Stud Connection

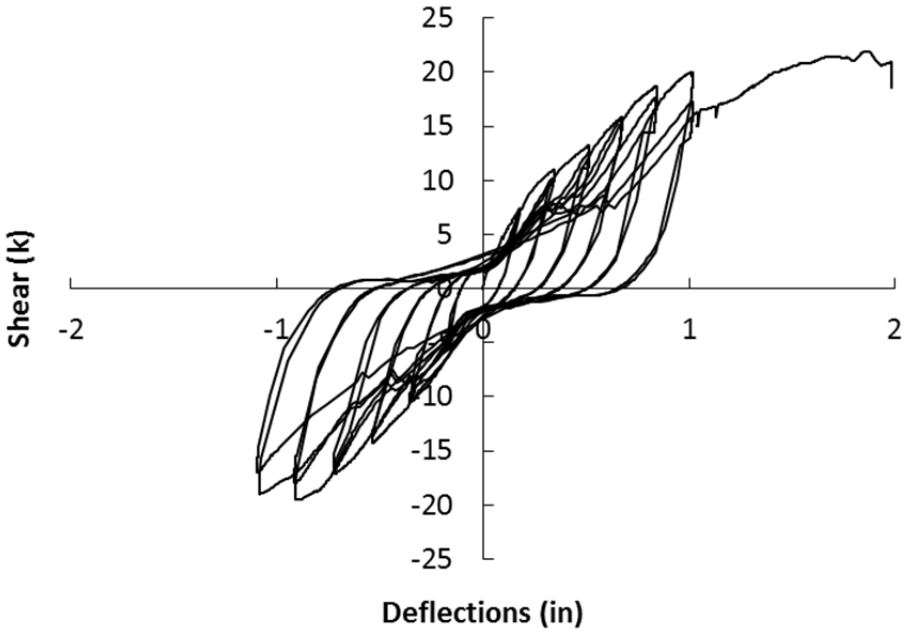

Figure A.7: *Panel Shear vs. Panel Deflections for All Displacement Cycles of Test 4*

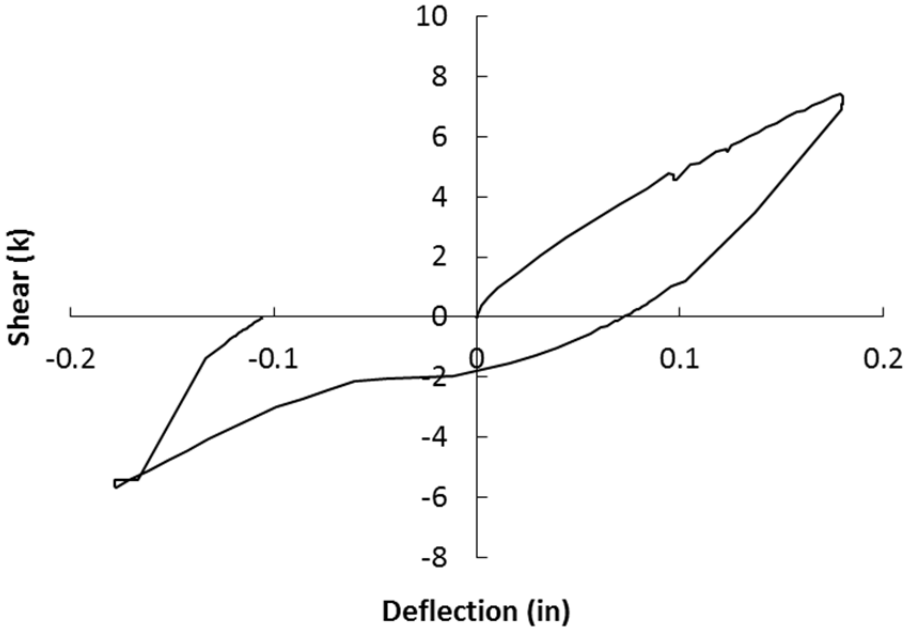

Figure A.8: *Panel Shear vs. Panel Deflections for Displacement Cycle 1 of Test 4*

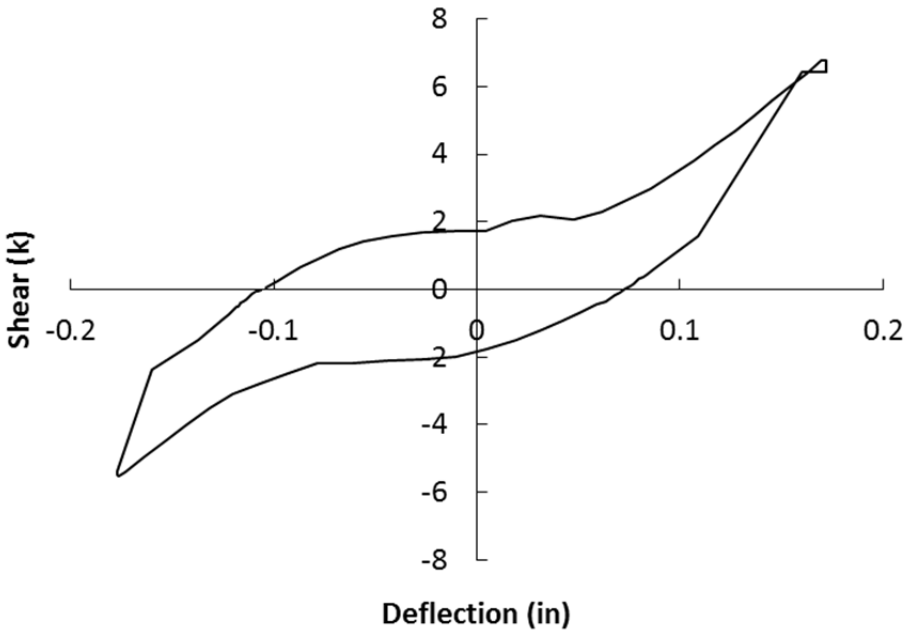

Figure A.9: *Panel Shear vs. Panel Deflections for Displacement Cycle 2 of Test 4*

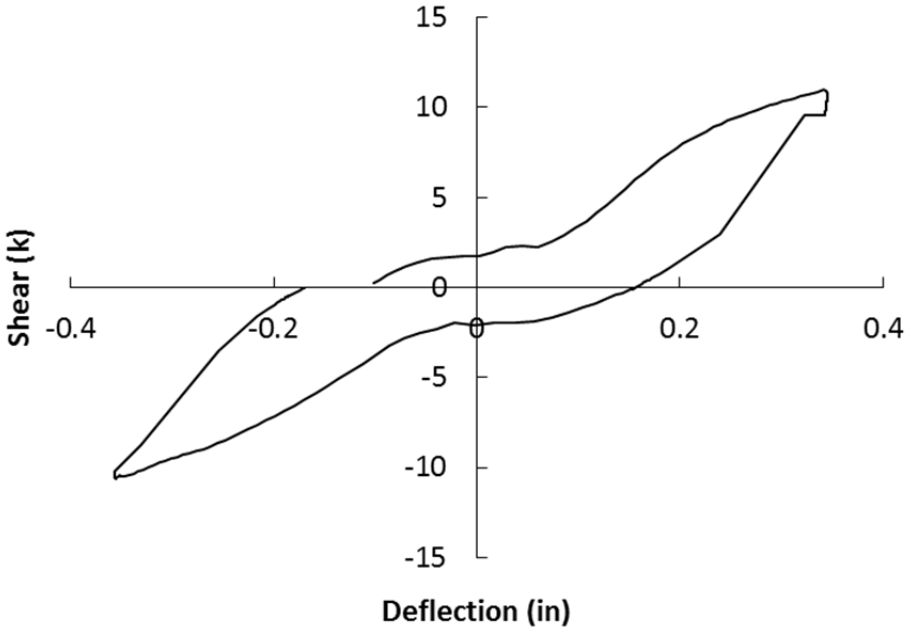

Figure A.10: *Panel Shear vs. Panel Deflections for Displacement Cycle 3 of Test 4*

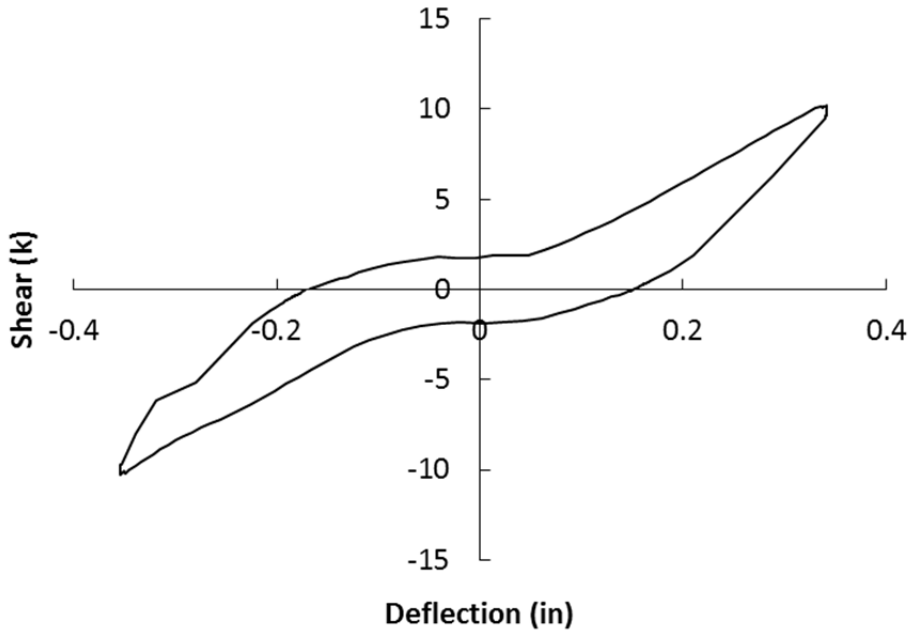

Figure A.11: *Panel Shear vs. Panel Deflections for Displacement Cycle 4 of Test 4*

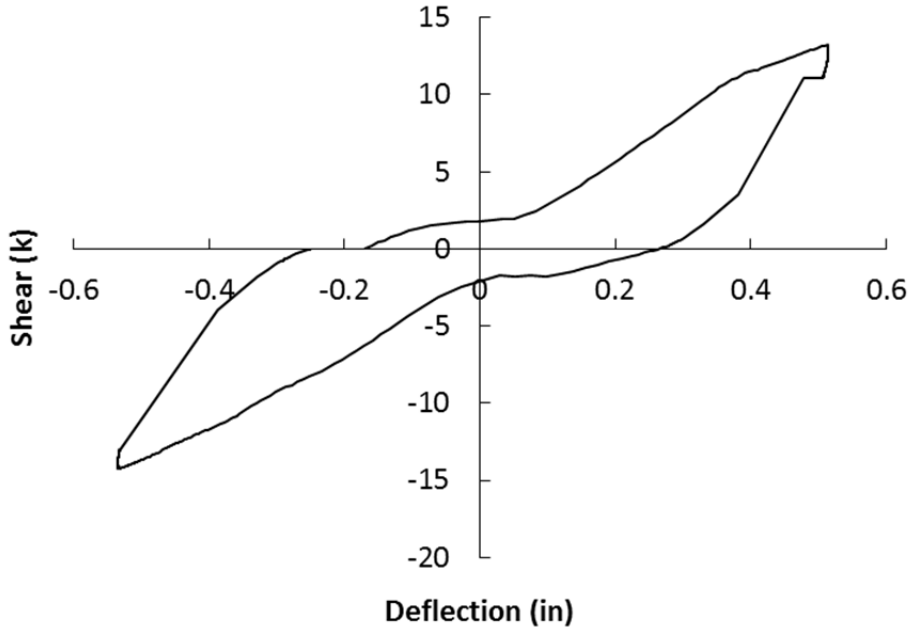

Figure A.12: *Panel Shear vs. Panel Deflections for Displacement Cycle 5 of Test 4*

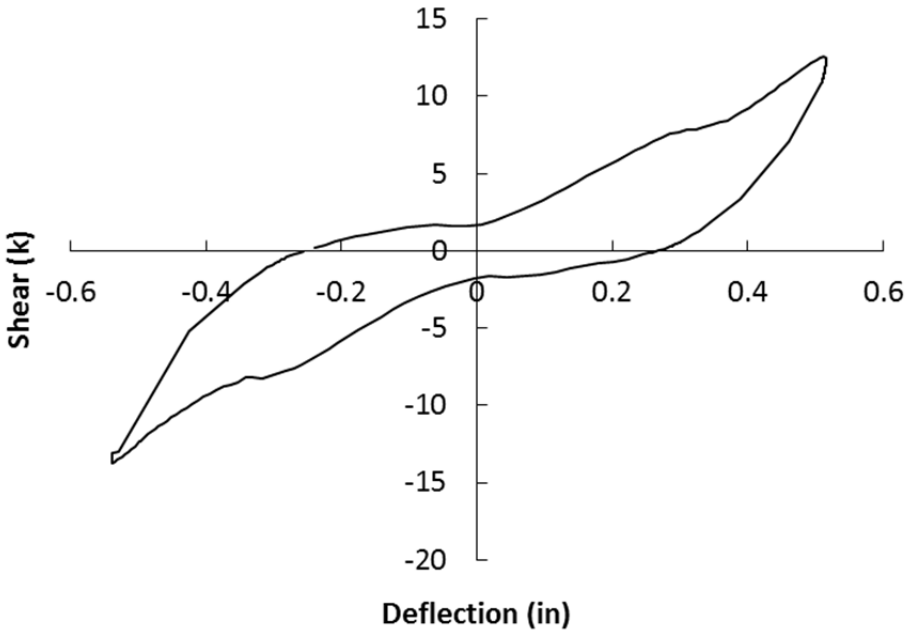

Figure A.13: *Panel Shear vs. Panel Deflections for Displacement Cycle 6 of Test 4*

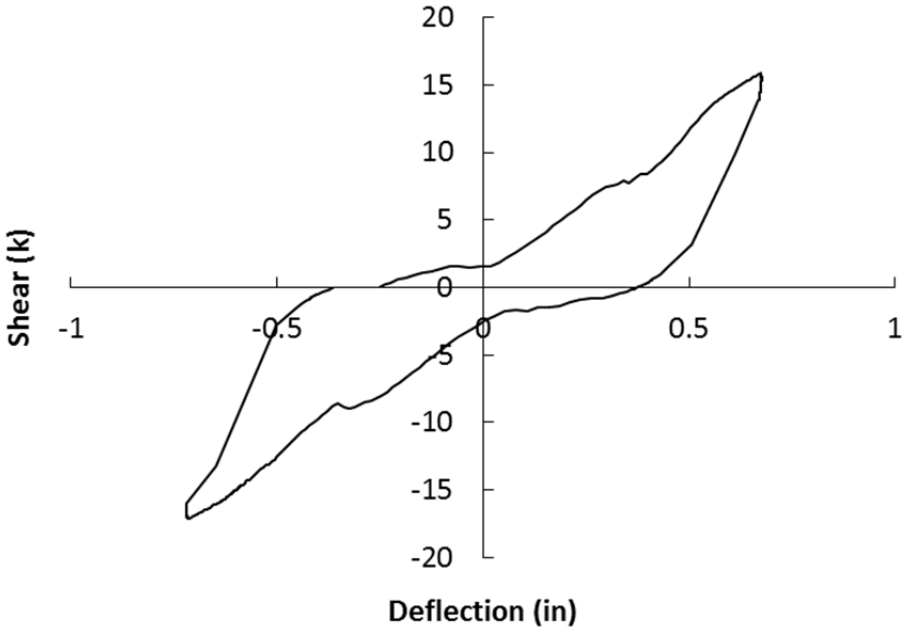

Figure A.14: *Panel Shear vs. Panel Deflections for Displacement Cycle 7 of Test 4*

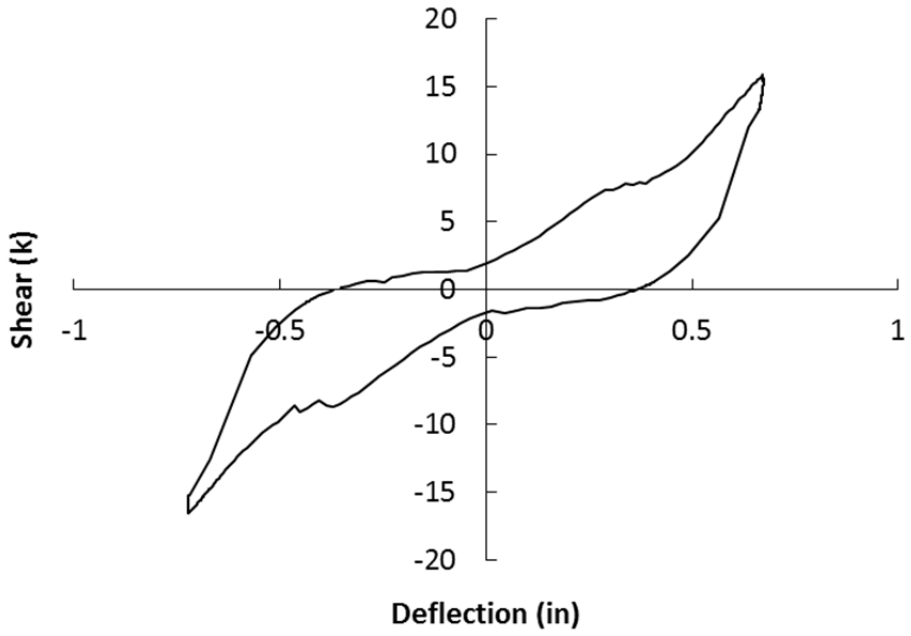

Figure A.15: *Panel Shear vs. Panel Deflections for Displacement Cycle 8 of Test 4*

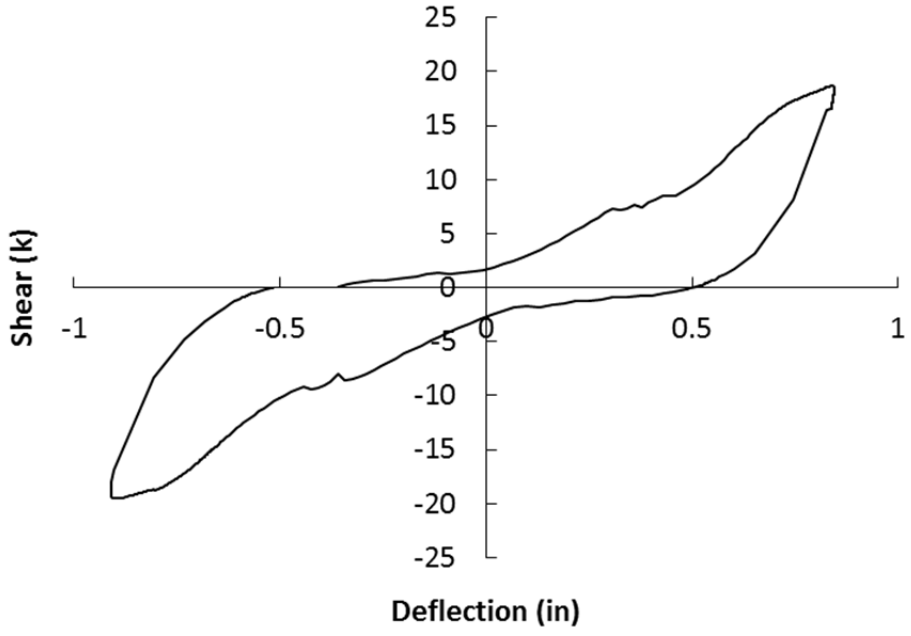

Figure A.16: *Panel Shear vs. Panel Deflections for Displacement Cycle 9 of Test 4*

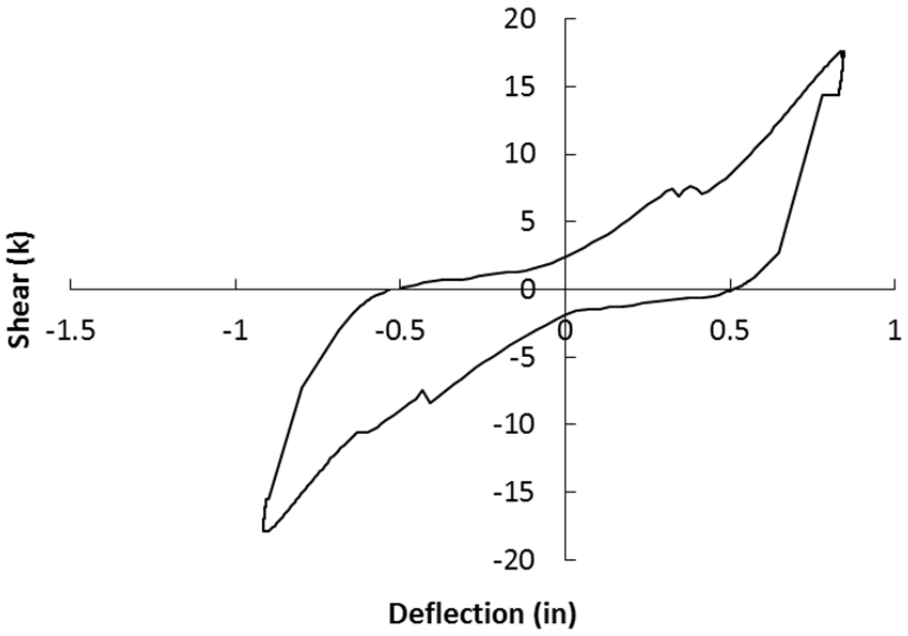

Figure A.17: *Panel Shear vs. Panel Deflections for Displacement Cycle 10 of Test 4*

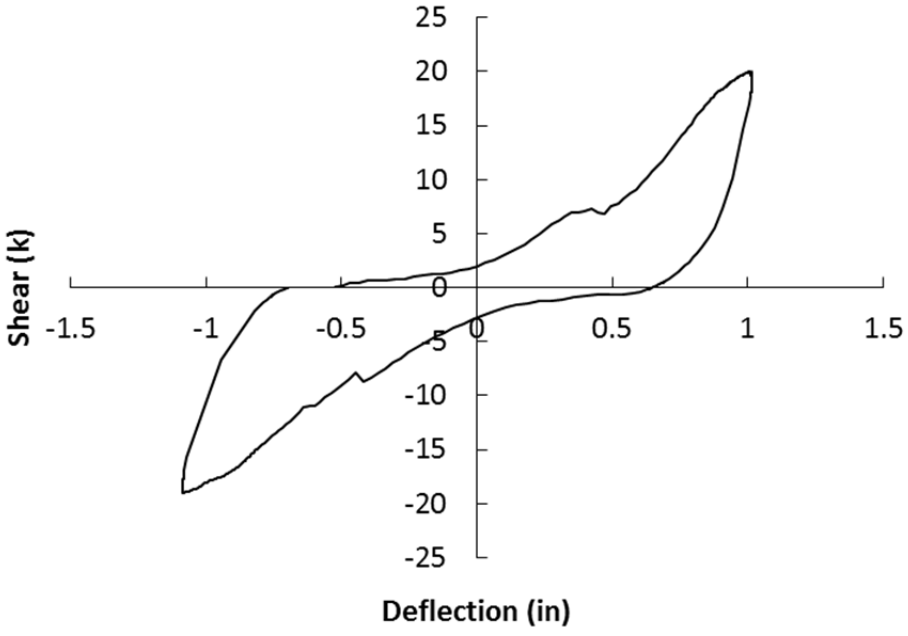

Figure A.18: *Panel Shear vs. Panel Deflections for Displacement Cycle 11 of Test 4*

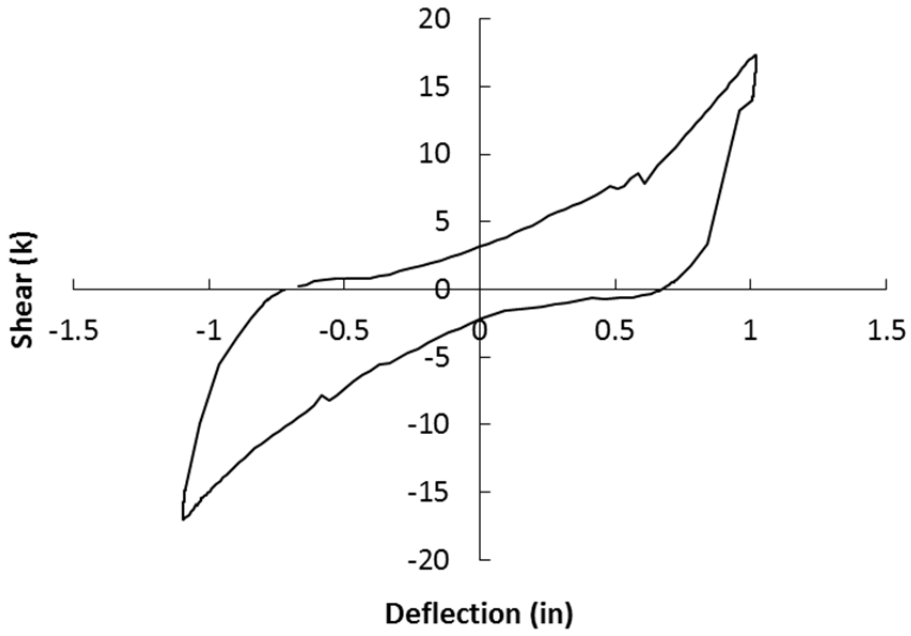

Figure A.19: *Panel Shear vs. Panel Deflections for Displacement Cycle 12 of Test 4*

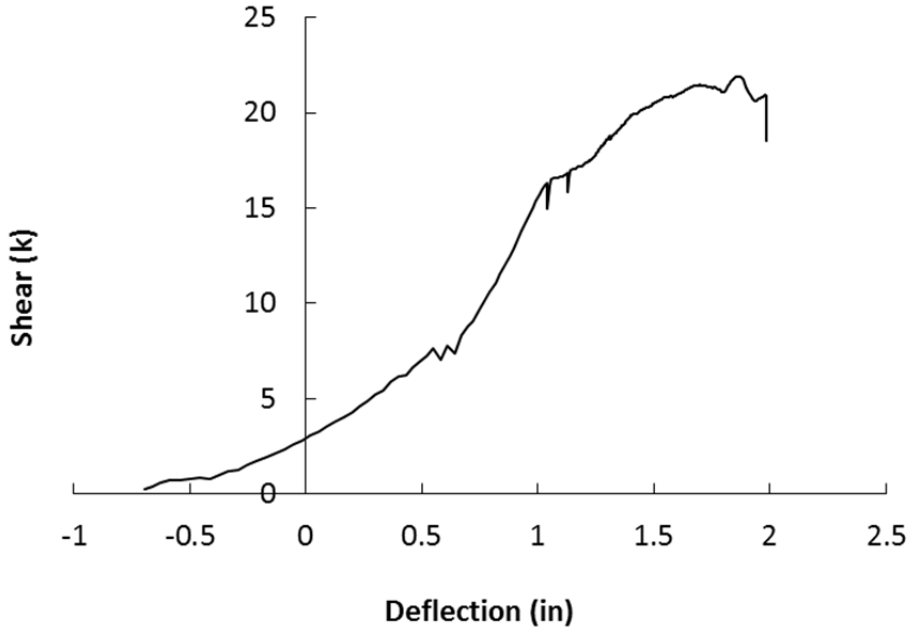

Figure A.20: *Panel Shear vs. Panel Deflections for Displacement Cycle 13 of Test 4*

A.2.3 Embedded Angle Connection

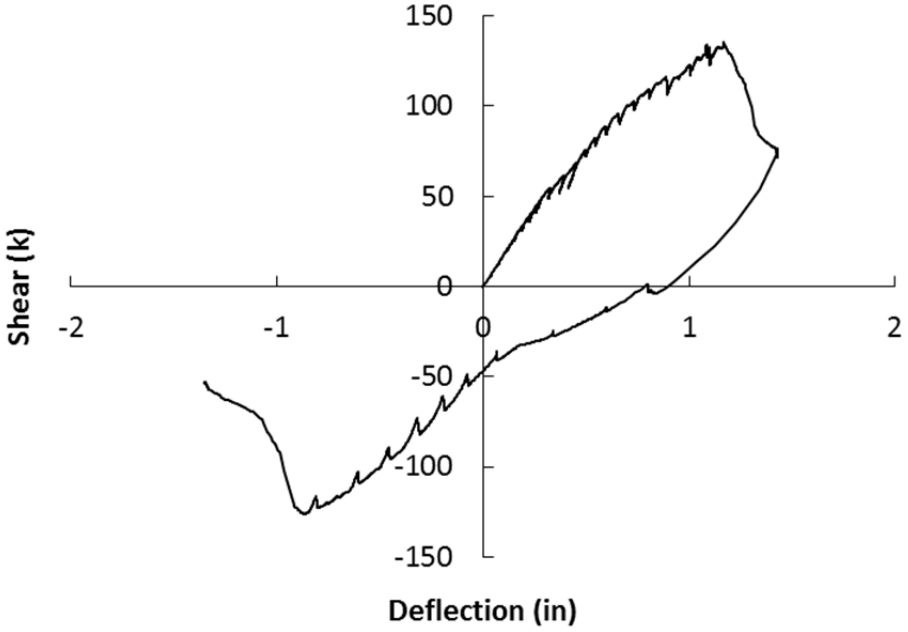

Figure A.21: *Panel Shear vs. Panel Deflections for Test 5*

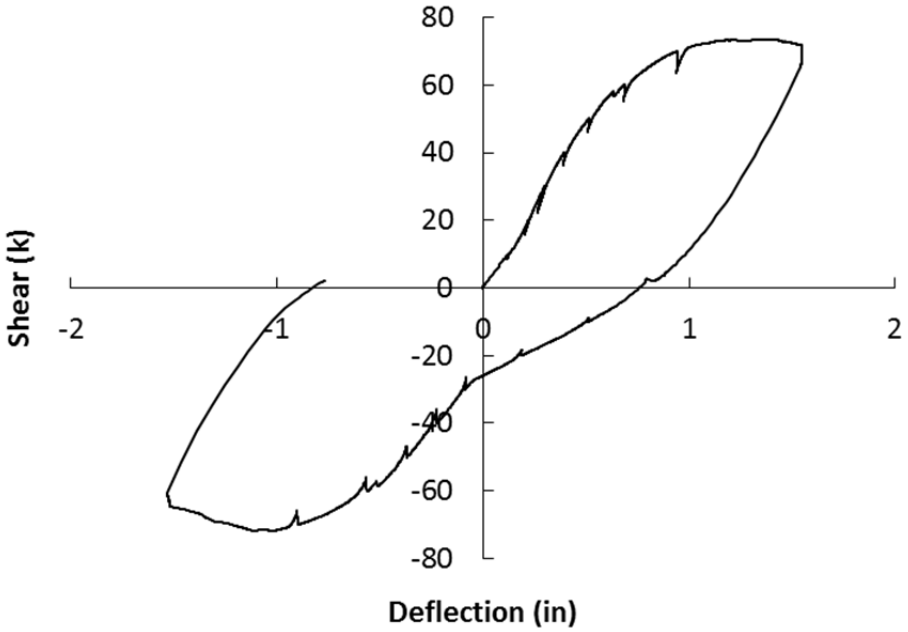

Figure A.22: *Panel Shear vs. Panel Deflections for Test 6*

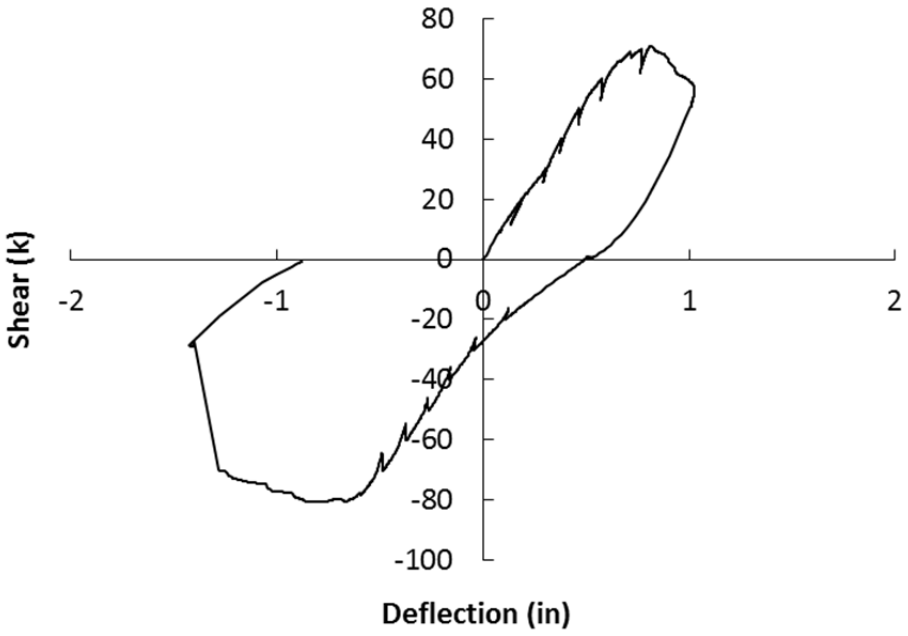

Figure A.23: *Panel Shear vs. Panel Deflections for Test 7*

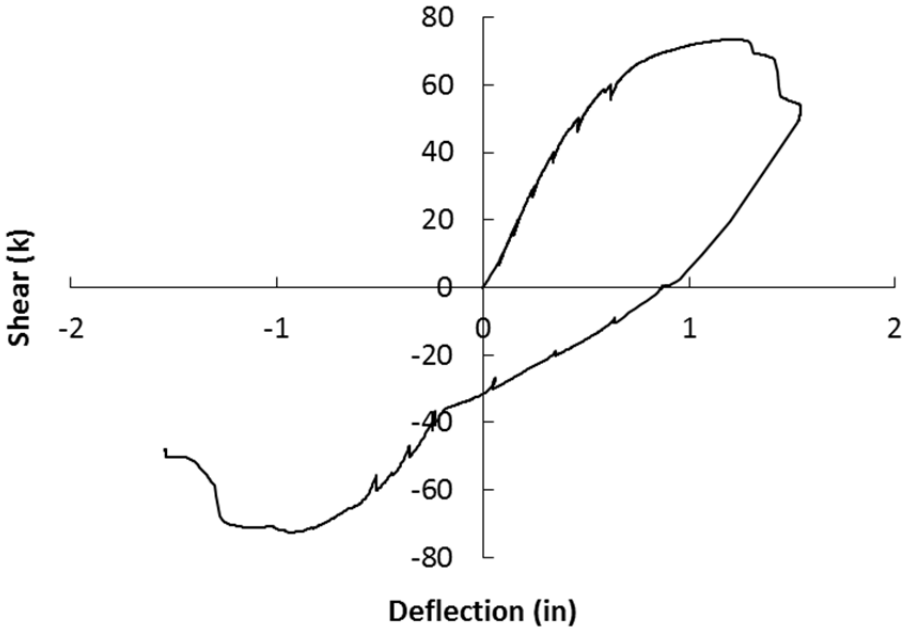

Figure A.24: *Panel Shear vs. Panel Deflections for Test 8*

References

Barker, J. M. (1975). Research, Application, and Experience with Precast Prestressed Bridge Deck Panels. PCI Journal, 66-85.

Bender, M. E. (1957). Prestressed Concrete Bridges for the Illinois Toll Highway. Proceedings World Conference on Prestressed Concrete, (pp. A11.1-A11.8). San Francisco, CA.

Bieschke, L. A., & Klingner, R. E. (1982). *The Effect of Transfer Strand Extensions on the Behavior of Precast Prestressed Panel Bridges.* No. 303-1F Res Rept., The University of Texas at Austin, Center for Transportation Research.

Buth, E., Furr, H. L., & Jones, H. L. (1972). Evaluation of a Prestressed Panel, Cast-In-Place Concrete Bridge. No. 145-3 Res Rept., Texas A&M University, Texas Transportation Institute.

Currah, R. M. (1993). Shear Strength and Shear Stiffness of Permanent Steel Bridge Deck Forms. (Master's Thesis), The University of Texas at Austin.

Eğilmez, O. Ö. (2005). Leteral Bracing of Steel Bridge Girders by Permanent Metal Deck Forms. (Doctoral Dissertation), University of Houston.

Fang, I.-K., Worley, J., Burns, N., & Klingner, R. (1990). Behavior of Isotropic R/C Bridge Decks on Steel Girders. *Journal of Structural Engineering, 116*(3), 659-678.

Furr, H. L., & Ingram, L. L. (1972). Cyclic Load Tests of Composite Prestressed-Reinforced Concrete Panels. No.145-4F Res Rept., Texas A&M University, Texas Transportation Institute.

Janney, J., & Eney, W. J. (1957). Full Scale Test of Bridge on Northern Illinois Toll Highway. Proceedings World Conference on Prestressed Concrete, (pp. A12.1-A12.18). San Francisco, CA.

Jones, H. L., & Furr, H. L. (1970). Development Length of Strands in Prestressed Panel Subdecks. No. 145-2 Res Rept., Texas A&M University, Texas Transportation Institute.

Jones, H. L., & Furr, H. L. (1970). Study of In-Service Bridges Constructed with Prestressed Panel Sub-Decks. No. 145-1 Res Rept., Texas A&M University, Texas Transportation Institute.

Kwon, K. (2012). *Design Recommendations for CIP-PCP Bridge Decks.* (Doctoral dissertation), The University of Texas at Austin.

Mander, T., Mander, J., & Head, M. (2011). Compound Shear-Flexural Capacity of Reinforced Concrete–Topped Precast Prestressed Bridge Decks. *Journal of Bridge Engineering, 16*(1), 4-11.

Merrill, B. D. (2002). Texas' Use of Precast Concrete Stay-In-Place Forms for Bridge Decks. *Procedings from the 2002 Concrete Bridge Conference.* Texas Department of Transportation.

Texas Highway Department. (undated). Test of Precast Concrete Bridge Deck Panels. Bridge Division Report.

Tsui, C., Burns, N., & Klingner, R. (1986). *Behavior of Ontario-Type Bridge Deck on Steel Girders: Negative Moment Region and Load Capacity.* No. 350-3 Res Rept., The University of Texas at Austin, Center for Transportation Research, Austin, Texas.

TxDOT. (2015). Prestressed Concrete Panels Deck Details (PCP). Standard Details. Texas Department of Transportation.

TxDOT. (2015). Prestressed Concrete Panels Panel Fabrication Details (PCP-FAB). Standard Details. Texas Department of Transportation.

TxDOT. (2015). Miscellaneous Details Steel Girders and Beams (SGMD). Standard Details. Texas Department of Transportation.

Vecchio, F. (1981). *The Response of Reinforced Concrete to In-Plane Shear and Normal Stresses.* (Doctoral Thesis), University of Toronto.

Vecchio, F. J. (2000). Disturbed Stress Field Model for Reinforced Concrete: Formulation. *Journal of Structural Engineering, 126*(9), 1070-1077.

Vecchio, F. J. (2001). Disturbed Stress Field Model for Reinforced Concrete: Implementation. *Journal of Structural Engineering, 127*(1), 12-20.

Vita

Victoria Elizabeth McCammon received her Bachelor of Science in Civil Engineering from the University of Texas at Austin in May, 2005. She was employed by the Texas Department of Transportation in Austin, Texas from March 2005 to the present. In August 2014 she entered the Graduate School of Engineering at the University of Texas at Austin.

Permanent email: Victoria.McCammon@utexas.edu

This thesis was typed by the author.